2 Constitutive Models of Creep

Analysis of creep in engineering structures requires the formulation and the solution of an initial-boundary value problem including the balance equations and the constitutive assumptions. Equations describing the kinematics of three-dimensional solids as well as balance equations of mechanics of media are presented in monographs and textbooks on continuum mechanics, e.g. [29, 35, 44, 57, 108, 131, 178, 199]. In what follows we discuss constitutive equations for the description of creep behavior in three-dimensional solids.

The starting point of the engineering creep theory is the introduction of the inelastic strain, the creep potential, the flow rule, the equivalent stress and internal state variables, Sect. 2.1. In Sect. 2.2 we discuss constitutive models of secondary creep. We start with the von Mises-Odqvist creep potential and the flow rule widely used in the creep mechanics. To account for stress state effects creep potentials that include three invariants of the stress tensor are introduced. Consideration of material symmetries provide restrictions for the creep potential. A novel direct approach to find scalar valued arguments of the creep potential for the given group of material symmetries is proposed. For several cases of material symmetry appropriate invariants of the stress tensor, equivalent stress and strain expressions as well as constitutive equations for anisotropic creep are derived. In Sect. 2.3 we review experimental foundations and models of transient creep behavior under different multi-axial loading conditions. Section 2.4 is devoted to the description of tertiary creep under multi-axial stress states. Various models within the framework of continuum damage mechanics are discussed.

All equations are presented in the direct tensor notation. This notation guarantees the invariance with respect to the choice of the coordinate system and has the advantage of clear and compact representation of constitutive assumptions, particularly in the case of anisotropic creep. The basic rules of the direct tensor calculus as well as some new results for basic sets of invariants with respect to different symmetry classes are presented in Appendix A.

2.1 General Remarks

The modeling of creep under multi-axial stress states is the key step in the adequate prediction of the long-term structural behavior. Such a modeling requires the introduction of tensors of stress, strain, strain rate and corresponding inelastic parts.

Usually, they are discussed within the framework of continuum mechanics starting from fundamental balance equations. One of the most important and fundamental questions is that of the definition (or even the existence) of a measure of the inelastic strain and the decomposition of the total strain into elastic and irreversible parts within the material description. From the theoretical point of view this is still a subject of many discussions within the non-linear continuum mechanics, e.g. [45, 46, 223, 246].

In engineering mechanics, these concepts are often introduced based on intuitive assumptions, available experimental data and applications. Therefore, a lot of formulations of multi-axial creep equations can be found in the literature. In what follows some of them will be discussed. First let us recall several assumptions usually made in the creep mechanics [58, 235].

The assumption of infinitesimal strains allows to neglect the difference between the true stresses and strains and the engineering stresses and strains. According to the continuum mechanics there are no differences between the Eulerian and the Lagrangian approaches within the material description. Creep equations in the geometrical non-linear case (finite strains) are discussed in the monograph [67], for example. Finite strain equations based on rheological models are presented in the monographs [175, 246]. The linearized equations of creep continuum mechanics can be used in the majority of engineering applications because structures are usually designed such that the displacements and strains arising as a consequence of the applied loading do not exceed the prescribed small values. The exception is the case of thin-walled shells, where geometrical non-linearities must be considered even if strains are infinitesimal, see Sect. 4.4.

The assumption of the classical non-polar continuum restricts the class of materials. The equations of motion within the continuum mechanics include the balance of momentum and the balance of angular momentum, e.g. [108]. These equations introduce the stress and the moment stress tensors. Polar materials are those which are characterized by constitutive equations with respect to both tensors (in general, they are non-symmetric). In addition, the rotation degrees of freedom, i.e. the rotation tensor and the angular velocity, are introduced as independent quantities. Models of polar media found application to granular or porous materials [97, 104, 214], fiber suspensions [22, 109], or other media with changing microstructure. At present, the moment stress tensor and the anti-symmetric part of the stress tensor are not considered in the engineering creep theories. The reason for this is the higher order complexity of the models and as a consequence increased effort for the identification of material characteristics.

The assumption of isothermal conditions makes it possible to decouple the thermal and the mechanical problem. Furthermore, heat transfer problems are not considered. The influence of the constant temperature on the creep rate is described by an Arrhenius function, see Sect. 2.2.3. Coupled thermo-mechanical problems of creep and damage are discussed in [291], where the influence of creep cavitation on thermal conductivity is considered.

In this chapter we shall use the following notation. Let $\boldsymbol{\sigma}$ be the Cauchy stress tensor and $\boldsymbol{\varepsilon}$ be the tensor of infinitesimal strains as they are defined in [29, 57, 199], among others. Let the symmetric second rank tensor $\dot{\boldsymbol{\varepsilon}}^{cr}$ be the tensor of the rate of infinitesimal inelastic strains induced by the creep process. For the infinitesimal strains one can assume the additive split of the total strain rate into elastic and creep parts, i.e. $\dot{\boldsymbol{\varepsilon}} = \dot{\boldsymbol{\varepsilon}}^{el} + \dot{\boldsymbol{\varepsilon}}^{cr}$. The constitutive equation relating the stress tensor and the elastic part of the strain tensor can be formulated according to the generalized Hooke's law [29, 55, 126, 199] and will be introduced later. Creep deformation is accompanied by various microstructural changes having different influences on the strain rate. The current state of the material microstructure is determined by the entire previous history of the creep process. It can be characterized by a set of additional field variables termed as internal or hidden state variables. In this chapter we shall discuss internal state variables characterizing the states of hardening/recovery and damage. In order to distinguish between the hardening and damage mechanisms we shall specify the "internal hardening variables" by H_i and the "internal damage variables" by ω_j. The number of such variables and the corresponding evolution equations (ordinary differential equations with respect to the time variable) is dictated by the knowledge of creep-damage mechanisms for a specified metal or alloy, the availability of experimental data on creep and long term strength as well as the type of the structural analysis application. In some cases the internal state variables must be introduced as tensors of different rank in order to include effects of the deformation or damage induced anisotropy.

Constitutive equations of multi-axial creep are usually based on the concept of the creep potential and the flow rule. The associated flow rule has the origin in the engineering theory of plasticity. The basic assumptions of this theory are:

– The existence of a yield condition (creep condition, see [55], for example) expressed by the equation $F(\boldsymbol{\sigma}) = 0$, where F is a scalar valued function. In the general case one can presume that F depends not only on the stress tensor but also on the internal state variables and the temperature [202, 265], i.e. the yield condition has a form

$$F(\boldsymbol{\sigma}, H_i, \omega_j, T) = 0, \quad i = 1, \ldots, n, \quad j = 1, \ldots, m \tag{2.1.1}$$

– The existence of a flow potential as a function of the stress tensor $\Phi(\boldsymbol{\sigma})$.

The flow rule (sometimes called the normality rule) is the following assumption for the inelastic strain rate tensor

$$\dot{\boldsymbol{\varepsilon}}^{in} = \dot{\eta} \frac{\partial \Phi}{\partial \boldsymbol{\sigma}}, \tag{2.1.2}$$

where $\dot{\eta}$ is a scalar factor. In the special case that the flow potential coincides with the yield function i.e. $\Phi = F$ (2.1.2) represents the associated flow rule. With respect to the variation of the stress tensor $\delta\boldsymbol{\sigma}$ one distinguishes between the cases of elastic state, unloading from an elastic-plastic state, neutral loading and loading, i.e.

$$\begin{cases} F(\boldsymbol{\sigma}) < 0, & & & \text{elastic state} \\ F(\boldsymbol{\sigma}) = 0, & \text{and} & \delta F = \delta\boldsymbol{\sigma} \cdot\cdot \dfrac{\partial F}{\partial \boldsymbol{\sigma}} < 0 & \text{unloading} \\ F(\boldsymbol{\sigma}) = 0, & \text{and} & \delta F = \delta\boldsymbol{\sigma} \cdot\cdot \dfrac{\partial F}{\partial \boldsymbol{\sigma}} = 0 & \text{neutral loading} \\ F(\boldsymbol{\sigma}) = 0, & \text{and} & \delta F = \delta\boldsymbol{\sigma} \cdot\cdot \dfrac{\partial F}{\partial \boldsymbol{\sigma}} > 0 & \text{loading} \end{cases}$$

For work hardening materials $\dot{\eta} > 0$ is set in the case of loading/neutral loading, otherwise $\dot{\eta} = 0$, see e.g. [201]. Further details of the flow theory as well as different arguments leading to (2.1.2) can be found in textbooks on theory of plasticity, e.g. [138, 151, 153, 161, 201, 206, 292].

Within the creep mechanics the flow theory is usually applied without the concept of the yield stress or yield condition. This is motivated by the fact that creep is a thermally activated process and the material starts to creep even under low and moderate stresses lying below the yield limit. Furthermore, at high temperatures $0.5T_m < T < 0.7T_m$ the main creep mechanism for metals and alloys is the diffusion of vacancies, e.g. [117]. Under this condition the existence of a yield or a creep limit cannot be verified experimentally. In [185], p.278 it is stated that "the concept of a loading surface and the loading-unloading criterion which was used in plasticity is no longer necessary". In monographs [55, 58, 201, 202, 250] the flow rule is applied as follows

$$\dot{\boldsymbol{\varepsilon}}^{cr} = \dot{\eta}\frac{\partial \Phi}{\partial \boldsymbol{\sigma}}, \quad \dot{\eta} > 0 \tag{2.1.3}$$

Equation (2.1.3) states the "normality" of the creep rate tensor to the surfaces $\Phi(\boldsymbol{\sigma}) = const$. The scalar factor $\dot{\eta}$ is determined according to the hypothesis of the equivalence of the dissipation power [2, 58]. The dissipation power is defined by $P = \dot{\boldsymbol{\varepsilon}}^{cr} \cdot\cdot \boldsymbol{\sigma}$. It is assumed that $P = \dot{\varepsilon}^{cr}_{eq}\sigma_{eq}$, where $\dot{\varepsilon}^{cr}_{eq}$ is an equivalent creep rate and σ_{eq} is an equivalent stress. The equivalent measures of stress and creep rate are convenient to compare experimental data under different stress states (see Sect. 1.1.2). From the above hypothesis follows

$$\dot{\eta} = \frac{P}{\dfrac{\partial \Phi}{\partial \boldsymbol{\sigma}} \cdot\cdot \boldsymbol{\sigma}} = \frac{\dot{\varepsilon}^{cr}_{eq}\sigma_{eq}}{\dfrac{\partial \Phi}{\partial \boldsymbol{\sigma}} \cdot\cdot \boldsymbol{\sigma}} \tag{2.1.4}$$

The equivalent creep rate is defined as a function of the equivalent stress according to the experimental data for uni-axial creep as well as creep mechanisms operating for the given stress range. An example is the power law stress function

$$\dot{\varepsilon}^{cr}_{eq}(\sigma_{eq}) = a\sigma^{n}_{eq} \tag{2.1.5}$$

Another form of the flow rule without the yield condition has been proposed by Odqvist, [234, 236]. The steady state creep theory by Odqvist, see [234], p.21 is based on the variational equation $\delta W = \delta\boldsymbol{\sigma} \cdot\cdot \dot{\boldsymbol{\varepsilon}}^{cr}$ leading to the flow rule

$$\dot{\boldsymbol{\varepsilon}}^{cr} = \frac{\partial W}{\partial \boldsymbol{\sigma}}, \tag{2.1.6}$$

where the scalar valued function $W(\boldsymbol{\sigma})$ plays the role of the creep potential[1]. In order to specify the creep potential, the equivalent stress $\sigma_{eq}(\boldsymbol{\sigma})$ is introduced. Taking into account that $W(\boldsymbol{\sigma}) = W(\sigma_{eq}(\boldsymbol{\sigma}))$ the flow rule (2.1.6) yields

$$\dot{\boldsymbol{\varepsilon}}^{cr} = \frac{\partial W}{\partial \sigma_{eq}} \frac{\partial \sigma_{eq}}{\partial \boldsymbol{\sigma}} = \dot{\varepsilon}^{cr}_{eq} \frac{\partial \sigma_{eq}}{\partial \boldsymbol{\sigma}}, \quad \dot{\varepsilon}^{cr}_{eq} \equiv \frac{\partial W}{\partial \sigma_{eq}} \tag{2.1.7}$$

The creep potential $W(\sigma_{eq})$ is defined according to experimental data of creep under uni-axial stress state for the given stress range. An example is the Norton-Bailey-Odqvist creep potential

$$W = \frac{\sigma_0}{n+1} \left(\frac{\sigma_{vM}}{\sigma_0} \right)^{n+1}, \tag{2.1.8}$$

widely used for the description of steady state creep of metals and alloys. In (2.1.8) σ_0 and n are material constants and σ_{vM} is the von Mises equivalent stress. Below we discuss various restrictions on the potentials, e.g. the symmetries of the creep behavior and the inelastic incompressibility.

In order to compare the flow rules (2.1.3) and (2.1.6) let us compute the dissipation power. From (2.1.7) it follows

$$P = \dot{\boldsymbol{\varepsilon}}^{cr} \cdot\cdot\, \boldsymbol{\sigma} = \frac{\partial W}{\partial \sigma_{eq}} \frac{\partial \sigma_{eq}}{\partial \boldsymbol{\sigma}} \cdot\cdot\, \boldsymbol{\sigma} = \dot{\varepsilon}^{cr}_{eq} \frac{\partial \sigma_{eq}}{\partial \boldsymbol{\sigma}} \cdot\cdot\, \boldsymbol{\sigma},$$

We observe that the equivalence of the dissipation power follows from (2.1.7) if the equivalent stress satisfies the following partial differential equation

$$\frac{\partial \sigma_{eq}}{\partial \boldsymbol{\sigma}} \cdot\cdot\, \boldsymbol{\sigma} = \sigma_{eq} \tag{2.1.9}$$

Furthermore, in this case the flow rules (2.1.3) and (2.1.6) lead to the same creep constitutive equation. Many proposed equivalent stress expressions satisfy (2.1.9).

The above potential formulations originate from the works of Richard von Mises, where the existence of variational principles is assumed in analogy to those known from the theory of elasticity (the principle of the minimum of the complementary elastic energy, for example). Richard von Mises wrote [320]: “Die Formänderung regelt sich derart, daß die pro Zeiteinheit von ihr verzehrte Arbeit unverändert bleibt gegenüber kleinen Variationen der Spannungen innerhalb der Fließgrenze. Da die Elastizitätstheorie einen ähnlichen Zusammenhang zwischen den Deformationsgrößen und dem elastischen Potential lehrt, so nenne ich die Spannungsfunktion F auch das “plastische Potential” oder “Fließpotential”.” It can be shown that the variational principles of linear elasticity are special cases of the energy balance equation (for isothermal or adiabatic processes), see e.g. [198], p. 148,

[1] The dependence on the temperature is dropped for the sake of brevity.

for example. Many attempts have been made to prove or to motivate the potential formulations within the framework of irreversible thermodynamics. For quasi-static irreversible processes various extremum principles (e.g. the principle of least irreversible force) are stipulated in [337]. Based on these principles and additional arguments like material stability, the potential formulations and the flow rules (2.1.1) and (2.1.6) can be verified. In [185], p. 63 a complementary dissipation potential as a function of the stress tensor as well as the number of additional forces conjugate to internal state variables is postulated, whose properties, e.g. the convexity, are sufficient conditions to satisfy the dissipation inequality. In [206] theories of plasticity and visco-plasticity are based on the notion of the dissipation pseudo-potentials. However, as far as we know, the flow rules (2.1.1) and (2.1.6) still represent the assumptions confirmed by various experimental observations of steady state creep in metals rather than consequences of the fundamental laws. The advantage of variational statements is that they are convenient for the formulation of initial-boundary value problems and for the numerical analysis of creep in engineering structures. The direct variational methods (for example, the Ritz method, the Galerkin method, the finite element method) can be applied for the numerical solution.

Finally, several creep theories without creep potentials may be found in the literature. In the monograph [246] various constitutive equations of elastic-plastic and elastic-visco-plastic behavior in the sense of rheological models are discussed without introducing the plasticity, creep or dissipation potentials. For example, the models of viscous flow of isotropic media known from rheology, e.g. [123, 269], can be formulated as the relations between two coaxial tensors

$$\boldsymbol{\sigma} = G_0 \boldsymbol{I} + G_1 \dot{\boldsymbol{\varepsilon}} + G_2 \dot{\boldsymbol{\varepsilon}} \cdot \dot{\boldsymbol{\varepsilon}} \tag{2.1.10}$$

or

$$\dot{\boldsymbol{\varepsilon}} = H_0 \boldsymbol{I} + H_1 \boldsymbol{\sigma} + H_2 \boldsymbol{\sigma} \cdot \boldsymbol{\sigma}, \tag{2.1.11}$$

where G_i is a function of invariants of $\dot{\boldsymbol{\varepsilon}}$ while H_i depend on invariants of $\boldsymbol{\sigma}$. The application of the dissipative inequality provides restrictions imposed on G_i or H_i. The existence of the potential requires that G_i or H_i must satisfy certain integrability conditions [58, 199].

2.2 Secondary Creep

Secondary or stationary creep is for many applications the most important creep model. After a relatively short transient period the material creeps in such a manner that an approximate equilibrium between hardening and softening processes can be assumed. This equilibrium exists for a long time and the long-term behavior of a structure can be analyzed assuming stationary creep processes. In this section several models of secondary creep are introduced. The secondary or stationary creep assumes constant or slowly varying loading and temperature conditions. Furthermore, the stress tensor is assumed to satisfy the condition of proportional loading, i.e. $\boldsymbol{\sigma}(t) = \varphi(t)\boldsymbol{\sigma}_0$, where $\varphi(t)$ is a slowly varying function of time and $\boldsymbol{\sigma}_0$ is a constant tensor.

2.2.1 Isotropic Creep

In many cases creep behavior can be assumed to be isotropic. In what follows the classical potential and the potential formulated in terms of three invariants of the stress tensor are introduced.

2.2.1.1 Classical Creep Equations. The starting point is the Odqvist flow rule (2.1.6). Under the assumption of the isotropic creep, the potential must satisfy the following restriction

$$W(\boldsymbol{Q}\cdot\boldsymbol{\sigma}\cdot\boldsymbol{Q}^T) = W(\boldsymbol{\sigma}) \tag{2.2.1}$$

for any symmetry transformation $\boldsymbol{Q}$, $\boldsymbol{Q}\cdot\boldsymbol{Q}^T = \boldsymbol{I}$, $\det\boldsymbol{Q} = \pm 1$. From (2.2.1) it follows that the potential depends only on the three invariants of the stress tensor (see Sect. A.3.1). Applying the principal invariants

$$\begin{aligned} &J_1(\boldsymbol{\sigma}) = \operatorname{tr}\boldsymbol{\sigma}, \quad J_2(\boldsymbol{\sigma}) = \frac{1}{2}[(\operatorname{tr}\boldsymbol{\sigma})^2 - \operatorname{tr}\boldsymbol{\sigma}^2], \\ &J_3(\boldsymbol{\sigma}) = \det\boldsymbol{\sigma} = \frac{1}{6}(\operatorname{tr}\boldsymbol{\sigma})^3 - \frac{1}{2}\operatorname{tr}\boldsymbol{\sigma}\operatorname{tr}\boldsymbol{\sigma}^2 + \frac{1}{3}\operatorname{tr}\boldsymbol{\sigma}^3 \end{aligned} \tag{2.2.2}$$

one can write

$$W(\boldsymbol{\sigma}) = W(J_1, J_2, J_3)$$

Any symmetric second rank tensor can be uniquely decomposed into the spherical part and the deviatoric part. For the stress tensor this decomposition can be written down as follows

$$\boldsymbol{\sigma} = \sigma_m\boldsymbol{I} + \boldsymbol{s}, \quad \operatorname{tr}\boldsymbol{s} = 0 \Rightarrow \sigma_m = \frac{1}{3}\operatorname{tr}\boldsymbol{\sigma},$$

where $\boldsymbol{s}$ is the stress deviator and σ_m is the mean stress. With the principal invariants of the stress deviator

$$J_{2D} = -\frac{1}{2}\operatorname{tr}\boldsymbol{s}^2 = -\frac{1}{2}\boldsymbol{s}\cdot\cdot\boldsymbol{s}, \quad J_{3D} = \frac{1}{3}\operatorname{tr}\boldsymbol{s}^3 = \frac{1}{3}(\boldsymbol{s}\cdot\boldsymbol{s})\cdot\cdot\boldsymbol{s}$$

the potential takes the form

$$W = W(J_1, J_{2D}, J_{3D}),$$

Applying the rule for the derivative of a scalar valued function with respect to a second rank tensor (see Sect. A.2.4) and (2.1.6) one can obtain

$$\dot{\boldsymbol{\varepsilon}}^{cr} = \frac{\partial W}{\partial J_1}\boldsymbol{I} - \frac{\partial W}{\partial J_{2D}}\boldsymbol{s} + \frac{\partial W}{\partial J_{3D}}\left(\boldsymbol{s}^2 - \frac{1}{3}\mathrm{tr}\,\boldsymbol{s}^2\boldsymbol{I}\right) \tag{2.2.3}$$

In the classical creep theory it is assumed that the inelastic deformation does not produce a significant change in volume. The spherical part of the creep rate tensor is neglected, i.e $\mathrm{tr}\,\dot{\boldsymbol{\varepsilon}}^{cr} = 0$. Setting the trace of (2.2.3) to zero results in

$$\mathrm{tr}\,\dot{\boldsymbol{\varepsilon}}^{cr} = 3\frac{\partial W}{\partial J_1} = 0 \quad \Rightarrow \quad W = W(J_{2D}, J_{3D})$$

From this follows that the creep behavior is not sensitive to the hydrostatic stress state $\boldsymbol{\sigma} = -p\boldsymbol{I}$, where $p > 0$ is the hydrostatic pressure. The creep equation (2.2.3) can be formulated as

$$\dot{\boldsymbol{\varepsilon}}^{cr} = -\frac{\partial W}{\partial J_{2D}}\boldsymbol{s} + \frac{\partial W}{\partial J_{3D}}\left(\boldsymbol{s}^2 - \frac{1}{3}\mathrm{tr}\,\boldsymbol{s}^2\boldsymbol{I}\right) \tag{2.2.4}$$

The last term in the right-hand side of (2.2.4) is non-linear with respect to the stress deviator $\boldsymbol{s}$. Equations of this type are called tensorial non-linear equations, e.g. [35, 58, 202, 265]. They allow to consider some non-classical or second order effects of the material behavior [35, 66]. As an example let us consider the pure shear stress state $\boldsymbol{s} = \tau(\boldsymbol{m}\otimes\boldsymbol{n} + \boldsymbol{n}\otimes\boldsymbol{m})$, where τ is the magnitude of the shear stress and $\boldsymbol{m}$ and $\boldsymbol{n}$ are orthogonal unit vectors. From (2.2.4) follows

$$\dot{\boldsymbol{\varepsilon}}^{cr} = -\frac{\partial W}{\partial J_{2D}}\tau(\boldsymbol{m}\otimes\boldsymbol{n} + \boldsymbol{n}\otimes\boldsymbol{m}) + \frac{\partial W}{\partial J_{3D}}\tau^2\left(\frac{1}{3}\boldsymbol{I} - \boldsymbol{p}\otimes\boldsymbol{p}\right),$$

where the unit vector $\boldsymbol{p}$ is orthogonal to the plane spanned on $\boldsymbol{m}$ and $\boldsymbol{n}$. We observe that the pure shear load leads to shear creep rate, and additionally to the axial creep rates (Poynting-Swift effect). Within the engineering creep mechanics such effects are usually neglected.

The assumption that the potential is a function of the second invariant of the stress deviator only, i.e.

$$W = W(J_2^D)$$

leads to the classical von Mises type potential [320]. In applications it is convenient to introduce the equivalent stress which allows to compare the creep behavior under different stress states including the uni-axial tension. The von Mises equivalent stress is defined as follows

$$\sigma_{vM} = \sqrt{\frac{3}{2}\boldsymbol{s}\cdot\cdot\,\boldsymbol{s}} = \sqrt{-3J_{2D}}, \tag{2.2.5}$$

where the factor $3/2$ is used for convenience (in the case of the uni-axial tension with the stress σ the above expression provides $\sigma_{vM} = \sigma$). With $W = W(\sigma_{vM}(\boldsymbol{\sigma}))$ the flow rule (2.1.6) results in

$$\dot{\boldsymbol{\varepsilon}}^{cr} = \frac{\partial W(\sigma_{vM})}{\partial \sigma_{vM}} \frac{\partial \sigma_{vM}}{\partial \boldsymbol{\sigma}} = \frac{\partial W(\sigma_{vM})}{\partial \sigma_{vM}} \frac{3}{2} \frac{\boldsymbol{s}}{\sigma_{vM}} \tag{2.2.6}$$

The second invariant of $\dot{\boldsymbol{\varepsilon}}^{cr}$ can be calculated as follows

$$\dot{\boldsymbol{\varepsilon}}^{cr} \cdot\cdot\, \dot{\boldsymbol{\varepsilon}}^{cr} = \frac{3}{2} \left[\frac{\partial W(\sigma_{vM})}{\partial \sigma_{vM}} \right]^2$$

Introducing the notation $\dot{\varepsilon}^2_{vM} = \frac{2}{3} \dot{\boldsymbol{\varepsilon}}^{cr} \cdot\cdot\, \dot{\boldsymbol{\varepsilon}}^{cr}$ and taking into account that

$$P = \frac{\partial W(\sigma_{vM})}{\partial \sigma_{vM}} \sigma_{vM} \geq 0$$

one can write

$$\dot{\boldsymbol{\varepsilon}}^{cr} = \frac{3}{2} \dot{\varepsilon}_{vM} \frac{\boldsymbol{s}}{\sigma_{vM}}, \quad \dot{\varepsilon}_{vM} = \frac{\partial W(\sigma_{vM})}{\partial \sigma_{vM}} \tag{2.2.7}$$

The constitutive equation of steady state creep (2.2.7) was proposed by Odqvist [236]. Experimental verifications of this equation can be found, for example, in [295] for steel 45, in [228] for titanium alloy Ti-6Al-4V and in [245] for alloys Al-Si, Fe-Co-V and XC 48. In these works tubular specimens were loaded by tension force and torque leading to the plane stress state $\boldsymbol{\sigma} = \sigma \boldsymbol{n} \otimes \boldsymbol{n} + \tau(\boldsymbol{n} \otimes \boldsymbol{m} + \boldsymbol{m} \otimes \boldsymbol{n})$, where σ and τ are the magnitudes of the normal and shear stresses (see Sect. 1.1.2). Surfaces $\sigma^2_{vM} = \sigma^2 + 3\tau^2 = const$ corresponding to the same steady state values of $\dot{\varepsilon}_{vM}$ were recorded. Assuming the Norton-Bailey type potential (2.1.8), from (2.2.7) it follows

$$\dot{\boldsymbol{\varepsilon}}^{cr} = \frac{3}{2} a \sigma_{vM}^{n-1} \boldsymbol{s} \tag{2.2.8}$$

This model is widely used in estimations of steady-state creep in structures, e.g. [77, 80, 236, 250, 265].

2.2.1.2 Creep Potentials with Three Invariants of the Stress Tensor. In some cases, deviations from the von Mises type equivalent stress were found in experiments. For example, different secondary creep rates under tensile and compressive loading were observed in [195] for Zircaloy-2, in [106] for aluminium alloy ALC101 and in [301], p. 118 for the nickel-based alloy René 95. One way to consider such effects is to construct the creep potential as a function of three invariants of the stress tensor. Below we discuss a generalized creep potential, proposed in [9]. This potential leads to tensorial non-linear constitutive equations and allows to predict the stress state dependent creep behavior and second order effects. The 6 unknown parameters in this law can be identified by some basic tests. Creep potentials formulated in terms of three invariants of the stress tensor are termed non-classical [9].

By analogy to the classical creep equations, the dependence on the stress tensor is defined by means of the equivalent stress σ_{eq}. Various equivalent stress expressions have been proposed in the literature for the formulation of yield or failure criteria, e.g. [27]. In the case of creep, different equivalent stress expressions are summarized in [160]. In [9] the following equivalent stress is proposed

$$\sigma_{eq} = \alpha\sigma_1 + \beta\sigma_2 + \gamma\sigma_3 \tag{2.2.9}$$

with the linear, the quadratic and the cubic invariants

$$\sigma_1 = \mu_1 I_1, \quad \sigma_2^2 = \mu_2 I_1^2 + \mu_3 I_2, \quad \sigma_3^3 = \mu_4 I_1^3 + \mu_5 I_1 I_2 + \mu_6 I_3, \tag{2.2.10}$$

where $I_i = \text{tr}\,\boldsymbol{\sigma}^i$ $(i = 1,2,3)$ are basic invariants of the stress tensor (see Sect. A.3.1), μ_j $(j = 1,\ldots,6)$ are parameters, which depend on the material properties. α, β, γ are numerical coefficients for weighting the influence of the different parts in the equivalent stress expression (2.2.9). Such a weighting is usual in phenomenological modelling of material behavior. For example, in [132] similar coefficients are introduced for characterizing different failure modes.

The von Mises equivalent stress (2.2.5) can be obtained from (2.2.9) by setting $\alpha = \gamma = 0$, $\beta = 1$ and $\mu_3 = 1.5$, $\mu_2 = -0.5$. In what follows we set $\beta = 1$ and the equivalent stress takes the form

$$\sigma_{eq} = \alpha\sigma_1 + \sigma_2 + \gamma\sigma_3 \tag{2.2.11}$$

It can be verified that the equivalent stress (2.2.11) satisfies (2.1.9).

The flow rule (2.1.6) allows to formulate the constitutive equation for the creep rate tensor

$$\dot{\boldsymbol{\varepsilon}}^{cr} = \frac{\partial W(\sigma_{eq})}{\partial \sigma_{eq}} \frac{\partial \sigma_{eq}}{\partial \boldsymbol{\sigma}} = \frac{\partial W(\sigma_{eq})}{\partial \sigma_{eq}} \left(\alpha \frac{\partial \sigma_1}{\partial \boldsymbol{\sigma}} + \frac{\partial \sigma_2}{\partial \boldsymbol{\sigma}} + \gamma \frac{\partial \sigma_3}{\partial \boldsymbol{\sigma}} \right) \tag{2.2.12}$$

Taking into account the relations between the invariants σ_i and the basic invariants I_i and using the rules for the derivatives of the invariants (see Sect. A.2.4), we obtain

$$\begin{aligned} \frac{\partial \sigma_1}{\partial \boldsymbol{\sigma}} &= \mu_1 \boldsymbol{I}, \quad \frac{\partial \sigma_2}{\partial \boldsymbol{\sigma}} = \frac{\mu_2 I_1 \boldsymbol{I} + \mu_3 \boldsymbol{\sigma}}{\sigma_2}, \\ \frac{\partial \sigma_3}{\partial \boldsymbol{\sigma}} &= \frac{\mu_4 I_1^2 \boldsymbol{I} + \frac{\mu_5}{3} I_2 \boldsymbol{I} + \frac{2}{3}\mu_5 I_1 \boldsymbol{\sigma} + \mu_6 \boldsymbol{\sigma}\cdot\boldsymbol{\sigma}}{\sigma_3^2} \end{aligned} \tag{2.2.13}$$

As a result, the creep constitutive equation can be formulated as follows

$$\dot{\boldsymbol{\varepsilon}}^{cr} = \frac{\partial W(\sigma_{eq})}{\partial \sigma_{eq}} \left[\alpha\mu_1 \boldsymbol{I} + \frac{\mu_2 I_1 \boldsymbol{I} + \mu_3 \boldsymbol{\sigma}}{\sigma_2} + \gamma \frac{\left(\mu_4 I_1^2 + \frac{\mu_5}{3} I_2\right) \boldsymbol{I} + \frac{2}{3}\mu_5 I_1 \boldsymbol{\sigma} + \mu_6 \boldsymbol{\sigma}\cdot\boldsymbol{\sigma}}{\sigma_3^2} \right] \tag{2.2.14}$$

Introducing the notation

$$\dot{\varepsilon}^{cr}_{eq} \equiv \frac{\partial W(\sigma_{eq})}{\partial \sigma_{eq}}$$

the constitutive equation takes the form

$$\dot{\boldsymbol{\varepsilon}}^{cr} = \dot{\varepsilon}^{cr}_{eq} \left[\alpha\mu_1 \boldsymbol{I} + \frac{\mu_2 I_1 \boldsymbol{I} + \mu_3 \boldsymbol{\sigma}}{\sigma_2} + \gamma \frac{\left(\mu_4 I_1^2 + \frac{\mu_5}{3} I_2\right) \boldsymbol{I} + \frac{2}{3}\mu_5 I_1 \boldsymbol{\sigma} + \mu_6 \boldsymbol{\sigma}\cdot\boldsymbol{\sigma}}{\sigma_3^2} \right] \tag{2.2.15}$$

Equation (2.2.15) is non-linear with respect to the stress tensor. Therefore, second order effects, e.g. [35, 56, 312] are included in the material behavior description. In addition, the volumetric creep rate can be calculated from (2.2.15) as follows

$$\dot{\varepsilon}^{cr}_{V} = \dot{\varepsilon}^{cr}_{eq} \left[3\alpha\mu_1 + \frac{(3\mu_2 + \mu_3) I_1}{\sigma_2} + \gamma \frac{(9\mu_4 + 2\mu_5) I_1^2 + 3(\mu_5 + \mu_6) I_2}{3\sigma_3^2} \right] \tag{2.2.16}$$

The volumetric creep rate is different from 0, i.e. the compressibility or dilatation can be considered.

The derived creep equation has the form (2.1.11) of the general relation between two coaxial tensors. The comparison of (2.1.11) and (2.2.15) provides

$$\begin{aligned} H_0 &= \dot{\varepsilon}^{cr}_{eq} \left(\alpha\mu_1 + \frac{\mu_2 I_1}{\sigma_2} + \gamma \frac{3\mu_4 I_1^2 + \mu_5 I_2}{3\sigma_3^2} \right), \\ H_1 &= \dot{\varepsilon}^{cr}_{eq} \left(\frac{\mu_3}{\sigma_2} + \gamma \frac{2\mu_5 I_1}{3\sigma_3^2} \right), \\ H_2 &= \dot{\varepsilon}^{cr}_{eq} \gamma \frac{\mu_6}{\sigma_3^2} \end{aligned} \tag{2.2.17}$$

In [9] the power law function of the equivalent stress (2.1.5) is applied to model creep behavior of several materials. Four independent creep tests are required to identify the material constants. The stress states realized in tests should include uni-axial tension, uni-axial compression, torsion and hydrostatic pressure. Let us note, that experimental data which allows to identify the full set of material constants in (2.2.15) are usually not available. In applications one may consider the following special cases of (2.2.15) with reduced number of material constants.

The classical creep equation based on the von Mises equivalent stress can be derived assuming the following values of material constants

$$\alpha = \gamma = 0, \quad \mu_2 = -1/2, \quad \mu_3 = 3/2, \tag{2.2.18}$$

$$\sigma_{eq} = \sigma_2 = \sqrt{-\frac{1}{2} I_1^2 + \frac{3}{2} I_2} = \sqrt{\frac{3}{2} \boldsymbol{s} \cdot\cdot \boldsymbol{s}} = \sigma_{vM} \tag{2.2.19}$$

The creep rate tensor takes the form

$$\dot{\boldsymbol{\varepsilon}}^{cr} = \dot{\varepsilon}^{cr}_{eq} \left(\sqrt{\frac{3}{2}\boldsymbol{s} \cdot\cdot \boldsymbol{s}} \right) \frac{3\boldsymbol{\sigma} - I_1 \boldsymbol{I}}{2\sqrt{\frac{3}{2}\boldsymbol{s} \cdot\cdot \boldsymbol{s}}} = \frac{3}{2} \frac{\dot{\varepsilon}^{cr}_{eq}(\sigma_{vM})}{\sigma_{vM}} \boldsymbol{s} \tag{2.2.20}$$

Assuming identical behavior in tension and compression and neglecting second order effects from $\alpha = \gamma = 0$, the following equivalent stress can be obtained

$$\sigma_{eq} = \sigma_2 = \sqrt{\mu_2 I_1^2 + \mu_3 I_2} \tag{2.2.21}$$

The corresponding creep constitutive equation takes the form

$$\dot{\boldsymbol{\varepsilon}}^{cr} = \dot{\varepsilon}^{cr}_{eq}(\sigma_2) \frac{\mu_2 I_1 \boldsymbol{I} + \mu_3 \boldsymbol{\sigma}}{\sigma_2} \tag{2.2.22}$$

The parameters μ_2 and μ_3 can be determined from uni-axial tension and torsion tests. Based on the experimental data presented in [165, 166] for technical pure copper M1E (Cu 99,9%) at T = 573 K the parameters μ_2 and μ_3 are identified in [24].

Neglecting the influence of the third invariant $(\gamma = 0)$, the creep rate tensor can be expressed as follows

$$\dot{\boldsymbol{\varepsilon}}^{cr} = \dot{\varepsilon}^{cr}_{eq}(\sigma_{eq}) \left(\alpha\mu_1 \boldsymbol{I} + \frac{\mu_2 I_1 \boldsymbol{I} + \mu_3 \boldsymbol{\sigma}}{\sigma_2} \right) \tag{2.2.23}$$

The above equation describes different behavior in tension and compression, and includes the volumetric creep rate. Three independent tests, e.g. tension, compression and torsion are required to identify the material constants μ_1, μ_2 and μ_3.

With the quadratic invariant and the reduced cubic invariant several special cases with three material constants can be considered. Setting ($\alpha\mu_1 = \mu_4 = \mu_5 = 0$) the tensorial non-linear equation can be obtained

$$\dot{\boldsymbol{\varepsilon}}^{cr} = \dot{\varepsilon}^{cr}_{eq}(\sigma_{eq}) \left(\frac{\mu_2 I_1 \boldsymbol{I} + \mu_3 \boldsymbol{\sigma}}{\sigma_2} + \gamma \frac{\mu_6 \boldsymbol{\sigma} \cdot \boldsymbol{\sigma}}{\sigma_3^2} \right) \tag{2.2.24}$$

With $\alpha\mu_1 = \mu_4 = \mu_6 = 0$ the creep rate tensor takes the form

$$\dot{\boldsymbol{\varepsilon}}^{cr} = \dot{\varepsilon}^{cr}_{eq}(\sigma_{eq}) \left(\frac{\mu_2 I_1 \boldsymbol{I} + \mu_3 \boldsymbol{\sigma}}{\sigma_2} + \gamma \frac{\mu_5 (I_2 \boldsymbol{I} + 2 I_1 \boldsymbol{\sigma})}{\sigma_3^2} \right) \tag{2.2.25}$$

The material constants in (2.2.23), (2.2.24) and (2.2.25) were identified in [2, 28] according to data from multi-axial creep tests for plastics (PVC) at room temperature [187] and aluminium alloy AK4-1T at 473 K [94, 125, 294]. Furthermore, simulations have been performed in [2, 28] to compare Eqs (2.2.23), (2.2.24) and (2.2.25) as they characterize creep behavior under different loading conditions. The conclusion was made that cubic invariants applied in (2.2.24) and (2.2.25) do not deliver any significant improvement in the material behavior description.

2.2.2 Creep of Initially Anisotropic Materials

Anisotropic creep behavior and anisotropic creep modeling are subjects which are rarely discussed in the classical monographs and textbooks on creep mechanics (only in some books one may found the flow potentials introduced by von Mises [320] and Hill [138]). The reason for this is that the experimental data from creep tests usually show large scatter within the range of 20% or even more. Therefore, it was often difficult to recognize whether the difference in creep curves measured for different specimens (cut from the same material in different directions) is the result of the anisotropy. Therefore, it was no use for anisotropic models with higher order complexity, since the identification of material constants was difficult or even impossible. In the last two decades the importance in modeling anisotropic creep behavior of materials and structures is discussed in many publications. In [47, 200, 259, 260, 261, 262] experimental results of creep of superalloys SRR99 and CMSX-4 are reported, which demonstrate significant anisotropy of creep behavior for different orientations of specimens with respect to the crystallographic axes. In [141] experimental creep curves of a 9CrMoNbV weld metal are presented. They show significant difference for specimens cut in longitudinal (welding) direction and transverse directions. Another example is a material reinforced by fibers, showing quite different creep behavior in direction of fibers and in the transverse direction, e.g. [273, 274].

Within the creep mechanics one usually distinguishes between two kinds of anisotropy: the initial anisotropy and the deformation or damage induced anisotropy. In what follows the first case will be introduced. The second case will be discussed in Sects 2.3.2 and 2.4.2.

The modeling of anisotropic behavior starts with the concepts of material symmetry, physical symmetry, symmetry transformation and symmetry group, e.g. [331]. The material symmetry group is related to the symmetries of the materials microstructure, e.g. the crystal symmetries, the symmetries due to the arrangement of fibers in a fiber-reinforced materials, etc. The symmetry transformations are described by means of orthogonal tensors. Two important of them are

– the reflection

$$\boldsymbol{Q}(\boldsymbol{n}) = \boldsymbol{I} - 2\boldsymbol{n} \otimes \boldsymbol{n}, \tag{2.2.26}$$

  where $\boldsymbol{n}$ is the unit normal to the mirror plane,
– the rotation about a fixed axis

$$\boldsymbol{Q}(\varphi \boldsymbol{m}) = \boldsymbol{m} \otimes \boldsymbol{m} + \cos\varphi(\boldsymbol{I} - \boldsymbol{m} \otimes \boldsymbol{m}) + \sin\varphi \boldsymbol{m} \times \boldsymbol{I}, \tag{2.2.27}$$

  where $\boldsymbol{m}$ is the axis of rotation and φ ($-\pi < \varphi < \pi$) is the angle of rotation.

Any arbitrary rotation of a rigid body can be described as a composition of three rotations (2.2.27) about three fixed axes [333]. Any symmetry transformation can be represented by means of rotations and reflections, i.e. the tensors of the type (2.2.26) and (2.2.27). The notion of the symmetry group as a set of symmetry transformations was introduced in [230]. The symmetry groups of polar and axial tensors are

discussed in [332]. According to [313], p. 82 a "simple solid" is called aelotropic or anisotropic, if its symmetry group is a proper subgroup of the orthogonal group.

The concept of the "physical symmetry group" is related to the symmetries of the material behavior, e.g. linear elasticity, thermal expansion, plasticity, creep, etc. It can only be established based on experimental observations. Physical symmetries must be considered in the formulation of constitutive equations and constitutive functions. As an example let us consider the symmetry group of the fourth rank elasticity tensor ${}^{(4)}\boldsymbol{C} = C^{ijkl}\boldsymbol{e}_i \otimes \boldsymbol{e}_j \otimes \boldsymbol{e}_k \otimes \boldsymbol{e}_l$ as the set of orthogonal tensors $\boldsymbol{Q}$ satisfying the equation, e.g. [25, 332],

$$ {}^{(4)}\boldsymbol{C}' = C^{ijkl}\boldsymbol{Q}\cdot\boldsymbol{e}_i \otimes \boldsymbol{Q}\cdot\boldsymbol{e}_j \otimes \boldsymbol{Q}\cdot\boldsymbol{e}_k \otimes \boldsymbol{Q}\cdot\boldsymbol{e}_l = {}^{(4)}\boldsymbol{C} \tag{2.2.28} $$

The physical symmetries or the set of orthogonal solutions of (2.2.28) can be found only if all the 21 coordinates of the elasticity tensor ${}^{(4)}\boldsymbol{C}$ for a selected basis are identified from tests. Vice versa, if the physical symmetry group is known then one can find the general structure of the elasticity tensor based on (2.2.28). Clearly, neither the elasticity tensor nor the physical symmetry group of the linear elastic behavior can be exactly found from tests. Establishment of physical symmetries of creep behavior is rather complicated due to relatively large scatter of experimental data. However, one can relate physical symmetries to the known symmetries of materials microstructure. According to the Neumann principle widely used in different branches of physics and continuum mechanics, e.g. [25, 232, 332]

> *The symmetry group of the reason belongs to the symmetry group of the consequence.*

Considering the material symmetries as one of the "reasons" and the physical symmetries as a "consequence" one can apply the following statement [331]

> *For a material element and for any of its physical properties every material symmetry transformation of the material element is a physical symmetry transformation of the physical property.*

In many cases the material symmetry elements are evident from the arrangement of the materials microstructure as a consequence of manufacturing conditions, for example. The above principle states that the physical behavior, e.g. the steady state creep, contains all elements of the material symmetry. The physical symmetry group usually possesses more elements than the material symmetry group, e.g. [232].

2.2.2.1 Classical Creep Equations. Here we discuss steady state creep equations based on the flow rule (2.1.6) and assumption that the creep potential has a quadratic form with respect to the invariants of the stress tensor. These invariants must be established according to the assumed symmetry elements of the creep behavior. The assumption of the quadratic form of the flow potential originates from the von Mises work on plasticity of crystals [320]. Therefore, the equations presented below may be termed as von Mises type equations.

Transverse Isotropy. In this case the potential $W(\boldsymbol{\sigma})$ must satisfy the following restriction

$$W(\boldsymbol{Q}\cdot\boldsymbol{\sigma}\cdot\boldsymbol{Q}^T)=W(\boldsymbol{\sigma}),\quad \boldsymbol{Q}(\varphi\boldsymbol{m})=\boldsymbol{m}\otimes\boldsymbol{m}+\cos\varphi(\boldsymbol{I}-\boldsymbol{m}\otimes\boldsymbol{m})+\sin\varphi\boldsymbol{m}\times\boldsymbol{I} \tag{2.2.29}$$

In (2.2.29) $\boldsymbol{Q}(\varphi\boldsymbol{m})$ is the assumed element of the symmetry group, whereby $\boldsymbol{m}$ is a constant unit vector and φ is the arbitrary angle of rotation about $\boldsymbol{m}$. From the restriction (2.2.29) follows that the potential W must satisfy the following partial differential equation (see Sect. A.3.2)

$$(\boldsymbol{m}\times\boldsymbol{\sigma}-\boldsymbol{\sigma}\times\boldsymbol{m})\cdot\cdot\left(\frac{\partial W}{\partial\boldsymbol{\sigma}}\right)^T=0 \tag{2.2.30}$$

The set of integrals of this equation represent the set of functionally independent scalar valued arguments of the potential W with respect to the symmetry transformation (2.2.29). The characteristic system of (2.2.30) is the system of ordinary differential equations

$$\frac{d\boldsymbol{\sigma}}{ds}=(\boldsymbol{m}\times\boldsymbol{\sigma}-\boldsymbol{\sigma}\times\boldsymbol{m}) \tag{2.2.31}$$

Any system of n linear ordinary differential equations has not more than $n-1$ functionally independent integrals [92]. Since $\boldsymbol{\sigma}$ is symmetric, (2.2.31) is a system of six ordinary differential equations and has not more than five functionally independent integrals. The lists of these integrals are presented by (A.3.15) and (A.3.26). Within the classical von Mises type theory second order effects are neglected. Therefore, we have to neglect the arguments which are cubic with respect to the stress tensor. In this case the difference between various kinds of transverse isotropy considered in Sect. A.3.2 vanishes. It is possible to use different lists of of scalar arguments. The linear and quadratic arguments from (A.3.15) are

$$\operatorname{tr}\boldsymbol{\sigma},\quad \operatorname{tr}\boldsymbol{\sigma}^2,\quad \boldsymbol{m}\cdot\boldsymbol{\sigma}\cdot\boldsymbol{m},\quad \boldsymbol{m}\cdot\boldsymbol{\sigma}^2\cdot\boldsymbol{m} \tag{2.2.32}$$

Instead of (2.2.32) one can use other arguments, for example [273],

$$\begin{aligned}&\operatorname{tr}\boldsymbol{\sigma},\quad \operatorname{tr}\boldsymbol{s}^2=\operatorname{tr}\boldsymbol{\sigma}^2-\frac{1}{3}(\operatorname{tr}\boldsymbol{\sigma})^2,\\ &\boldsymbol{m}\cdot\boldsymbol{s}\cdot\boldsymbol{m}=\boldsymbol{m}\cdot\boldsymbol{\sigma}\cdot\boldsymbol{m}-\frac{1}{3}\operatorname{tr}\sigma,\\ &\boldsymbol{m}\cdot\boldsymbol{s}^2\cdot\boldsymbol{m}=\boldsymbol{m}\cdot\boldsymbol{\sigma}^2\cdot\boldsymbol{m}-\frac{2}{3}\boldsymbol{m}\cdot\boldsymbol{s}\cdot\boldsymbol{m}\operatorname{tr}\boldsymbol{\sigma}-\frac{1}{9}(\operatorname{tr}\boldsymbol{\sigma})^2\end{aligned} \tag{2.2.33}$$

In what follows we prefer another set of invariants which can be related to (2.2.32) but has a more clear mechanical interpretation. Let us decompose the stress tensor as follows

$$\boldsymbol{\sigma}=\sigma_{mm}\boldsymbol{m}\otimes\boldsymbol{m}+\boldsymbol{\sigma}_p+\boldsymbol{\tau}_m\otimes\boldsymbol{m}+\boldsymbol{m}\otimes\boldsymbol{\tau}_m \tag{2.2.34}$$

with the projections

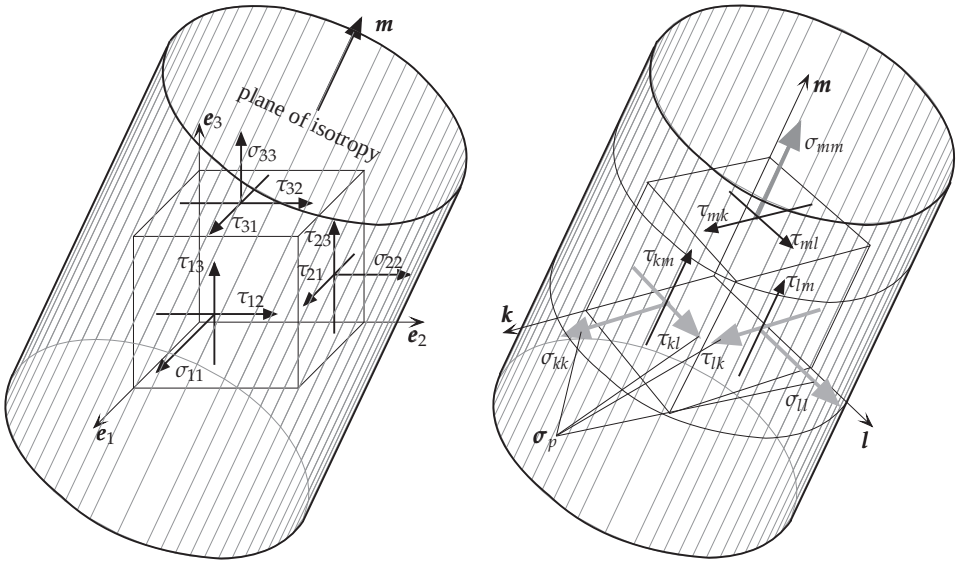

Figure 2.1 Stress state in a transversely isotropic medium and corresponding projections σ_{mm}, $\boldsymbol{\sigma}_p$ and $\boldsymbol{\tau}_m$

$$\begin{aligned}
&\sigma_{mm} = \boldsymbol{m}\cdot\boldsymbol{\sigma}\cdot\boldsymbol{m},\\
&\boldsymbol{\sigma}_p = (\boldsymbol{I}-\boldsymbol{m}\otimes\boldsymbol{m})\cdot\boldsymbol{\sigma}\cdot(\boldsymbol{I}-\boldsymbol{m}\otimes\boldsymbol{m}),\\
&\boldsymbol{\tau}_m = \boldsymbol{m}\cdot\boldsymbol{\sigma}\cdot(\boldsymbol{I}-\boldsymbol{m}\otimes\boldsymbol{m})
\end{aligned} \tag{2.2.35}$$

The meaning of the decomposition (2.2.34) is obvious. σ_{mm} is the normal stress acting in the plane with the unit normal $\boldsymbol{m}$, $\boldsymbol{\sigma}_p$ stands for the "plane" part of the stress tensor representing the stress state in the isotropy plane. $\boldsymbol{\tau}_m$ is the shear stress vector in the plane with the unit normal $\boldsymbol{m}$. For the orthonormal basis $\boldsymbol{k}$, $\boldsymbol{l}$ and $\boldsymbol{m}$ the projections are (see Fig. 2.1)

$$\begin{aligned}
&\boldsymbol{\tau}_m = \tau_{mk}\boldsymbol{k} + \tau_{ml}\boldsymbol{l},\\
&\boldsymbol{\sigma}_p = \sigma_{kk}\boldsymbol{k}\otimes\boldsymbol{k} + \sigma_{ll}\boldsymbol{l}\otimes\boldsymbol{l} + \tau_{kl}(\boldsymbol{k}\otimes\boldsymbol{l} + \boldsymbol{l}\otimes\boldsymbol{k})
\end{aligned}$$

The plane part of the stress tensor can be further decomposed as follows

$$\boldsymbol{\sigma}_p = \boldsymbol{s}_p + \frac{1}{2}\operatorname{tr}\boldsymbol{\sigma}_p(\boldsymbol{I}-\boldsymbol{m}\otimes\boldsymbol{m}), \quad \operatorname{tr}\boldsymbol{s}_p = 0 \tag{2.2.36}$$

Now we can introduce the following set of transversely isotropic invariants

$$
\begin{aligned}
I_{1m} &= \sigma_{mm} = \boldsymbol{m}\cdot\boldsymbol{\sigma}\cdot\boldsymbol{m},\\
I_{2m} &= \operatorname{tr}\boldsymbol{\sigma}_p = \operatorname{tr}\boldsymbol{\sigma} - \boldsymbol{m}\cdot\boldsymbol{\sigma}\cdot\boldsymbol{m},\\
I_{3m} &= \frac{1}{2}\operatorname{tr}\boldsymbol{s}_p^2 = \frac{1}{2}\operatorname{tr}\boldsymbol{\sigma}_p^2 - \frac{1}{4}(\operatorname{tr}\boldsymbol{\sigma}_p)^2\\
&= \frac{1}{2}\left(\operatorname{tr}\boldsymbol{\sigma}^2 + (\boldsymbol{m}\cdot\boldsymbol{\sigma}\cdot\boldsymbol{m})^2\right) - \boldsymbol{m}\cdot\boldsymbol{\sigma}^2\cdot\boldsymbol{m} - \frac{1}{4}(\operatorname{tr}\boldsymbol{\sigma} - \boldsymbol{m}\cdot\boldsymbol{\sigma}\cdot\boldsymbol{m})^2,\\
I_{4m} &= \boldsymbol{\tau}_m\cdot\boldsymbol{\tau}_m = \boldsymbol{m}\cdot\boldsymbol{\sigma}^2\cdot\boldsymbol{m} - (\boldsymbol{m}\cdot\boldsymbol{\sigma}\cdot\boldsymbol{m})^2 = (\boldsymbol{m}\times\boldsymbol{\sigma}\cdot\boldsymbol{m})\cdot(\boldsymbol{m}\times\boldsymbol{\sigma}\cdot\boldsymbol{m})
\end{aligned}
\tag{2.2.37}
$$

In the above list I_{2m} and I_{3m} are two invariants of $\boldsymbol{\sigma}_p$ and $I_{4m} = \boldsymbol{\tau}_m^2 = \boldsymbol{\tau}_m\cdot\boldsymbol{\tau}_m$ is the square of the length of the shear stress vector acting in the plane with the unit normal $\boldsymbol{m}$. It is shown in Sect. A.3.2 that the above invariants are integrals of (2.2.31).

Taking into account the relations

$$
\frac{\partial I_{1m}}{\partial\boldsymbol{\sigma}} = \boldsymbol{m}\otimes\boldsymbol{m}, \quad \frac{\partial I_{2m}}{\partial\boldsymbol{\sigma}} = \boldsymbol{I} - \boldsymbol{m}\otimes\boldsymbol{m},
$$
$$
\frac{\partial I_{3m}}{\partial\boldsymbol{\sigma}} = \boldsymbol{s}_p, \quad \frac{\partial I_{4m}}{\partial\boldsymbol{\sigma}} = \boldsymbol{\tau}_{\boldsymbol{m}}\otimes\boldsymbol{m} + \boldsymbol{m}\otimes\boldsymbol{\tau}_{\boldsymbol{m}}
$$

and the flow rule (2.1.6) we obtain the following creep equation

$$
\begin{aligned}
\dot{\boldsymbol{\varepsilon}}^{cr} &= \frac{\partial W}{\partial I_{1m}}\boldsymbol{m}\otimes\boldsymbol{m} + \frac{\partial W}{\partial I_{2m}}(\boldsymbol{I} - \boldsymbol{m}\otimes\boldsymbol{m}) + \frac{\partial W}{\partial I_{3m}}\boldsymbol{s}_p\\
&+ \frac{\partial W}{\partial I_{4m}}(\boldsymbol{\tau}_{\boldsymbol{m}}\otimes\boldsymbol{m} + \boldsymbol{m}\otimes\boldsymbol{\tau}_{\boldsymbol{m}})
\end{aligned}
\tag{2.2.38}
$$

The next assumption of the classical theory is the zero volumetric creep rate. Taking the trace of (2.2.38) we obtain

$$
\operatorname{tr}\dot{\boldsymbol{\varepsilon}}^{cr} = \frac{\partial W}{\partial I_{1m}} + 2\frac{\partial W}{\partial I_{2m}} = 0 \quad \Rightarrow \quad W = W(I_{1m} - \frac{1}{2}I_{2m}, I_{3m}, I_{4m}) \tag{2.2.39}
$$

Introducing the notation

$$
J_m \equiv I_{1m} - \frac{1}{2}I_{2m} = \boldsymbol{m}\cdot\boldsymbol{\sigma}\cdot\boldsymbol{m} - \frac{1}{2}\operatorname{tr}\boldsymbol{\sigma}_p
$$

the creep equation (2.2.38) takes the form

$$
\dot{\boldsymbol{\varepsilon}}^{cr} = \frac{1}{2}\frac{\partial W}{\partial J_m}(3\boldsymbol{m}\otimes\boldsymbol{m} - \boldsymbol{I}) + \frac{\partial W}{\partial I_{3m}}\boldsymbol{s}_p + \frac{\partial W}{\partial I_{4m}}(\boldsymbol{\tau}_{\boldsymbol{m}}\otimes\boldsymbol{m} + \boldsymbol{m}\otimes\boldsymbol{\tau}_{\boldsymbol{m}}) \tag{2.2.40}
$$

By analogy to the isotropic case we formulate the equivalent stress as follows

$$
\begin{aligned}
\sigma_{eq}^2 &= \alpha_1 J_m^2 + 3\alpha_2 I_{3m} + 3\alpha_3 I_{4m}\\
&= \alpha_1\left(\boldsymbol{m}\cdot\boldsymbol{\sigma}\cdot\boldsymbol{m} - \frac{1}{2}\operatorname{tr}\boldsymbol{\sigma}_p\right)^2 + \frac{3}{2}\alpha_2\operatorname{tr}\boldsymbol{s}_p^2 + 3\alpha_3\tau_{\boldsymbol{m}}^2
\end{aligned}
\tag{2.2.41}
$$

The positive definiteness of the quadratic form (2.2.41) is provided by the conditions $\alpha_i > 0$, $i = 1,2,3$. The deviatoric part $\boldsymbol{s}$ of the stress tensor and its second invariant can be computed by

$$\begin{aligned} \boldsymbol{s} &= J_m \left(\boldsymbol{m} \otimes \boldsymbol{m} - \frac{1}{3}\boldsymbol{I} \right) + \boldsymbol{s}_p + \boldsymbol{\tau}_m \otimes \boldsymbol{m} + \boldsymbol{m} \otimes \boldsymbol{\tau}_m, \\ \operatorname{tr} \boldsymbol{s}^2 &= \frac{2}{3} J_m^2 + \operatorname{tr} \boldsymbol{s}_p^2 + 2\tau_{\boldsymbol{m}}^2 \end{aligned}$$

Consequently, the von Mises equivalent stress (2.2.5) follows from (2.2.41) by setting $\alpha_1 = \alpha_2 = \alpha_3 = 1$.

The advantage of the introduced invariants over (2.2.32) or (2.2.33) is that they can be specified independently from each other. For example, set the second invariant in (2.2.32) to zero, i.e. $\operatorname{tr} \boldsymbol{\sigma}^2 = \boldsymbol{\sigma} \cdot\cdot \boldsymbol{\sigma} = 0$. From this follows that $\boldsymbol{\sigma} = \boldsymbol{0}$ and consequently all other invariants listed in (2.2.32) are simultaneously equal to zero. In addition, the introduced invariants can be related to typical stress states which should be realized in creep tests for the identification of constitutive functions and material constants. With the equivalent stress (2.2.41) the creep equation (2.2.40) can be rewritten as follows

$$\dot{\boldsymbol{\varepsilon}}^{cr} = \frac{3}{2\sigma_{eq}} \frac{\partial W}{\partial \sigma_{eq}} \left[\alpha_1 J_m \left(\boldsymbol{m} \otimes \boldsymbol{m} - \frac{1}{3}\boldsymbol{I} \right) + \alpha_2 \boldsymbol{s}_p + \alpha_3 (\boldsymbol{\tau}_m \otimes \boldsymbol{m} + \boldsymbol{m} \otimes \boldsymbol{\tau}_m) \right] \tag{2.2.42}$$

With the notation $\dot{\varepsilon}_{eq}^{cr} \equiv \frac{\partial W}{\partial \sigma_{eq}}$ (2.2.42) takes the form

$$\dot{\boldsymbol{\varepsilon}}^{cr} = \frac{3}{2} \frac{\dot{\varepsilon}_{eq}^{cr}}{\sigma_{eq}} \left[\alpha_1 J_m \left(\boldsymbol{m} \otimes \boldsymbol{m} - \frac{1}{3}\boldsymbol{I} \right) + \alpha_2 \boldsymbol{s}_p + \alpha_3 (\boldsymbol{\tau}_m \otimes \boldsymbol{m} + \boldsymbol{m} \otimes \boldsymbol{\tau}_m) \right] \tag{2.2.43}$$

Let us introduce the following parts of the creep rate tensor

$$\begin{aligned} \dot{\varepsilon}_{mm}^{cr} &\equiv \boldsymbol{m} \cdot \dot{\boldsymbol{\varepsilon}}^{cr} \cdot \boldsymbol{m}, \\ \dot{\boldsymbol{\varepsilon}}_p^{cr} &\equiv (\boldsymbol{I} - \boldsymbol{m} \otimes \boldsymbol{m}) \cdot \dot{\boldsymbol{\varepsilon}}^{cr} \cdot (\boldsymbol{I} - \boldsymbol{m} \otimes \boldsymbol{m}), \\ \dot{\boldsymbol{\epsilon}}_p^{cr} &\equiv \dot{\boldsymbol{\varepsilon}}_p^{cr} - \frac{1}{2} \dot{\varepsilon}_{mm}^{cr} (\boldsymbol{I} - \boldsymbol{m} \otimes \boldsymbol{m}), \\ \dot{\boldsymbol{\gamma}}_m^{cr} &\equiv \boldsymbol{m} \cdot \dot{\boldsymbol{\varepsilon}}^{cr} \cdot (\boldsymbol{I} - \boldsymbol{m} \otimes \boldsymbol{m}) \end{aligned} \tag{2.2.44}$$

From (2.2.42) we obtain

$$\dot{\varepsilon}_{mm}^{cr} = \alpha_1 \frac{\dot{\varepsilon}_{eq}^{cr}}{\sigma_{eq}} J_m, \qquad \dot{\boldsymbol{\epsilon}}_p^{cr} = \frac{3}{2} \alpha_2 \frac{\dot{\varepsilon}_{eq}^{cr}}{\sigma_{eq}} \boldsymbol{s}_p, \qquad \dot{\boldsymbol{\gamma}}_m^{cr} = \frac{3}{2} \alpha_3 \frac{\dot{\varepsilon}_{eq}^{cr}}{\sigma_{eq}} \boldsymbol{\tau}_m \tag{2.2.45}$$

Similarly to the isotropic case the equivalent creep rate can be calculated as follows

$$\dot{\varepsilon}_{eq}^{cr} = \sqrt{\frac{1}{\alpha_1} (\dot{\varepsilon}_{mm}^{cr})^2 + \frac{2}{3} \frac{1}{\alpha_2} \dot{\boldsymbol{\epsilon}}_p^{cr} \cdot\cdot \dot{\boldsymbol{\epsilon}}_p^{cr} + \frac{4}{3} \frac{1}{\alpha_3} \dot{\boldsymbol{\gamma}}_m^{cr} \cdot \dot{\boldsymbol{\gamma}}_m^{cr}} \tag{2.2.46}$$

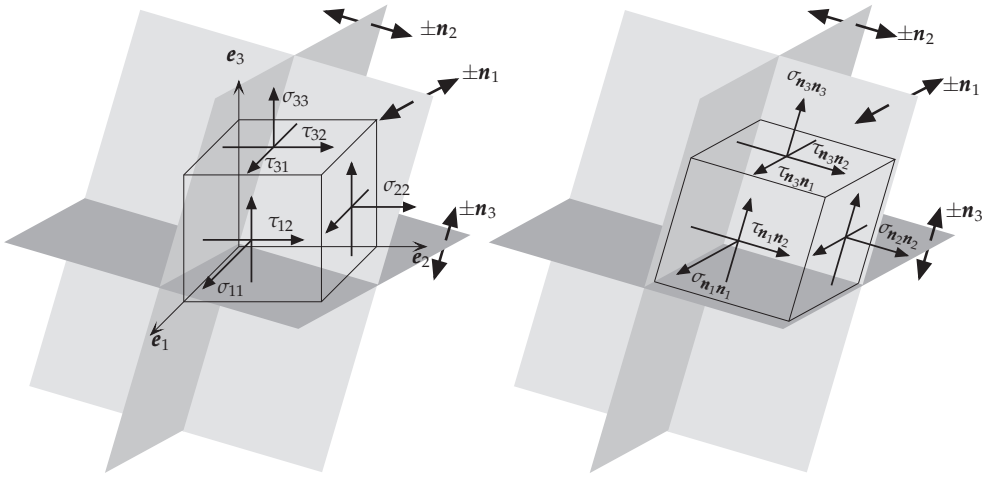

Figure 2.2 Stress state in an orthotropic medium and corresponding projections $\sigma_{\boldsymbol{n}_i\boldsymbol{n}_i}$, $\tau_{\boldsymbol{n}_i\boldsymbol{n}_j}$

The equivalent creep rate (2.2.46) is useful for the verification of the creep potential hypothesis and the assumed quadratic form of the equivalent stress with respect to the transversely isotropic invariants of the stress tensor. The introduced creep equation contains three material constants α_i and the equivalent creep rate $\dot{\varepsilon}^{cr}_{eq}$.

The assumptions of transverse isotropy and the quadratic form of the equivalent stress are widely used in models of elasticity, plasticity, creep and failure of fiber reinforced composites, e.g. [7, 74, 273, 274, 279, 298], and directionally solidified superalloys [42, 213]. The proposed equations will be applied in Sect. 3.2 to the description of anisotropic creep in a multi-pass weld metal.

Orthotropic Symmetry. In this case the potential $W(\boldsymbol{\sigma})$ must satisfy the following restriction

$$W(\boldsymbol{Q}_i \cdot \boldsymbol{\sigma} \cdot \boldsymbol{Q}_i^T) = W(\boldsymbol{\sigma}), \quad \boldsymbol{Q}_i = \boldsymbol{I} - \boldsymbol{n}_i \otimes \boldsymbol{n}_i, \quad i = 1,2,3 \tag{2.2.47}$$

In (2.2.47) $\boldsymbol{Q}_i$ denote the assumed symmetry elements - three reflections with respect to the planes with unit normals $\pm\boldsymbol{n}_i$, Fig. 2.2. The unit vectors $\pm\boldsymbol{n}_1, \pm\boldsymbol{n}_2, \pm\boldsymbol{n}_3$ are assumed to be orthogonal, i.e. $\boldsymbol{n}_i \cdot \boldsymbol{n}_j = 0$, $i \neq j$. In Sect. A.3.3 a set of scalar arguments which satisfy the above restrictions is presented by (A.3.32). As in the previous paragraph we assume the quadratic form of the potential with respect to the stress tensor. One can use different sets of scalar arguments of the stress tensor satisfying (2.2.47), see for example [73],

$$\begin{aligned} &\boldsymbol{n}_1 \cdot \boldsymbol{\sigma} \cdot \boldsymbol{n}_1, \quad \boldsymbol{n}_2 \cdot \boldsymbol{\sigma} \cdot \boldsymbol{n}_2, \quad \boldsymbol{n}_3 \cdot \boldsymbol{\sigma} \cdot \boldsymbol{n}_3, \\ &\boldsymbol{n}_1 \cdot \boldsymbol{\sigma}^2 \cdot \boldsymbol{n}_1, \quad \boldsymbol{n}_2 \cdot \boldsymbol{\sigma}^2 \cdot \boldsymbol{n}_2, \quad \boldsymbol{n}_3 \cdot \boldsymbol{\sigma}^2 \cdot \boldsymbol{n}_3 \end{aligned}$$

Figure 2.2 shows the components of the stress tensor in a Cartesian frame $\boldsymbol{e}_i$, three planes of symmetry characterized by the unit vectors $\pm\boldsymbol{n}_i$ and components of the stress tensor with respect to the planes of symmetry. The stress tensor can be represented as follows

$$\begin{aligned}\boldsymbol{\sigma} &= \sigma_{\boldsymbol{n}_1\boldsymbol{n}_1}\boldsymbol{n}_1\otimes\boldsymbol{n}_1+\sigma_{\boldsymbol{n}_2\boldsymbol{n}_2}\boldsymbol{n}_2\otimes\boldsymbol{n}_2+\sigma_{\boldsymbol{n}_3\boldsymbol{n}_3}\boldsymbol{n}_3\otimes\boldsymbol{n}_3\\ &+ \tau_{\boldsymbol{n}_1\boldsymbol{n}_2}(\boldsymbol{n}_1\otimes\boldsymbol{n}_2+\boldsymbol{n}_2\otimes\boldsymbol{n}_1)+\tau_{\boldsymbol{n}_1\boldsymbol{n}_3}(\boldsymbol{n}_1\otimes\boldsymbol{n}_3+\boldsymbol{n}_3\otimes\boldsymbol{n}_1)\\ &+ \tau_{\boldsymbol{n}_2\boldsymbol{n}_3}(\boldsymbol{n}_2\otimes\boldsymbol{n}_3+\boldsymbol{n}_3\otimes\boldsymbol{n}_2)\end{aligned}$$

with

$$\begin{aligned}&\sigma_{\boldsymbol{n}_1\boldsymbol{n}_1}=\boldsymbol{n}_1\cdot\boldsymbol{\sigma}\cdot\boldsymbol{n}_1,\quad \sigma_{\boldsymbol{n}_2\boldsymbol{n}_2}=\boldsymbol{n}_2\cdot\boldsymbol{\sigma}\cdot\boldsymbol{n}_2,\quad \sigma_{\boldsymbol{n}_3\boldsymbol{n}_3}=\boldsymbol{n}_3\cdot\boldsymbol{\sigma}\cdot\boldsymbol{n}_3,\\ &\tau_{\boldsymbol{n}_1\boldsymbol{n}_2}=\boldsymbol{n}_1\cdot\boldsymbol{\sigma}\cdot\boldsymbol{n}_2,\quad \tau_{\boldsymbol{n}_1\boldsymbol{n}_3}=\boldsymbol{n}_1\cdot\boldsymbol{\sigma}\cdot\boldsymbol{n}_3,\quad \tau_{\boldsymbol{n}_2\boldsymbol{n}_3}=\boldsymbol{n}_2\cdot\boldsymbol{\sigma}\cdot\boldsymbol{n}_3\end{aligned}$$

According to Sect. A.3.3 we use the following orthotropic invariants of the stress tensor

$$\begin{aligned}&I_{\boldsymbol{n}_1\boldsymbol{n}_1}=\sigma_{\boldsymbol{n}_1\boldsymbol{n}_1},\quad I_{\boldsymbol{n}_2\boldsymbol{n}_2}=\sigma_{\boldsymbol{n}_2\boldsymbol{n}_2},\quad I_{\boldsymbol{n}_3\boldsymbol{n}_3}=\sigma_{\boldsymbol{n}_3\boldsymbol{n}_3},\\ &I_{\boldsymbol{n}_1\boldsymbol{n}_2}=\tau^2_{\boldsymbol{n}_1\boldsymbol{n}_2},\quad I_{\boldsymbol{n}_1\boldsymbol{n}_3}=\tau^2_{\boldsymbol{n}_1\boldsymbol{n}_3},\quad I_{\boldsymbol{n}_2\boldsymbol{n}_3}=\tau^2_{\boldsymbol{n}_2\boldsymbol{n}_3}\end{aligned}\tag{2.2.48}$$

Assuming that the creep potential is a function of six arguments introduced, the flow rule (2.1.6) leads to the following creep equation

$$\begin{aligned}\dot{\boldsymbol{\varepsilon}}^{cr} &= \frac{\partial W}{\partial I_{\boldsymbol{n}_1\boldsymbol{n}_1}}\boldsymbol{n}_1\otimes\boldsymbol{n}_1+\frac{\partial W}{\partial I_{\boldsymbol{n}_2\boldsymbol{n}_2}}\boldsymbol{n}_2\otimes\boldsymbol{n}_2+\frac{\partial W}{\partial I_{\boldsymbol{n}_3\boldsymbol{n}_3}}\boldsymbol{n}_3\otimes\boldsymbol{n}_3\\ &+ \frac{\partial W}{\partial I_{\boldsymbol{n}_1\boldsymbol{n}_2}}\boldsymbol{n}_1\cdot\boldsymbol{\sigma}\cdot\boldsymbol{n}_2(\boldsymbol{n}_1\otimes\boldsymbol{n}_2+\boldsymbol{n}_2\otimes\boldsymbol{n}_1)\\ &+ \frac{\partial W}{\partial I_{\boldsymbol{n}_1\boldsymbol{n}_3}}\boldsymbol{n}_1\cdot\boldsymbol{\sigma}\cdot\boldsymbol{n}_3(\boldsymbol{n}_1\otimes\boldsymbol{n}_3+\boldsymbol{n}_3\otimes\boldsymbol{n}_1)\\ &+ \frac{\partial W}{\partial I_{\boldsymbol{n}_2\boldsymbol{n}_3}}\boldsymbol{n}_2\cdot\boldsymbol{\sigma}\cdot\boldsymbol{n}_3(\boldsymbol{n}_2\otimes\boldsymbol{n}_3+\boldsymbol{n}_3\otimes\boldsymbol{n}_2)\end{aligned}\tag{2.2.49}$$

The assumption of zero volumetric creep rate leads to

$$\operatorname{tr}\dot{\boldsymbol{\varepsilon}}^{cr}=\frac{\partial W}{\partial I_{\boldsymbol{n}_1\boldsymbol{n}_1}}+\frac{\partial W}{\partial I_{\boldsymbol{n}_2\boldsymbol{n}_2}}+\frac{\partial W}{\partial I_{\boldsymbol{n}_3\boldsymbol{n}_3}}=0\tag{2.2.50}$$

From the partial differential equation (2.2.50) follows that the potential W is a function of five scalar arguments of the stress tensor. The characteristic system of (2.2.50) is

$$\frac{dI_{\boldsymbol{n}_1\boldsymbol{n}_1}}{ds}=1,\quad \frac{dI_{\boldsymbol{n}_2\boldsymbol{n}_2}}{ds}=1,\quad \frac{dI_{\boldsymbol{n}_3\boldsymbol{n}_3}}{ds}=1\tag{2.2.51}$$

The above system of three ordinary differential equations has two independent integrals. One can verify that the following invariants

$$J_1=\frac{1}{2}(I_{\boldsymbol{n}_2\boldsymbol{n}_2}-I_{\boldsymbol{n}_3\boldsymbol{n}_3}),\quad J_2=\frac{1}{2}(I_{\boldsymbol{n}_3\boldsymbol{n}_3}-I_{\boldsymbol{n}_1\boldsymbol{n}_1}),\quad J_3=\frac{1}{2}(I_{\boldsymbol{n}_1\boldsymbol{n}_1}-I_{\boldsymbol{n}_2\boldsymbol{n}_2})\tag{2.2.52}$$

are integrals of (2.2.51). Only two of them are independent due to the relation $J_1+J_2+J_3=0$. If the principal directions of the stress tensor coincide with the directions $\boldsymbol{n}_i$ then $\tau_{\boldsymbol{n}_i\boldsymbol{n}_j}=0, i\neq j$ and the above invariants represent the principal shear stresses. An alternative set of integrals of (2.2.51) is

$$\tilde{J}_1 = I_{\boldsymbol{n}_1\boldsymbol{n}_1} - \frac{1}{3}\mathrm{tr}\,\boldsymbol{\sigma}, \quad \tilde{J}_2 = I_{\boldsymbol{n}_2\boldsymbol{n}_2} - \frac{1}{3}\mathrm{tr}\,\boldsymbol{\sigma}, \quad \tilde{J}_3 = I_{\boldsymbol{n}_3\boldsymbol{n}_3} - \frac{1}{3}\mathrm{tr}\,\boldsymbol{\sigma} \tag{2.2.53}$$

If the principal directions of the stress tensor coincide with $\boldsymbol{n}_i$ then the above invariants are the principal values of the stress deviator. For the formulation of the creep potential in terms of invariants the relation $\tilde{J}_1 + \tilde{J}_2 + \tilde{J}_3 = 0$ must be taken into account.

In what follows we apply the invariants (2.2.52). The equivalent stress can be formulated as follows

$$\begin{aligned} \sigma_{eq}^2 &= 2\beta_1 J_1^2 + 2\beta_2 J_2^2 + 2\beta_3 J_3^2 \\ &+ 3\beta_{12} I_{\boldsymbol{n}_1\boldsymbol{n}_2} + 3\beta_{13} I_{\boldsymbol{n}_1\boldsymbol{n}_3} + 3\beta_{23} I_{\boldsymbol{n}_2\boldsymbol{n}_3} \end{aligned} \tag{2.2.54}$$

The von Mises equivalent stress (2.2.5) follows from (2.2.54) by setting $\beta_1 = \beta_2 = \beta_3 = \beta_{12} = \beta_{13} = \beta_{23} = 1$. Applying the flow rule (2.1.6) we obtain the following creep equation

$$\begin{aligned} \dot{\boldsymbol{\varepsilon}}^{cr} = \frac{\dot{\varepsilon}_{eq}^{cr}}{\sigma_{eq}} & \Big[\beta_1 J_1(\boldsymbol{n}_2 \otimes \boldsymbol{n}_2 - \boldsymbol{n}_3 \otimes \boldsymbol{n}_3) \\ & + \beta_2 J_2(\boldsymbol{n}_3 \otimes \boldsymbol{n}_3 - \boldsymbol{n}_1 \otimes \boldsymbol{n}_1) \\ & + \beta_3 J_3(\boldsymbol{n}_1 \otimes \boldsymbol{n}_1 - \boldsymbol{n}_2 \otimes \boldsymbol{n}_2) \\ & + \frac{3}{2}\beta_{12}\tau_{\boldsymbol{n}_1\boldsymbol{n}_2}(\boldsymbol{n}_1 \otimes \boldsymbol{n}_2 + \boldsymbol{n}_2 \otimes \boldsymbol{n}_1) \\ & + \frac{3}{2}\beta_{13}\tau_{\boldsymbol{n}_1\boldsymbol{n}_3}(\boldsymbol{n}_1 \otimes \boldsymbol{n}_3 + \boldsymbol{n}_3 \otimes \boldsymbol{n}_1) \\ & + \frac{3}{2}\beta_{23}\tau_{\boldsymbol{n}_2\boldsymbol{n}_3}(\boldsymbol{n}_2 \otimes \boldsymbol{n}_3 + \boldsymbol{n}_3 \otimes \boldsymbol{n}_2)\Big] \end{aligned} \tag{2.2.55}$$

The equivalent stress and the creep equation includes six independent material constants. Therefore six independent homogeneous stress states should be realized in order to identify the whole set of constants. In addition, the dependence of the creep rate on the equivalent stress must be fitted from the results of uni-axial creep tests for different constant stress values. For example, if the power law stress function provides a satisfactory description of steady-state creep then the constant n must be additionally identified.

An example of orthotropic creep is discussed in [163] for the aluminium alloy D16AT. Plane specimens were removed from rolled sheet along three directions: the rolling direction, the transverse direction as well as under the angle of 45° to the rolling direction. Uni-axial creep tests were performed at 273°C and 300°C within the stress range 63-90 MPa. The results have shown that at 273°C creep curves depend on the loading direction while at 300°C the creep behavior is isotropic.

Other cases. The previous models are based on the assumption of the quadratic form of the creep potential with respect to the stress tensor. The most general quadratic form can be formulated as follows

$$\sigma_{eq}^2 = \frac{1}{2}\boldsymbol{\sigma} \cdot\cdot\, {}^{(4)}\boldsymbol{B} \cdot\cdot\, \boldsymbol{\sigma}, \tag{2.2.56}$$

where σ_{eq} plays the role of the equivalent stress. The fourth rank tensor ${}^{(4)}\boldsymbol{B}$ must satisfy the following restrictions

$$\begin{aligned} &\boldsymbol{a} \cdot\cdot\, {}^{(4)}\boldsymbol{B} \cdot\cdot\, \boldsymbol{a} \geq 0, \quad \boldsymbol{a} \cdot\cdot\, {}^{(4)}\boldsymbol{B} = {}^{(4)}\boldsymbol{B} \cdot\cdot\, \boldsymbol{a}, \quad \boldsymbol{c} \cdot\cdot\, {}^{(4)}\boldsymbol{B} = \boldsymbol{0}, \\ &\forall \boldsymbol{a}, \boldsymbol{c} \text{ with } \boldsymbol{a} = \boldsymbol{a}^T,\ \boldsymbol{c} = -\boldsymbol{c}^T, \end{aligned} \tag{2.2.57}$$

where $\boldsymbol{a}$ and $\boldsymbol{c}$ are second rank tensors. Additional restrictions follow from the assumed symmetries of the steady state creep behavior. For example, if the orthogonal tensor $\boldsymbol{Q}$ stands for a symmetry element, the structure of the tensor ${}^{(4)}\boldsymbol{B}$ can be established from the following equation

$${}^{(4)}\boldsymbol{B}' = B^{ijkl}\boldsymbol{Q}\cdot\boldsymbol{e}_i \otimes \boldsymbol{Q}\cdot\boldsymbol{e}_j \otimes \boldsymbol{Q}\cdot\boldsymbol{e}_k \otimes \boldsymbol{Q}\cdot\boldsymbol{e}_l = {}^{(4)}\boldsymbol{B}, \tag{2.2.58}$$

where $\boldsymbol{e}_i$, $i = 1,2,3$ are basis vectors.

The flow rule (2.1.6) provides the following generalized anisotropic creep equation

$$\dot{\boldsymbol{\varepsilon}}^{cr} = \frac{\dot{\varepsilon}^{cr}_{eq}}{2\sigma_{eq}} {}^{(4)}\boldsymbol{B} \cdot\cdot\, \boldsymbol{\sigma}, \quad \dot{\varepsilon}^{cr}_{eq} \equiv \frac{\partial W}{\partial \sigma_{eq}} \tag{2.2.59}$$

The fourth rank tensors satisfying the restrictions (2.2.57) are well-known from the theory of linear elasticity. They are used to represent elastic material properties in the generalized Hooke's law. The components of these tensors in a Cartesian coordinate system are given in the matrix notation in many textbooks on linear elasticity as well as in books and monographs on composite materials, e.g. [6, 7, 29, 122, 256, 309]. Furthermore, different coordinate free representations of fourth rank tensors of this type are discussed in the literature. For a review we refer to [76]. One of these representations - the projector representation is applied in [47, 48, 200] to constitutive modeling of creep in single crystal alloys under assumption of the cubic symmetry.

Let us recall that (2.2.59) is the consequence of the creep potential hypothesis and the quadratic form of the equivalent stress with respect to the stress tensor. Similarly to the case of linear elasticity [309] one can prove that only eight basic symmetry classes are relevant according to these assumptions. The basic symmetry classes and the corresponding number of independent coordinates of the tensor ${}^{(4)}\boldsymbol{B}$ are listed in Table 2.1. The number of independent coordinates indicates the number of material constants which should be identified from creep tests. This number can be reduced if the volume constancy is additionally assumed. For example, in the cases of transverse isotropy and orthotropic symmetry the number of independent coordinates of $\boldsymbol{B}$ reduces to 3 and 5, respectively (see previous paragraphs).

2.2.2.2 Non-classical Creep Equations. Non-classical effects are the dependence of secondary creep rate on the kind of loading and second order effects, see Sect. 2.2.1. Examples of such behavior are different creep rates under tensile and compressive stress or the effect of reversal of the shear stress. The last case is observed in creep tests on tubular specimens under applied torque. The change of the direction of the applied torque leads to different values of the shear

Table 2.1 Basic symmetry classes and number of independent coordinates of the tensor ${}^{(4)}\boldsymbol{B}$

Symmetry class	Number of independent coordinates of ${}^{(4)}\boldsymbol{B}$
triclinic symmetry	21
monoclinic symmetry	13
orthotropic or rhombic symmetry	9
trigonal symmetry	6
tetragonal symmetry	6
transverse isotropy or hexagonal symmetry	5
cubic symmetry	3
isotropic symmetry	2

strain rate. The effect of shear stress reversal is usually explained to be the result of the anisotropy induced by the deformation process (e.g. anisotropic hardening) or anisotropy induced by damage evolution. Phenomenological models of induced anisotropy will be introduced in Sect. 2.3.2 and 2.4. Here we consider the case of initial anisotropy without discussion of histories of the deformation, damage or manufacturing processes. Nevertheless, a phenomenological model of anisotropic creep should be able to reflect the above mentioned effects since they are observed experimentally. In order to describe non-classical effects the quadratic form of the creep potential should be replaced by a more general form including all invariants of the stress tensor for the assumed symmetry group. In this case the number of material constants rapidly increases. Furthermore, the identification and verification of the model requires creep tests under combined multi-axial stress states. In what follows we limit ourselves to some remarks regarding the general structure of constitutive equations and kinds of tests for the identification.

Transverse isotropy. The creep potential must satisfy the restriction (2.2.29) leading to the partial differential equation (2.2.30). The integrals represent the set of functionally independent arguments of the creep potential. The integrals are presented in Sect. A.3.2 for two transverse isotropy groups. The first group is formed by all the rotations about a given axis $\boldsymbol{m}$, i.e

$$\boldsymbol{Q}(\psi\boldsymbol{m}) = \boldsymbol{m}\otimes\boldsymbol{m} + \cos\psi(\boldsymbol{I} - \boldsymbol{m}\otimes\boldsymbol{m}) + \sin\psi\boldsymbol{m}\times\boldsymbol{I}$$

The second group additionally includes rotations on the angle π about any axis orthogonal to $\boldsymbol{m}$, i.e.

$$\boldsymbol{Q}_1 = \boldsymbol{Q}(\pi\boldsymbol{p}) = 2\boldsymbol{p}\otimes\boldsymbol{p} - \boldsymbol{I}, \quad \det\boldsymbol{Q} = 1, \quad \boldsymbol{p}\cdot\boldsymbol{m} = 0$$

Let us note that there is an essential difference in these two groups since the creep potential depends on different non-quadratic arguments of the stress tensor. Here we limit our considerations to the second case which is widely discussed in the literature on anisotropic elasticity, plasticity and creep [58, 73, 84, 279, 286], where

the following invariants are applied [2]

$$\mathrm{tr}\,\boldsymbol{\sigma}, \quad \mathrm{tr}\,\boldsymbol{\sigma}^2, \quad \mathrm{tr}\,\boldsymbol{\sigma}^3, \quad \boldsymbol{m}\cdot\boldsymbol{\sigma}\cdot\boldsymbol{m}, \quad \boldsymbol{m}\cdot\boldsymbol{\sigma}^2\cdot\boldsymbol{m} \tag{2.2.60}$$

To be consistent with derivations in Sect. 2.2.2.1 let us use the decomposition of the stress tensor (2.2.34) leading to the following set of invariants

$$\begin{aligned}
I_{1m} &= \sigma_{mm} = \boldsymbol{m}\cdot\boldsymbol{\sigma}\cdot\boldsymbol{m},\\
I_{2m} &= \mathrm{tr}\,\boldsymbol{\sigma}_p = \mathrm{tr}\,\boldsymbol{\sigma} - \boldsymbol{m}\cdot\boldsymbol{\sigma}\cdot\boldsymbol{m},\\
I_{3m} &= \frac{1}{2}\mathrm{tr}\,\boldsymbol{s}_p^2 = \frac{1}{2}\mathrm{tr}\,\boldsymbol{\sigma}_p^2 - \frac{1}{4}(\mathrm{tr}\,\boldsymbol{\sigma}_p)^2\\
&= \frac{1}{2}\left[\mathrm{tr}\,\boldsymbol{\sigma}^2 + (\boldsymbol{m}\cdot\boldsymbol{\sigma}\cdot\boldsymbol{m})^2\right] - \boldsymbol{m}\cdot\boldsymbol{\sigma}^2\cdot\boldsymbol{m} - \frac{1}{4}(\mathrm{tr}\,\boldsymbol{\sigma} - \boldsymbol{m}\cdot\boldsymbol{\sigma}\cdot\boldsymbol{m})^2,\\
I_{4m} &= \boldsymbol{\tau}_m\cdot\boldsymbol{\tau}_m = \boldsymbol{m}\cdot\boldsymbol{\sigma}^2\cdot\boldsymbol{m} - (\boldsymbol{m}\cdot\boldsymbol{\sigma}\cdot\boldsymbol{m})^2 = (\boldsymbol{m}\times\boldsymbol{\sigma}\cdot\boldsymbol{m})\cdot(\boldsymbol{m}\times\boldsymbol{\sigma}\cdot\boldsymbol{m})\\
I_{5m} &= \boldsymbol{\tau}_m\cdot\boldsymbol{s}_p\cdot\boldsymbol{\tau}_m = \boldsymbol{m}\cdot\boldsymbol{\sigma}^3\cdot\boldsymbol{m} - 2(\boldsymbol{m}\cdot\boldsymbol{\sigma}\cdot\boldsymbol{m})(\boldsymbol{m}\cdot\boldsymbol{\sigma}^2\cdot\boldsymbol{m})\\
&+ (\boldsymbol{m}\cdot\boldsymbol{\sigma}\cdot\boldsymbol{m})^3 - \frac{1}{2}(\mathrm{tr}\,\boldsymbol{\sigma} - \boldsymbol{m}\cdot\boldsymbol{\sigma}\cdot\boldsymbol{m})\left[\boldsymbol{m}\cdot\boldsymbol{\sigma}^2\cdot\boldsymbol{m} - (\boldsymbol{m}\cdot\boldsymbol{\sigma}\cdot\boldsymbol{m})^2\right]
\end{aligned} \tag{2.2.61}$$

The meaning of the first four invariants is explained in in Sect. 2.2.2.1. The last cubic invariant is introduced instead $\mathrm{tr}\,\boldsymbol{\sigma}^3$. One can prove the following relation

$$\mathrm{tr}\,\boldsymbol{\sigma}^3 = I_{1m}^3 + 3I_{1m}I_{4m} + 3I_{2m}I_{3m} + \frac{3}{2}I_{2m}I_{4m} + \frac{1}{2}I_{2m}^3 + 3I_{5m}$$

Assuming that the creep potential W is a function of five scalar arguments (2.2.61) and applying the flow rule (2.1.6) we obtain the following creep equation

$$\begin{aligned}
\dot{\boldsymbol{\varepsilon}}^{cr} &= h_1\boldsymbol{m}\otimes\boldsymbol{m} + (h_2 - \frac{1}{2}h_5 I_{4m})(\boldsymbol{I} - \boldsymbol{m}\otimes\boldsymbol{m}) + h_3\boldsymbol{\sigma}_p + h_4(\boldsymbol{\tau}_m\otimes\boldsymbol{m} + \boldsymbol{m}\otimes\boldsymbol{\tau}_m)\\
&+ h_5\left(\boldsymbol{\tau}_m\otimes\boldsymbol{\tau}_m + \boldsymbol{m}\otimes\boldsymbol{\sigma}_p\cdot\boldsymbol{\tau}_m + \boldsymbol{\tau}_m\cdot\boldsymbol{\sigma}_p\otimes\boldsymbol{m}\right),
\end{aligned} \tag{2.2.62}$$

where

$$h_i = \frac{\partial W}{\partial I_{im}}, \quad i = 1,2,\ldots,5$$

The last term in the right-hand side of (2.2.62) describes second order effects. The meaning of these effects is obvious. In the case of non-zero "transverse shear stress" vector

$$\boldsymbol{\tau}_m = \boldsymbol{m}\cdot\boldsymbol{\sigma}\cdot(\boldsymbol{I} - \boldsymbol{m}\otimes\boldsymbol{m})$$

the elongation in the direction of $\boldsymbol{\tau}_m$ can be considered. The vector $\boldsymbol{\varsigma}_m = \boldsymbol{s}_p\cdot\boldsymbol{\tau}_m$ belongs to the isotropy plane, i.e. $\boldsymbol{\varsigma}_m\cdot\boldsymbol{m} = 0$. In the case that $\boldsymbol{\varsigma}_m \neq \boldsymbol{0}$ (2.2.62) describes an additional "transverse shear strain rate" effect.

[2] For the description of elastic material behavior instead of $\boldsymbol{\sigma}$ a strain tensor, e.g. the Cauchy-Green strain tensor is introduced. The five transversely isotropic invariants are the arguments of the strain energy density function.

In order to formulate the creep constitutive equation one should specify an expression for the equivalent stress as a function of the introduced invariants. As an example we present the equivalent stress by use of polynomials of the type (2.2.9) and (2.2.10)

$$\sigma_{eq} = \alpha\sigma_1 + \sigma_2 + \gamma\sigma_3, \tag{2.2.63}$$

with

$$\begin{aligned}
\sigma_1 &= \mu_{11} I_{1m} + \mu_{12} I_{2m}, \\
\sigma_2 &= \mu_{21} I_{1m}^2 + \mu_{22} I_{1m} I_{2m} + \mu_{23} I_{2m}^2 + \mu_{24} I_{3m} + \mu_{25} I_{4m}, \\
\sigma_3 &= \mu_{31} I_{1m}^3 + \mu_{32} I_{1m}^2 I_{2m} + \mu_{33} I_{1m} I_{2m}^2 + \mu_{34} I_{2m}^3 + \mu_{35} I_{1m} I_{3m} \\
&+ \mu_{36} I_{2m} I_{3m} + \mu_{37} I_{1m} I_{4m} + \mu_{38} I_{2m} I_{4m} + \mu_{39} I_{5m}
\end{aligned} \tag{2.2.64}$$

The equivalent stress (2.2.63) includes 16 material constants μ_{ij} and two weighting factors α and γ. The identification of all material constants requires different independent creep tests under multi-axial stress states. For example, in order to find the constant μ_{39} creep tests under stress states with nonzero cubic invariant I_{5m} should be carried out. An example is the tension in the isotropy plane combined with the transverse shear stress leading to the stress state of the type $\boldsymbol{\sigma} = \sigma_0 \boldsymbol{n}_1 \otimes \boldsymbol{n}_1 + \tau_0(\boldsymbol{n}_1 \otimes \boldsymbol{m} + \boldsymbol{m} \otimes \boldsymbol{n}_1)$, where $\sigma_0 > 0$ and $\tau_0 > 0$ are the magnitudes of the applied stresses, $\boldsymbol{n}_1$ is the direction of tension and $\boldsymbol{n}_1 \cdot \boldsymbol{m} = 0$. In this case

$$\boldsymbol{s}_p = \frac{1}{2}\sigma_0(\boldsymbol{n}_1 \otimes \boldsymbol{n}_1 - \boldsymbol{n}_2 \otimes \boldsymbol{n}_2), \quad \boldsymbol{n}_1 \cdot \boldsymbol{n}_2 = 0, \qquad \boldsymbol{\tau}_m = \tau_0 \boldsymbol{n}_1, \quad I_{5m} = \frac{1}{2}\sigma_0 \tau_0^2$$

By analogy to the non-classical models of isotropic creep discussed in Sect. 2.2.1 different special cases can be introduced. Setting $\gamma = 0$ in (2.2.64), second order effects will be neglected. The resulting constitutive model takes into account different behavior under tension and compression. To find the constants μ_{11} and μ_{12} creep tests under tension (compression) along the direction $\boldsymbol{m}$ as well as tension (compression) along any direction in the isotropy plane should be carried out. Setting $\alpha = 0$ the model with the quadratic form of the creep potential with 5 constants can be obtained. The assumption of the zero volumetric creep rate will lead to the model discussed in Sect. 2.2.2.1.

Second order effects of anisotropic creep were discussed by Betten [52, 58]. He found disagreements between creep equations based on the theory of isotropic functions and the creep equation of the type (2.2.62) according to the potential hypothesis and the flow rule. The conclusion was made that the potential theory leads to restrictive forms of constitutive equations if compared to the representations of tensor functions.

Let us recall the results following from the algebra of isotropic tensor functions [71]. In the case of transverse isotropy group characterized by the symmetry elements (A.3.18) the statement of the problem is to find the general representation of the isotropic tensor function of the stress tensor $\boldsymbol{\sigma}$ and the dyad $\boldsymbol{m} \otimes \boldsymbol{m}$ (so-called

structure tensor). The constitutive equation describing the creep behavior must be found as follows

$$\dot{\boldsymbol{\varepsilon}}^{cr} = \boldsymbol{f}(\boldsymbol{\sigma}, \boldsymbol{m} \otimes \boldsymbol{m}),$$

where $\boldsymbol{f}$ is an isotropic tensor function of two tensor arguments. The general representation of this function is [73]

$$\begin{aligned} \boldsymbol{f}(\boldsymbol{\sigma}, \boldsymbol{m} \otimes \boldsymbol{m}) &= f_1 \boldsymbol{m} \otimes \boldsymbol{m} + f_2(\boldsymbol{I} - \boldsymbol{m} \otimes \boldsymbol{m}) + f_3 \boldsymbol{\sigma} + f_4 \boldsymbol{\sigma}^2 \\ &+ f_5(\boldsymbol{m} \otimes \boldsymbol{m} \cdot \boldsymbol{\sigma} + \boldsymbol{\sigma} \cdot \boldsymbol{m} \otimes \boldsymbol{m}) + f_6(\boldsymbol{m} \otimes \boldsymbol{m} \cdot \boldsymbol{\sigma}^2 + \boldsymbol{\sigma}^2 \cdot \boldsymbol{m} \otimes \boldsymbol{m}), \end{aligned} \tag{2.2.65}$$

where the scalars f_i, $i = 1, \ldots, 6$, depend on the five invariants of the stress tensor (2.2.60). Betten found that the last term in (2.2.65) is missing in the constitutive equation which is based on the potential theory. In order to discuss the meaning of the last term in (2.2.65) let us introduce the identities which follow from the decomposition of the stress tensor by Eqs (2.2.34) and (2.2.36)

$$\begin{aligned} \boldsymbol{\sigma}^2 &= I_{2m} \boldsymbol{s}_p + (I_{3m} + \frac{1}{4} I_{2m}^2)(\boldsymbol{I} - \boldsymbol{m} \otimes \boldsymbol{m}) + \boldsymbol{m} \otimes \boldsymbol{s}_p \cdot \boldsymbol{\tau}_m + \boldsymbol{\tau}_m \cdot \boldsymbol{s}_p \otimes \boldsymbol{m} \\ &+ (I_{1m} + \frac{1}{2} I_{2m})(\boldsymbol{\tau}_m \otimes \boldsymbol{m} + \boldsymbol{m} \otimes \boldsymbol{\tau}_m) + (I_{1m}^2 + I_{4m}) \boldsymbol{m} \otimes \boldsymbol{m} + \boldsymbol{\tau}_m \otimes \boldsymbol{\tau}_m, \end{aligned} \tag{2.2.66}$$

$$\boldsymbol{m} \otimes \boldsymbol{m} \cdot \boldsymbol{\sigma} + \boldsymbol{\sigma} \cdot \boldsymbol{m} \otimes \boldsymbol{m} = \boldsymbol{\tau}_m \otimes \boldsymbol{m} + \boldsymbol{m} \otimes \boldsymbol{\tau}_m + 2 I_{1m} \boldsymbol{m} \otimes \boldsymbol{m},$$

$$\begin{aligned} \boldsymbol{m} \otimes \boldsymbol{m} \cdot \boldsymbol{\sigma}^2 + \boldsymbol{\sigma}^2 \cdot \boldsymbol{m} \otimes \boldsymbol{m} &= \boldsymbol{m} \otimes \boldsymbol{s}_p \cdot \boldsymbol{\tau}_m + \boldsymbol{\tau}_m \cdot \boldsymbol{s}_p \otimes \boldsymbol{m} \\ &+ (I_{1m} + \frac{1}{2} I_{2m})(\boldsymbol{\tau}_m \otimes \boldsymbol{m} + \boldsymbol{m} \otimes \boldsymbol{\tau}_m) \\ &+ 2(I_{4m} + I_{1m}^2) \boldsymbol{m} \otimes \boldsymbol{m} \end{aligned}$$

After inserting (2.2.66), (2.2.34) and (2.2.36) into (2.2.65) we obtain the following creep equation

$$\begin{aligned} \dot{\boldsymbol{\varepsilon}}^{cr} &= g_1 \boldsymbol{m} \otimes \boldsymbol{m} + g_2(\boldsymbol{I} - \boldsymbol{m} \otimes \boldsymbol{m}) + g_3 \boldsymbol{s}_p + g_4(\boldsymbol{m} \otimes \boldsymbol{\tau}_m + \boldsymbol{\tau}_m \otimes \boldsymbol{m}) \\ &+ g_5(\boldsymbol{m} \otimes \boldsymbol{s}_p \cdot \boldsymbol{\tau}_m + \boldsymbol{\tau}_m \cdot \boldsymbol{s}_p \otimes \boldsymbol{m}) + g_6 \boldsymbol{\tau}_m \otimes \boldsymbol{\tau}_m \end{aligned} \tag{2.2.67}$$

with

$$\begin{aligned} g_1 &= f_1 + f_4(I_{1m}^2 + I_{4m}) + 2 f_5 I_{1m} + 2 f_6(I_{4m} + I_{1m}^2), \\ g_2 &= f_2 + \frac{1}{2} f_3 I_{2m} + f4(I_{3m} + \frac{1}{4} I_{2m}^2), \\ g_3 &= f_3 + I_{2m} f_4, \\ g_4 &= (f_4 + f_6)(I_{1m} + \frac{1}{2} I_{2m}) + f_5, \\ g_5 &= f_4 + f_6, \\ g_6 &= f_4 \end{aligned}$$

We observe that Eq. (2.2.67) based on the theory of isotropic tensor functions does not deliver any new second order effect in comparison to (2.2.62). The only difference is that the two last terms in (2.2.67) characterizing the second order effects appear with two different influence functions. The comparison of (2.2.67) with (2.2.62) provides the following conditions for the existence of the potential

$$\frac{\partial W}{\partial I_{1m}} = g_1, \quad \frac{\partial W}{\partial I_{2m}} = g_2 + \frac{1}{2} g_5 I_{4m},$$
$$\frac{\partial W}{\partial I_{3m}} = g_3, \quad \frac{\partial W}{\partial I_{4m}} = g_4, \quad \frac{\partial W}{\partial I_{5m}} = g_5, \quad g_6 = g_5$$

Furthermore, the functions g_i must satisfy the integrability conditions which can be obtained by equating the mixed derivatives of the potential with respect to invariants, i.e.

$$\frac{\partial^2 W}{\partial I_{im} \partial I_{km}} = \frac{\partial^2 W}{\partial I_{km} \partial I_{im}}, \quad i \neq k, \quad i,k = 1,2,\ldots,5$$

Let us note that the models (2.2.62) and (2.2.67) are restricted to the special case of transverse isotropy. In the general case one should analyze the creep potential with the invariants listed in (A.3.26).

Other cases. Alternatively a phenomenological constitutive equation of anisotropic creep can be formulated with the help of material tensors, e.g. [2]. Introducing three material tensors $\boldsymbol{A}$, ${}^{(4)}\boldsymbol{B}$ and ${}^{(6)}\boldsymbol{C}$ the equivalent stress (2.2.63) can be generalized as follows

$$\sigma_{eq} = \alpha\sigma_1 + \sigma_2 + \gamma\sigma_3 \tag{2.2.68}$$

with

$$\sigma_1 = \boldsymbol{A} \cdot\cdot\, \boldsymbol{\sigma}, \quad \sigma_2^2 = \boldsymbol{\sigma} \cdot\cdot\, {}^{(4)}\boldsymbol{B} \cdot\cdot\, \boldsymbol{\sigma}, \quad \sigma_3^3 = \boldsymbol{\sigma} \cdot\cdot\, (\boldsymbol{\sigma} \cdot\cdot\, {}^{(6)}\boldsymbol{C} \cdot\cdot\, \boldsymbol{\sigma}) \tag{2.2.69}$$

The structure of the material tensors must be established from the following restrictions

$$\begin{aligned}
&\boldsymbol{A}' = \boldsymbol{Q} \cdot \boldsymbol{A} \cdot \boldsymbol{Q}^T = A^{ij} \boldsymbol{Q} \cdot \boldsymbol{e}_i \otimes \boldsymbol{Q} \cdot \boldsymbol{e}_j = \boldsymbol{A}, \\
&{}^{(4)}\boldsymbol{B}' = B^{ijkl} \boldsymbol{Q} \cdot \boldsymbol{e}_i \otimes \boldsymbol{Q} \cdot \boldsymbol{e}_j \otimes \boldsymbol{Q} \cdot \boldsymbol{e}_k \otimes \boldsymbol{Q} \cdot \boldsymbol{e}_l = {}^{(4)}\boldsymbol{B}, \\
&{}^{(6)}\boldsymbol{C}' = C^{ijklmn} \boldsymbol{Q} \cdot \boldsymbol{e}_i \otimes \boldsymbol{Q} \cdot \boldsymbol{e}_j \otimes \boldsymbol{Q} \cdot \boldsymbol{e}_k \otimes \boldsymbol{Q} \cdot \boldsymbol{e}_l \otimes \boldsymbol{Q} \cdot \boldsymbol{e}_m \otimes \boldsymbol{Q} \cdot \boldsymbol{e}_n = {}^{(6)}\boldsymbol{C},
\end{aligned} \tag{2.2.70}$$

where $\boldsymbol{Q}$ is an element of the physical symmetry group. The creep potential hypothesis and the flow rule (2.1.6) lead to the following creep equation

$$\dot{\boldsymbol{\varepsilon}}^{cr} = \frac{\partial W}{\partial \sigma_{eq}} \left(\alpha \frac{\partial \sigma_1}{\partial \boldsymbol{\sigma}} + \frac{\partial \sigma_2}{\partial \boldsymbol{\sigma}} + \gamma \frac{\partial \sigma_3}{\partial \boldsymbol{\sigma}} \right) \tag{2.2.71}$$

Taking into account the relations

$$\frac{\partial \sigma_1}{\partial \boldsymbol{\sigma}} = \boldsymbol{A}, \quad \frac{\partial \sigma_2}{\partial \boldsymbol{\sigma}} = \frac{{}^{(4)}\boldsymbol{B} \cdot\cdot\, \boldsymbol{\sigma}}{\sigma_2}, \quad \frac{\partial \sigma_3}{\partial \boldsymbol{\sigma}} = \frac{\boldsymbol{\sigma} \cdot\cdot\, {}^{(6)}\boldsymbol{C} \cdot\cdot\, \boldsymbol{\sigma}}{\sigma_3^2} \tag{2.2.72}$$

a generalized anisotropic creep equation can be formulated as follows

$$\dot{\boldsymbol{\varepsilon}}^{cr} = \dot{\varepsilon}^{cr}_{eq}\left(\alpha\boldsymbol{A} + \frac{{}^{(4)}\boldsymbol{B}\cdot\cdot\boldsymbol{\sigma}}{\sigma_2} + \gamma\frac{\boldsymbol{\sigma}\cdot\cdot\,{}^{(6)}\boldsymbol{C}\cdot\cdot\boldsymbol{\sigma}}{\sigma_3^2}\right), \quad \dot{\varepsilon}^{cr}_{eq} \equiv \frac{\partial W}{\partial\sigma_{eq}} \tag{2.2.73}$$

In [51, 265] the following anisotropic creep equation is proposed

$$\dot{\boldsymbol{\varepsilon}}^{cr} = \boldsymbol{H} + {}^{(4)}\boldsymbol{M}\cdot\cdot\boldsymbol{\sigma} + ({}^{(6)}\boldsymbol{L}\cdot\cdot\boldsymbol{\sigma})\cdot\cdot\boldsymbol{\sigma} \tag{2.2.74}$$

Comparing the Eqs (2.2.73) and (2.2.74) the material tensors $\boldsymbol{H}$, ${}^{(4)}\boldsymbol{M}$ and ${}^{(6)}\boldsymbol{L}$ can be related to the tensors $\boldsymbol{A}$, ${}^{(4)}\boldsymbol{B}$ and ${}^{(6)}\boldsymbol{C}$.

The tensors $\boldsymbol{A}$, ${}^{(4)}\boldsymbol{B}$ and ${}^{(6)}\boldsymbol{C}$ contain 819 coordinates ($\boldsymbol{A}$ - 9, ${}^{(4)}\boldsymbol{B}$ - 81, ${}^{(6)}\boldsymbol{C}$ - 729). From the symmetry of the stress tensor and the creep rate tensor as well as from the potential hypothesis follows that "only" 83 coordinates are independent ($\boldsymbol{A}$ - 6, ${}^{(4)}\boldsymbol{B}$ - 21, ${}^{(6)}\boldsymbol{C}$ - 56). Further reduction is based on the symmetry considerations. The structure of material tensors and the number of independent coordinates can be obtained by solving (2.2.70).

Another possibility of simplification is the establishing of special cases of (2.2.73). For instance, equations with a reduced number of parameters can be derived as follows

– $\alpha = 1, \gamma = 0$:

$$\sigma_{eq} = \sigma_1 + \sigma_2, \quad \dot{\boldsymbol{\varepsilon}}^{cr} = \dot{\varepsilon}^{cr}_{eq}\left(\boldsymbol{A} + \frac{{}^{(4)}\boldsymbol{B}\cdot\cdot\boldsymbol{\sigma}}{\sigma_2}\right), \tag{2.2.75}$$

– $\alpha = 0, \gamma = 1$:

$$\sigma_{eq} = \sigma_2 + \sigma_3, \quad \dot{\boldsymbol{\varepsilon}}^{cr} = \dot{\varepsilon}^{cr}_{eq}\left(\frac{{}^{(4)}\boldsymbol{B}\cdot\cdot\boldsymbol{\sigma}}{\sigma_2} + \frac{\boldsymbol{\sigma}\cdot\cdot\,{}^{(6)}\boldsymbol{C}\cdot\cdot\boldsymbol{\sigma}}{\sigma_3^2}\right), \tag{2.2.76}$$

– $\alpha = 0, \gamma = 0$:

$$\sigma_{eq} = \sigma_2, \quad \dot{\boldsymbol{\varepsilon}}^{cr} = \dot{\varepsilon}^{cr}_{eq}\left(\frac{{}^{(4)}\boldsymbol{B}\cdot\cdot\boldsymbol{\sigma}}{\sigma_2}\right) \tag{2.2.77}$$

The last case has been discussed in Sect. 2.2.2.1. Examples of application of constitutive equation (2.2.73) as well as different cases of symmetries are discussed in [2, 9].

2.2.3 Functions of Stress and Temperature

In all constitutive equations discussed in Sects 2.2.1 and 2.2.2 the creep potential or the equivalent creep rate must be specified as functions of the equivalent stress and the temperature, i.e.

$$\dot{\varepsilon}^{cr}_{eq} = \frac{\partial W}{\partial\sigma_{eq}} = f(\sigma_{eq}, T)$$

In [176] the function f is termed to be the constitutive or response function. For the formulation of constitutive functions one may apply theoretical foundations from materials science with regard to mechanisms of creep deformation and related forms of stress and temperature functions. Furthermore, experimental data including families of creep curves obtained from uni-axial creep tests for certain ranges of stress and temperature are required. It is convenient to present these families in a form of minimum creep rate vs. stress and minimum creep rate vs. temperature curves in order to find mechanical properties of the material within the steady-state creep range.

Many empirical functions of stress and temperature which allow to fit experimental data have been proposed in the literature, e.g. [236, 250, 266, 292]. The starting point is the assumption that the creep rate may be descried as a product of two separate functions of stress and temperature

$$\dot{\varepsilon}_{eq}^{cr} = f_\sigma(\sigma_{eq}) f_T(T)$$

The widely used functions of stress are:

– power law

$$f_\sigma(\sigma_{eq}) = \dot{\varepsilon}_0 \left| \frac{\sigma_{eq}}{\sigma_0} \right|^{n-1} \frac{\sigma_{eq}}{\sigma_0} \tag{2.2.78}$$

The power law contains three constants $(\dot{\varepsilon}_0, \sigma_0, n)$ but only two of them are independent. Instead of $\dot{\varepsilon}_0$ and σ_0 one material constant

$$a \equiv \frac{\dot{\varepsilon}_0}{\sigma_0^n}$$

can be introduced.

– power law including the creep limit

$$f_\sigma(\sigma_{eq}) = \dot{\varepsilon}_0' \left(\frac{\sigma_{eq}}{\sigma_0'} - 1 \right)^{n'}, \quad \sigma_{eq} > \sigma_0'$$

If $\sigma_{eq} \leq \sigma_0'$ the creep rate is equal zero. In this case σ_0' is the assumed creep limit. Let us note that the experimental identification of its value is difficult, e.g. [266].

– exponential law

$$f_\sigma(\sigma_{eq}) = \dot{\varepsilon}_0 \exp \frac{\sigma_{eq}}{\sigma_0}$$

$\dot{\varepsilon}_0, \sigma_0$ are material constants. The disadvantage of this expression is that it predicts a nonzero creep rate for a zero equivalent stress

$$f_\sigma(0) = \dot{\varepsilon}_0 \neq 0$$

– hyperbolic sine law

$$f_\sigma(\sigma_{eq}) = \dot{\varepsilon}_0 \sinh \frac{\sigma_{eq}}{\sigma_0}$$

For low stress values this function provides the linear dependence on the stress

$$f_\sigma(\sigma_{eq}) \approx \dot{\varepsilon}_0 \frac{\sigma_{eq}}{\sigma_0}$$

Assuming the constant temperature equations for the equivalent creep rate can be summarized as follows

$$\begin{aligned}
&\dot{\varepsilon}^{cr}_{eq} = a\sigma^n_{eq} && \text{Norton, 1929, Bailey, 1929,}\\
&\dot{\varepsilon}^{cr}_{eq} = b\left(\exp\frac{\sigma_{eq}}{\sigma_0} - 1\right) && \text{Soderberg, 1936,}\\
&\dot{\varepsilon}^{cr}_{eq} = a\sinh\frac{\sigma_{eq}}{\sigma_0} && \text{Prandtl, 1928, Nadai, 1938, McVetty, 1943,}\\
&\dot{\varepsilon}^{cr}_{eq} = a_1\sigma^{n_1}_{eq} + a_2\sigma^{n_2}_{eq} && \text{Johnson et al., 1963,}\\
&\dot{\varepsilon}^{cr}_{eq} = a\left(\sinh\frac{\sigma_{eq}}{\sigma_0}\right)^n && \text{Garofalo, 1965,}
\end{aligned} \tag{2.2.79}$$

where $a, b, a_1, a_2, \sigma_0, n, n_1$ and n_2 are material constants. The dependence on the temperature is usually expressed by the Arrhenius law

$$f_T(T) = \exp[-Q/RT],$$

where Q and R denote the activation energy and the Boltzmann's constant, respectively.

For the use of stress and temperature functions one should take into account that different deformation mechanisms may operate for different specific ranges of stress and temperature. An overview is provided by the deformation mechanisms maps proposed by Frost and Ashby [117], Fig. 2.3. Contours of constant strain rates are presented as functions of the normalized equivalent stress σ_{eq}/G and the homologous temperature T/T_m, where G is the shear modulus and T_m is the melting temperature. For a given combination of the stress and the temperature, the map provides the dominant creep mechanism and the strain rate.

Let us briefly discuss different regions on the map, the mechanisms of creep deformation and constitutive functions derived in materials science. For comprehensive reviews one may consult [116, 156, 222]. The origins of the inelastic deformation at the temperature range $0.5 < T/T_m < 0.7$ are transport processes associated with motion and interaction of dislocations and diffusion of vacancies. Here we limit our consideration to the two classes of physical models - dislocation and diffusion creep. Various creep rate equations within the dislocation creep range are based on the Bailey-Orowan recovery hypothesis. An internal barrier stress σ_{int} being opposed to the dislocation movement is assumed. When the plastic strain occurs the internal stress increases as a result of work hardening due to accumulation of deformation and due to increase of the dislocation density. As the material is subjected to the load and temperature over certain time, the internal stress σ_{int} recovers. In the uni-axial case the rate of change of the internal stress is assumed as follows

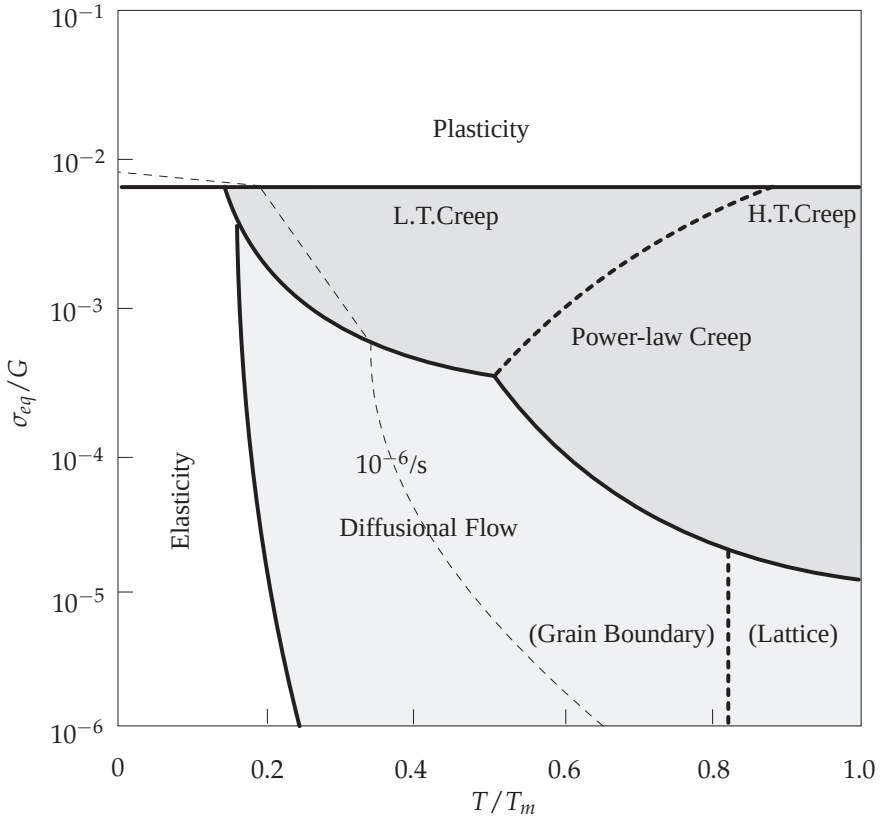

Figure 2.3 Schematic deformation-mechanism map (L.T.Creep - low temperature creep, H.T.Creep - high temperature creep)

$$\dot{\sigma}_{int} = h\dot{\varepsilon}^{cr} - r\sigma_{int},$$

where h and r are material properties related to hardening and recovery, respectively. In the steady state $\dot{\sigma}_{int} = 0$ so that

$$\dot{\varepsilon}^{cr} = \frac{r\sigma_{int}}{h}$$

Specifying the values for r, h and σ_{int} various models for the steady state creep rate have been derived. An example is the following expression (for details of derivation we refer to [116])

$$\dot{\varepsilon}^{cr} \propto \frac{D}{RT}\frac{\sigma^4}{G^3}\exp\left(-\frac{Q}{RT}\right),$$

where D is the diffusion coefficient.

Further models of dislocation creep are discussed under the assumption of the climb-plus-glide deformation mechanism. At high temperatures and moderate stresses, dislocations can climb as well as glide. The glide of dislocations produced by the applied stress is opposed by obstacles. Due to diffusion of vacancies, the

dislocations can climb around strengthening particles. The inelastic strain is then controlled by the glide, while its rate is determined by the climb. The climb-plus-glide mechanism can be related to the recovery-hardening hypothesis. The hardening results from the resistance to glide due to interaction of moving dislocations with other dislocations, precipitates, etc. The recovery mechanism is the diffusion controlled climb which releases the glide barriers. The climb-plus-glide based creep rate models can be found in [116, 117, 222]. The common result is the power-law creep

$$\dot{\varepsilon}_{eq}^{cr} \propto \left(\frac{\sigma_{eq}}{G}\right)^{n} \exp\left(-\frac{Q}{RT}\right) \tag{2.2.80}$$

Equation (2.2.80) can be used to fit experimental data for a range of stresses up to $10^{-3}G$. The exponent n varies from 3 to about 10 for metallic materials. At higher stresses above $10^{-3}G$ the power law (2.2.80) breaks down. The measured strain rate is greater than the Eq. (2.2.80) predicts. Within the range of the power-law break down a transition from the climb-plus-glide to the glide mechanism is assumed [117]. The following empirical equation can be applied, e.g. [117, 222],

$$\dot{\varepsilon}_{eq}^{cr} \propto \left[\sinh\left(\alpha\frac{\sigma_{eq}}{G}\right)\right]^{n} \exp\left(-\frac{Q}{RT}\right), \tag{2.2.81}$$

where α is a material constant. If $\alpha\sigma_{eq}/G < 1$ then (2.2.81) reduces to (2.2.80).

At higher temperatures ($T/T_m > 0.7$) diffusion mechanisms control the creep rate. The deformation occurs at much lower stresses and results from diffusion of vacancies. The mechanism of grain boundary diffusion (Coble creep) assumes diffusive transport of vacancies through and around the surfaces of grains. The deviatoric part of the stress tensor changes the chemical potential of atoms at the grain boundaries. Because of different orientations of grain boundaries a potential gradient occurs. This gradient is the driving force for the grain boundary diffusion. The diffusion through the matrix (bulk diffusion) is the dominant creep mechanism (Nabarro-Herring creep) for temperatures close to the melting point. For details concerning the Coble and the Nabarro-Herring creep models we refer to [116, 222]. These models predict the diffusion controlled creep rate to be a linear function of the stress.

In addition to the dislocation and the diffusion creep, the grain boundary sliding is the important mechanism for poly-crystalline materials. This mechanism occurs because the grain boundaries are weaker than the ordered crystalline structure of the grains [222, 271]. Furthermore, the formation of voids and micro-cracks on grain boundaries contributes to the sliding. The whole deformation rate depends on the grain size and the grain aspect ratio (ratio of the grain dimensions parallel and perpendicular to the tensile stress direction). Samples with a larger grain size usually exhibit a lower strain rate.

2.3 Primary Creep and Creep Transients

In structural analysis applications it is often desirable to consider stress redistributions from the beginning of the creep process up to the creep with constant rate. Let us note, that in a statically undetermined structure stress redistributions take place even if primary creep is ignored. In the case of rapid changes of external loading one must take into account transient effects of the material behavior. Let us discuss some experimental results related to creep under variable multi-axial loading conditions. The majority of multi-axial creep tests have been performed on thin-walled tubes under combined action of tension (compression) force and torque. In this case the uniform stress state $\boldsymbol{\sigma} = \sigma \boldsymbol{n} \otimes \boldsymbol{n} + \tau(\boldsymbol{n} \otimes \boldsymbol{m} + \boldsymbol{m} \otimes \boldsymbol{n})$ is assumed, where σ and τ are calculated from the force and torque as well as the geometry of the cross section (see Sect. 1.1.2). Figure 2.4 presents a sketch of experimental data for type

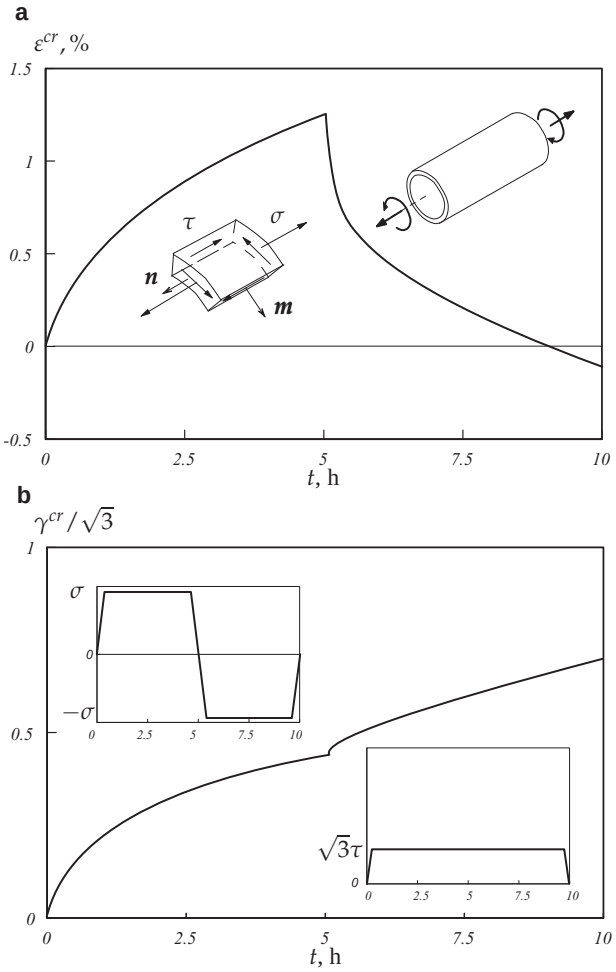

Figure 2.4 Transient creep at combined tension and torsion. Effect of the normal stress reversal. **a** Normal strain vs. time, **b** shear strain vs. time (after [148])

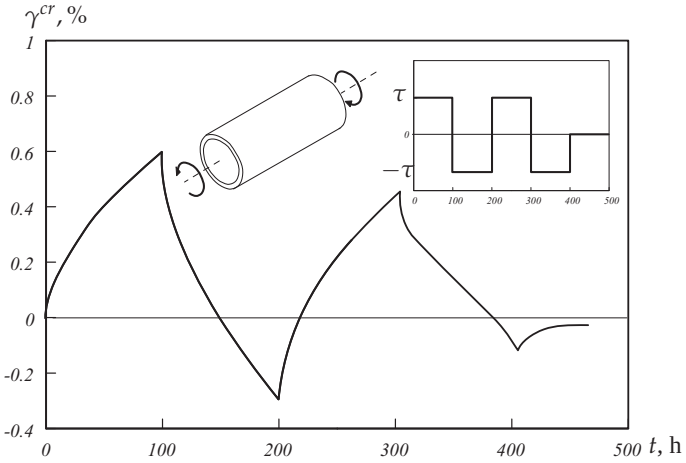

Figure 2.5 Creep under shear stress reversals (after [248])

304 steel ($2\frac{1}{4}$Cr-1Mo) at 600°C [148]. A tube was loaded the first 5 hours by the constant tension force and the constant torque. After that the direction of the force was reversed while the torque kept constant. The normal strain vs. time creep curve under compressive force after the reversal differs substantially from the reference creep curve under tensile force, Fig. 2.4a. The absolute value of the strain rates before and after the reversal differs significantly. Furthermore, the shear strain vs. time creep curve is influenced by the reversal of the axial force, Fig. 2.4b.

Figure 2.5 shows a sketch of experimental results obtained in [248] for INCONEL Alloy 617 (NiCr22Co12Mo) tubes at 900°C under cyclic torsion. Every 100 h the applied torque was reversed leading to the change of the sign of the shear stress. The inelastic shear strain accumulated after each cycle of positive (negative) torque decreases rapidly after few cycles of reversals. Similar behavior is reported in [238] for the type 304 steel, where, in addition, the effect of thermal exposure before and during the loading is discussed. Creep behavior of steels is usually accompanied by the thermally induced evolution of structure of carbide precipitates (coarsening or new precipitation). The effect of ageing has a significant influence on the transient creep of steels as discussed in [238]. For example, the decrease of inelastic shear strain under alternating torsion was not observed if tubular specimens were subjected to the thermal exposure within the time interval of 500 h before the loading.

Additional effects have been observed in the case of reversals of the applied torque combined with the constant tension force, Fig. 2.6. First, the axial strain response is significantly influenced by the cyclic torsion. Second, the rate of the shear strain depends on the sign of the applied torque. Such a response indicates the anisotropic nature of the hardening processes.

Multi-axial creep behavior is significantly influenced by the deformation history. As an example, Fig. 2.7 presents a sketch of results reported in [157] for type 304 stainless steel. Tubular specimens were first loaded up to the stress σ_1 leading to

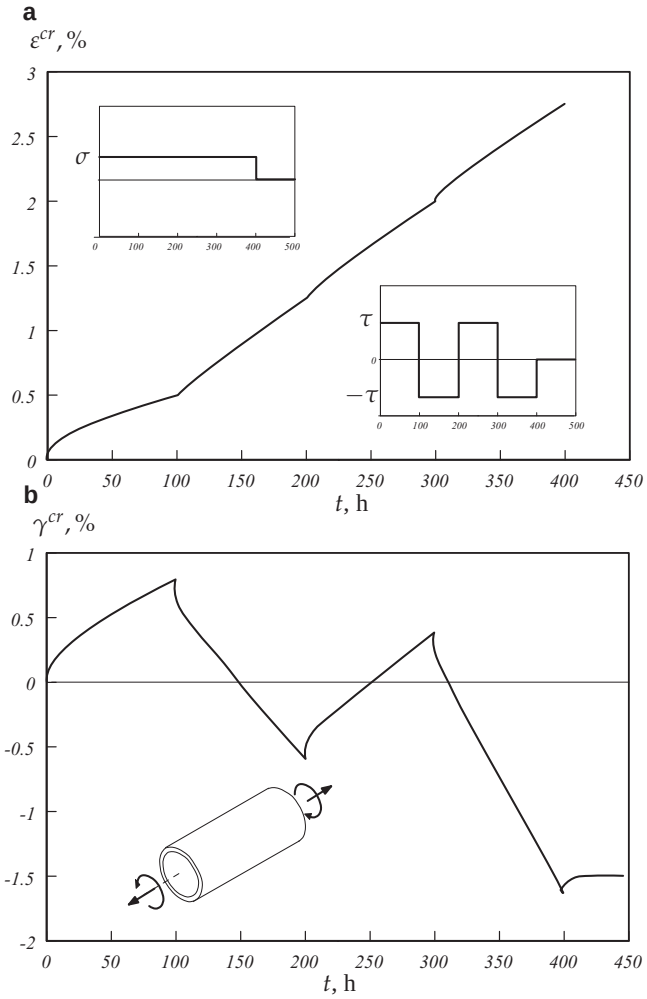

Figure 2.6 Creep at combined tension and torsion. Effect of the shear stress reversals. **a** Normal strain vs. time, **b** shear strain vs. time (after [248])

the plastic strain of 3%. After that the specimens were unloaded to σ_0. Subsequent creep tests have been performed under combined constant normal strain σ and shear strain τ. Different stress states leading to the same value of the von Mises stress $\sigma_{vM} = \sqrt{\sigma^2 + 3\tau^2} = \sigma_0$ were realized. The results show that the tensile creep curve of the material after plastic pre-straining differs significantly from the creep curve of the "virgin material" (curve a). Furthermore, the von Mises creep strain vs. time curves after plastic pre-straining depend significantly on the type of the applied stress state (compare, for example, tension, curve a, torsion, curve b, and compression, curve e).

In this section we discuss phenomenological models to describe primary creep and creep transients under multi-axial stress states. We start with models of time and strain hardening. After that we introduce the concept of kinematic hardening which

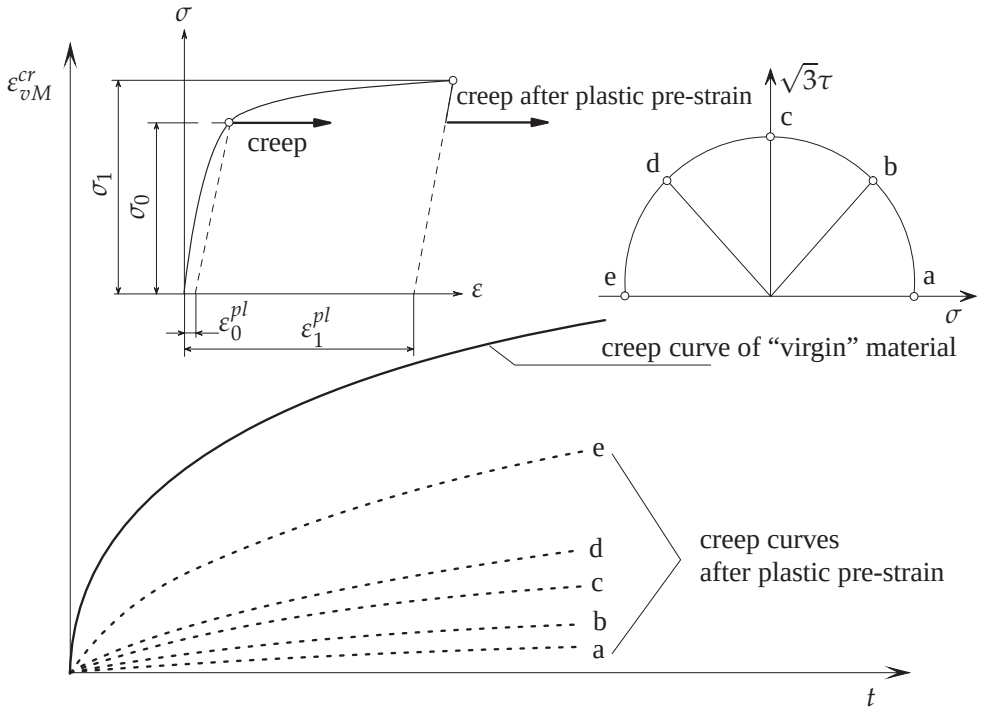

Figure 2.7 Effect of initial tensile plastic strain on subsequent creep behavior under combined tension and torsion, for details see [157]

is widely used for the characterization of transient creep effects under constant and varying loading. Our purpose is to discuss general ideas rather than enter into details of empirical functions of stress and temperature as well as different forms of evolution equations for hardening variables (the so-called hardening rules). Regarding the hardening rules one may consult the comprehensive reviews [87, 237] and monographs [174, 185, 208, 301]. For classification and assessment of different unified models of plasticity-creep interaction we refer to [148, 149].

2.3.1 Time and Strain Hardening

The time hardening model assumes a relationship between the equivalent creep rate, the equivalent stress and the time at fixed temperature, i.e.

$$f_t(\dot{\varepsilon}_{eq}^{cr}, \sigma_{eq}, t) = 0$$

The strain hardening model postulates a relationship between the equivalent creep rate, the equivalent creep strain and the equivalent stress at fixed temperature. In this case

$$f_s(\dot{\varepsilon}_{eq}^{cr}, \varepsilon_{eq}^{cr}, \sigma_{eq}) = 0$$

Figure 2.8 illustrates the uni-axial creep response after reloading (stress jump from σ_1 to σ_2 at $t = t_r$). Based on the time hardening model the strain rate at $t \geq t_r$ is

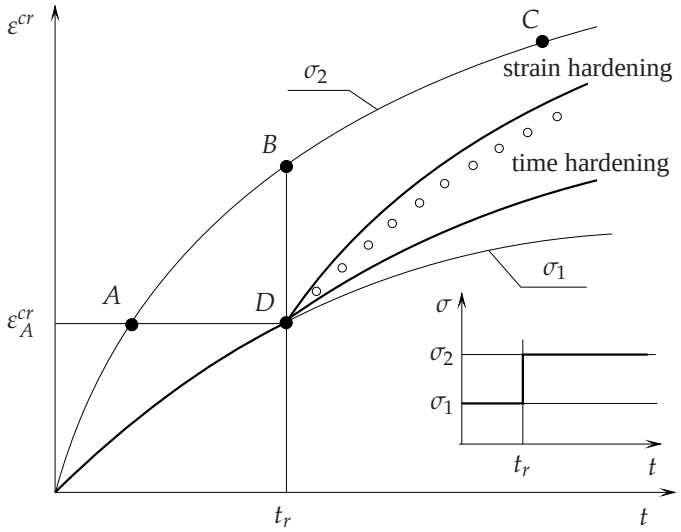

Figure 2.8 Creep response at variable loading (the open circles denote typical experimental values)

determined by the stress σ_2 and the time t_r only. Thus the creep curve for $t \geq t_r$ can be obtained by translation of the curve BC to the point D. Following the strain hardening model the strain rate depends on the stress and the accumulated strain. The creep curve after the stress jump can be determined by translating the curve AC (the creep curve for the stress σ_2 starting from the creep strain ε^{cr}_A accumulated in time t_r) along the time axis. It can be shown that for specific functions of stress, time and strain as well as under the assumption of the constant stress and temperature the strain and the time hardening models lead to the same description. For example, if we set

$$\dot{\varepsilon}^{cr}_{eq} = a\sigma^n_{eq} t^m \tag{2.3.1}$$

according to the time hardening with a, n and m as the material constants the integration with respect to the time variable assuming $\sigma_{eq} = const$ and $\varepsilon^{cr}_{eq} = 0$ at $t = 0$ leads to

$$\varepsilon^{cr}_{eq} = a\sigma^n_{eq} \frac{1}{m+1} t^{m+1} \tag{2.3.2}$$

On the other hand applying the strain hardening model, the creep equation can be formulated as

$$\dot{\varepsilon}^{cr}_{eq} = b\sigma^k_{eq} (\varepsilon^{cr}_{eq})^l \tag{2.3.3}$$

Taking into account (2.3.2) the time variable can be eliminated from (2.3.1). As a result the following relations between the material constants can be obtained

$$b = [a(m+1)^m]^{\frac{1}{m+1}}, \quad k = \frac{n}{m+1}, \quad l = \frac{m}{m+1}$$

Vice versa, the strain hardening equation (2.3.2) can be integrated for the special choice of k and l and for $\sigma_{eq} = const$. Again, if $\varepsilon^{cr}_{eq} = 0$ at $t = 0$ we obtain (2.3.2).

Applying the time hardening model the von Mises-Odqvist creep theory (see Sect. 2.2) can be generalized as follows

$$\dot{\boldsymbol{\varepsilon}}^{cr} = \frac{3}{2} a \sigma_{vM}^{n-1} t^m \boldsymbol{s} \tag{2.3.4}$$

By analogy one can formulate the creep constitutive equation with the strain hardening

$$\dot{\boldsymbol{\varepsilon}}^{cr} = \frac{3}{2} b \sigma_{vM}^{k-1} (\varepsilon_{vM}^{cr})^l \boldsymbol{s} \tag{2.3.5}$$

The time and the strain hardening models provide simple empirical description of the uni-axial creep curve within the range of primary creep and are still popular in characterizing the material behavior, e.g. [137, 145, 171]. Despite the simplicity, both the models suffer from significant limitations, even if applied stress and temperature are constant. The disadvantage of the time hardening model is that the time variable appears explicitly in equation (2.3.1) for the creep rate. An additional drawback is that the constants m and l take usually the values $-1 < m < 0$, $-1 < l < 0$ as the result of curve fitting. If $\varepsilon_{eq}^{cr} = 0$ at $t = 0$ then Eq. (2.3.3) provides an infinite starting creep rate. One can avoid this problem in a time-step based numerical procedure assuming a small non-zero creep equivalent strain at the starting time step. Finally, both models can be applied only for the case of the constant or slowly varying stresses. Transient creep effects under rapid changes of loading and particularly in the case of stress reversals cannot be described.

Further details of time and strain hardening models can be found in [173, 250]. In [173] a modified strain hardening model is proposed based on the idea of creep strain origins.

2.3.2 Kinematic Hardening

The common approach in describing transient creep effects under complex loading paths is the introduction of internal state variables and appropriate evolution equations (the so-called hardening rules). The scalar-valued internal state variables are introduced in the literature to characterize isotropic hardening and ageing processes. An example will be discussed in Sect. 2.4.1.3. Several "non-classical" effects observed in tests under non-proportional loading have motivated the use of tensor-valued variables (usually second rank tensors).

The idea of kinematic hardening (translation of the yield surface in the stress space) originates from the theory of plasticity and has been introduced by Prager [257]. In the creep mechanics the kinematic hardening was proposed by Malinin and Khadjinsky [203, 204]. The starting point is the additive decomposition of the stress tensor into two parts: $\boldsymbol{\sigma} = \bar{\boldsymbol{\sigma}} + \boldsymbol{\alpha}$, where $\bar{\boldsymbol{\sigma}}$ is called the active or the effective part of the stress tensor and $\boldsymbol{\alpha}$ denotes the additional or translation part of the stress tensor (back stress tensor). The introduced tensors can be further decomposed into spherical and deviatoric parts

$$\begin{aligned}
\bar{\boldsymbol{\sigma}} &= \frac{1}{3}\mathrm{tr}\,\bar{\boldsymbol{\sigma}}\boldsymbol{I} + \bar{\boldsymbol{s}}, && \mathrm{tr}\,\bar{\boldsymbol{s}} = 0, \\
\boldsymbol{\alpha} &= \frac{1}{3}\mathrm{tr}\,\boldsymbol{\alpha}\boldsymbol{I} + \boldsymbol{\beta}, && \mathrm{tr}\,\boldsymbol{\beta} = 0, \\
\boldsymbol{\sigma} &= \frac{1}{3}(\mathrm{tr}\,\bar{\boldsymbol{\sigma}} + \mathrm{tr}\,\boldsymbol{\alpha})\boldsymbol{I} + \boldsymbol{s}, && \boldsymbol{s} = \bar{\boldsymbol{s}} + \boldsymbol{\beta}
\end{aligned} \tag{2.3.6}$$

It is assumed that the inelastic strain rate is determined by the active part of the stress tensor. The creep potential is then a function of the active part of the stress tensor, i.e. $W = W(\bar{\boldsymbol{\sigma}}) = W(\boldsymbol{\sigma} - \boldsymbol{\alpha})$, e.g. [245]. As in the case of the classical isotropic creep (Sect. 2.2.1.1) only the second invariant of the deviator $\bar{\boldsymbol{s}}$ is considered. Introducing the von Mises equivalent stress

$$\bar{\sigma}_{vM} \equiv \sqrt{\frac{3}{2}\bar{\boldsymbol{s}} \cdot\cdot\, \bar{\boldsymbol{s}}} = \sqrt{\frac{3}{2}(\boldsymbol{s} - \boldsymbol{\beta}) \cdot\cdot\, (\boldsymbol{s} - \boldsymbol{\beta})} \tag{2.3.7}$$

the flow rule (2.1.6) leads to the following constitutive equation

$$\dot{\boldsymbol{\varepsilon}}^{cr} = \frac{3}{2}\frac{\dot{\varepsilon}^{cr}_{vM}}{\bar{\sigma}_{vM}}\bar{\boldsymbol{s}}, \quad \dot{\varepsilon}_{vM} \equiv \sqrt{\frac{2}{3}\dot{\boldsymbol{\varepsilon}}^{cr} \cdot\cdot\, \dot{\boldsymbol{\varepsilon}}^{cr}} \tag{2.3.8}$$

The equivalent creep rate can be expressed by the use of stress and temperature functions discussed in Sect. 2.2.3. For example, with the power law stress function and the Arrhenius temperature dependence

$$\dot{\varepsilon}^{cr}_{vM} = a\bar{\sigma}^{n}_{vM}, \quad a = a_0 \exp\left(-\frac{Q}{RT}\right) \tag{2.3.9}$$

Equations (2.3.8) contain the deviatoric part of the back stress $\boldsymbol{\beta}$. This internal state variable is defined by the evolution equation and the initial condition. In [201, 202] the following evolution equation is postulated

$$\dot{\boldsymbol{\beta}} = \frac{2}{3}b\dot{\boldsymbol{\varepsilon}}^{cr} - \frac{g(\alpha_{vM})}{\alpha_{vM}}\boldsymbol{\beta} \tag{2.3.10}$$

with

$$\alpha_{vM} \equiv \sqrt{\frac{3}{2}\boldsymbol{\beta} \cdot\cdot\, \boldsymbol{\beta}}$$

For the function g various empirical relations were proposed. One example is [201, 202]

$$g(\alpha_{vM}) = c\alpha^{n}_{vM}, \quad c = c_0 \exp\left(-\frac{Q_r}{RT}\right)$$

Equation (2.3.10) is the multi-axial utilization of the Bailey-Orowan recovery hypothesis, see Sect. 2.2.3. b and c_0 are material constants and Q_r is the activation energy of recovery.

Let us show how the model behaves for the uni-axial homogeneous stress state $\boldsymbol{\sigma}(t) = \sigma(t)\boldsymbol{n} \otimes \boldsymbol{n}$, where $\sigma(t)$ is the magnitude of the applied stress and $\boldsymbol{n}$ is the

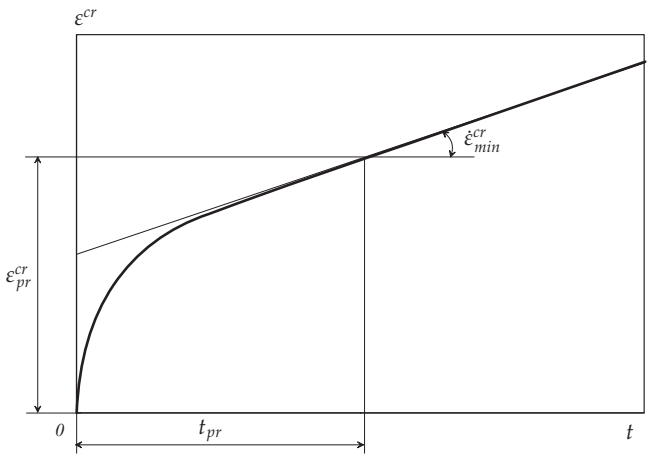

Figure 2.9 Primary and secondary creep stages of a uni-axial creep curve

unit vector. With $\boldsymbol{\alpha}(0) = \mathbf{0}$ one can assume that $\boldsymbol{\alpha}(t)$ is coaxial with the stress tensor. Therefore one can write [201, 202]

$$\boldsymbol{\alpha} = \alpha \boldsymbol{n} \otimes \boldsymbol{n}, \quad \boldsymbol{\beta} = \alpha \left(\boldsymbol{n} \otimes \boldsymbol{n} - \frac{1}{3} \boldsymbol{I} \right), \quad \bar{\sigma}_{vM} = |\sigma - \alpha|, \quad \alpha_{vM} = |\alpha|$$

From Eqs (2.3.9) and (2.3.10) follows

$$\begin{aligned} &\dot{\varepsilon}^{cr} = a \text{sign}(\sigma - \alpha)|\sigma - \alpha|^n, \quad \dot{\varepsilon}^{cr} \equiv \boldsymbol{n} \cdot \dot{\boldsymbol{\varepsilon}}^{cr} \cdot \boldsymbol{n}, \\ &\dot{\alpha} = b\dot{\varepsilon}^{cr} - c \text{sign}\alpha |\alpha|^n \end{aligned} \tag{2.3.11}$$

Let us assume that $\sigma(t) = \sigma_0 > 0$, $\alpha(0) = 0$, $\sigma_0 - \alpha > 0$ and introduce the variable $H = \alpha / \sigma_0$. From (2.3.11) we obtain

$$\begin{aligned} &\dot{\varepsilon}^{cr} = a\sigma_0^n (1 - H)^n, \\ &\dot{H} = \sigma_0^{n-1} [ba(1 - H)^n - cH^n] \end{aligned} \tag{2.3.12}$$

The constitutive and evolution Eqs (2.3.12) describe the primary and the secondary stages of a uni-axial creep curve, Fig. 2.9. In the considered case of the uni-axial tension the parameter $0 \leq H < H_* < 1$ is equal to zero at the beginning of the creep process and increases over time. In the steady state $H = H_*$, where H_* is the saturation value. From the second equation in (2.3.12) we obtain

$$H_* = \frac{1}{1 + \mu^{\frac{1}{n}}}, \quad \mu \equiv \frac{c}{ab} \tag{2.3.13}$$

The minimum creep rate in the steady state is calculated by

$$\dot{\varepsilon}^{cr}_{min} = a\sigma_0^n (1 - H_*)^n = \tilde{a}\sigma_0^n, \quad \tilde{a} \equiv a(1 - H_*)^n \tag{2.3.14}$$

The constants $\tilde{a}$ and n can be obtained from the experimental data of steady state creep. For the given value of H_* the second equation in (2.3.12) can be integrated providing the duration time of primary creep t_{pr} (see Fig. 2.9)

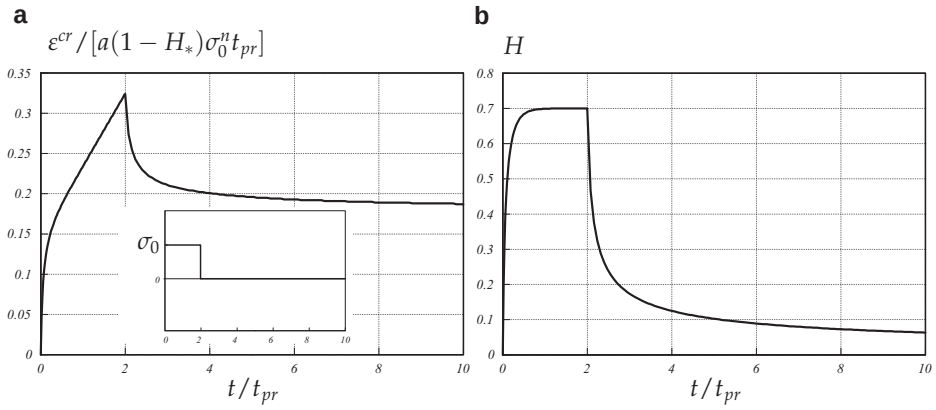

Figure 2.10 Uni-axial creep after unloading. Simulations based on Eqs (2.3.15) for the case $n = 3$ and $H_* = 0.7$. **a** Creep strain vs. time, **b** hardening variable vs. time.

$$t_{pr} = \frac{\varphi(H_*)}{ba\sigma_0^n}, \quad \varphi(H_*) = \int_0^{H_*} \frac{dH}{(1-H)^n - \mu H^n}$$

From the first equation in (2.3.12) the creep strain ε_{pr}^{cr} follows at $t = t_{pr}$ (see Fig. 2.9) as

$$\varepsilon_{pr}^{cr} = \frac{\sigma_0}{b} \int_0^{H_*} \frac{(1-H)^n dH}{(1-H)^n - \mu H^n}$$

The above equations can be used for the identification of material constants.

To discuss the model predictions for the case of the uni-axial cyclic loading let us introduce the following dimensionless variables

$$\tilde{\sigma} = \frac{\sigma(t)}{\sigma_0}, \quad \tau = \frac{t}{t_{pr}}, \quad \epsilon = \frac{\varepsilon^{cr}}{a(1-H_*)\sigma_0^n t_{pr}},$$

where σ_0 denotes the constant stress value in the first loading cycle. Equations (2.3.11) take the form

$$\begin{aligned} \frac{d\epsilon}{d\tau} &= a\,\mathrm{sign}(\tilde{\sigma} - H)\frac{|\tilde{\sigma} - H|^n}{1 - H*}, \\ \frac{dH}{d\tau} &= \varphi(H_*)\left[\mathrm{sign}(\tilde{\sigma} - H)|\tilde{\sigma} - H|^n - \mathrm{sign}(H)\left(\frac{1-H_*}{H_*}\right)^n |H|^n\right] \end{aligned} \tag{2.3.15}$$

Figures 2.10 and 2.11 illustrate the results of the numerical integration of (2.3.15) with $n = 3$, $H_* = 0.7$ and the initial conditions $\epsilon(0) = 0$ and $H(0) = 0$. In the first case presented in Fig. 2.10 we assume $\sigma = \sigma_0$ within the time interval $[0, 2t_{pr}]$, so that the hardening variable increases up to the saturation value and remains constant. The creep curve exhibits both the primary and the secondary stages, Fig. 2.10b. At $t = 2t_{pr}$ we assume a spontaneous unloading, i.e. $\sigma = 0$. We observe that the model

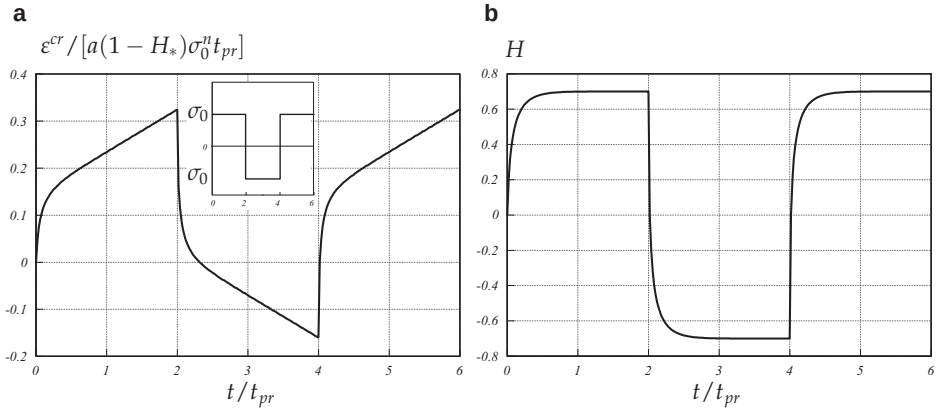

Figure 2.11 Uni-axial creep under cyclic loading. Simulations based on Eqs (2.3.15) for the case $n = 3$ and $H_* = 0.7$. **a** Creep strain vs. time, **b** hardening variable vs. time.

(2.3.15) is able to describe the creep recovery (see Fig. 1.3b). Figure 2.11 presents the numerical results for the case of cyclic loading. Three loading cycles with the constant stresses $\pm\sigma_0$ and the holding time $\Delta t = 2t_{pr}$, Fig. 2.11a, are considered. We observe that the model (2.3.15) predicts identical creep responses for the first and the third loading cycle.

Let us give some comments on the model predictions under multi-axial stress states. For this purpose we consider the case that the stress deviator $\boldsymbol{s}$ is the known constant tensor within a given interval of time $[t_0, t]$. Equations (2.3.8) and (2.3.10) can be rewritten as follows

$$\begin{aligned} \dot{\boldsymbol{\varepsilon}}^{cr} &= \frac{3}{2}\frac{f(\bar{\sigma}_{vM})}{\bar{\sigma}_{vM}}(\boldsymbol{s}-\boldsymbol{\beta}), \\ \dot{\boldsymbol{\beta}} &= b\frac{f(\bar{\sigma}_{vM})}{\bar{\sigma}_{vM}}(\boldsymbol{s}-\boldsymbol{\beta}) - \frac{g(\alpha_{vM})}{\alpha_{vM}}\boldsymbol{\beta} \end{aligned} \tag{2.3.16}$$

In the steady creep state $\boldsymbol{\beta} = \boldsymbol{\beta}_*$, where $\boldsymbol{\beta}_*$ is the saturation value of the back stress deviator. From the second equation in (2.3.16) it follows

$$b\frac{f(\bar{\sigma}_{vM_*})}{\bar{\sigma}_{vM_*}}(\boldsymbol{s}-\boldsymbol{\beta}_*) = \frac{g(\alpha_{vM_*})}{\alpha_{vM_*}}\boldsymbol{\beta}_*, \tag{2.3.17}$$

where

$$\bar{\sigma}_{vM_*} = \sqrt{\frac{3}{2}(\boldsymbol{s}-\boldsymbol{\beta}_*)\cdot\cdot(\boldsymbol{s}-\boldsymbol{\beta}_*)}, \quad \alpha_{vM_*} = \sqrt{\frac{3}{2}\boldsymbol{\beta}_*\cdot\cdot\boldsymbol{\beta}_*}$$

The double inner product of (2.3.17) with itself results in

$$[bf(\bar{\sigma}_{vM_*})]^2 = [g(\alpha_{vM_*})]^2$$

Since $f(\bar{\sigma}_{vM_*}) > 0$ and $g(\alpha_{vM_*}) > 0$ we obtain

$$bf(\bar{\sigma}_{vM_*}) = g(\alpha_{vM_*}) \tag{2.3.18}$$

From (2.3.17) it follows

$$\boldsymbol{\beta}_* = \frac{\alpha_{vM_*}}{\bar{\sigma}_{vM_*} + \alpha_{vM_*}}\boldsymbol{s} \quad \Rightarrow \quad \bar{\sigma}_{vM_*} = \sigma_{vM} + \alpha_{vM_*} \tag{2.3.19}$$

Now the steady state value of the back stress deviator can be calculated

$$\boldsymbol{\beta}_* = \alpha_{vM_*}\frac{\boldsymbol{s}}{\sigma_{vM}} \tag{2.3.20}$$

Let us assume power functions for f and g. Then from (2.3.18) it follows

$$ba(\sigma_{vM} - \alpha_{vM_*})^n = c\alpha_{vM_*}^n$$

As in the uni-axial case we introduce the hardening variable $H = \alpha_{vM}/\sigma_{vM}$. The saturation value H_* is then determined by (2.3.13). From the first Eq. in (2.3.16) we obtain

$$\dot{\boldsymbol{\varepsilon}}_{st}^{cr} = \frac{3}{2}\tilde{a}\sigma_{vm}^{n-1}\boldsymbol{s}, \quad \tilde{a} \equiv a(1 - H_*)^n \tag{2.3.21}$$

We observe that the kinematic hardening model (2.3.16) results in the classical Norton-Bailey-Odqvist constitutive equation of steady-state creep discussed in Sect. 2.2.1. This model predicts isotropic steady state creep independently from the initial condition for the back stress deviator $\boldsymbol{\beta}$. Furthermore, different stress states leading to the same value of the von Mises equivalent stress will provide the same steady state value of the equivalent creep rate.

The model (2.3.16) is applied in [202, 245] for the description of creep for different materials under simple or non-proportional loading conditions. It is demonstrated that the predictions agree with experimental results. However, in many cases deviations from the Norton-Bailey-Odqvist type steady state creep can be observed in experiments. For example, in the case shown in Fig. 2.6 the steady state shear creep rate changes significantly after the shear stress reversals, although the von Mises equivalent stress remains constant. The results presented in Fig. 2.7 indicate that the initial hardening state due to plastic pre-strain is the reason for the stress state dependence of the subsequent creep behavior. This effect cannot be described by the model (2.3.16).

The models with the back stress of the type (2.3.16) are usually termed to be the models with anisotropic hardening, e.g. [202]. The type of anisotropy is then determined by the symmetry group of the back stress tensor or deviator. The symmetry group of any symmetric second rank tensor includes always nine elements, e.g. [199]. For the tensor $\boldsymbol{\beta}$ the symmetry elements are

$$\boldsymbol{Q}_{\boldsymbol{\beta}} = \pm\boldsymbol{n}_1 \otimes \boldsymbol{n}_1 \pm \boldsymbol{n}_2 \otimes \boldsymbol{n}_2 \pm \boldsymbol{n}_3 \otimes \boldsymbol{n}_3, \tag{2.3.22}$$

where $\boldsymbol{n}_i$ are the principal axes. In order to verify the assumed symmetries of hardening one should perform creep tests with non-proportional loading of the following type. During the first cycle a homogeneous constant stress state with the deviatoric part $\boldsymbol{s}$ should be applied over a period of time $[0, t_1]$, $t_1 < t_{pr}$. During the second

loading cycle the stress states $\boldsymbol{Q}_i \cdot \boldsymbol{s} \cdot \boldsymbol{Q}_i^T$ should be applied, where the orthogonal tensors $\boldsymbol{Q}_i$ do not belong to the symmetry group of $\boldsymbol{s}$. Among all stress states of this type the stress states $\boldsymbol{Q}_{\boldsymbol{\beta}} \cdot \boldsymbol{s} \cdot \boldsymbol{Q}_{\boldsymbol{\beta}}^T$ should exist leading to the same (with respect to the scatter of experimental data) creep response after reloading.

As shown in [72] kinematic hardening of the type (2.3.16) leads to a restrictive form of orthotropic inelastic behavior. In order to demonstrate this let us write down the back stress deviator in the following form

$$\begin{aligned} \boldsymbol{\beta} &= \beta_1 \boldsymbol{n}_1 \otimes \boldsymbol{n}_1 + \beta_2 \boldsymbol{n}_2 \otimes \boldsymbol{n}_2 - (\beta_1 + \beta_2) \boldsymbol{n}_3 \otimes \boldsymbol{n}_3 \\ &= \beta_1 (\boldsymbol{n}_1 \otimes \boldsymbol{n}_1 - \boldsymbol{n}_3 \otimes \boldsymbol{n}_3) + \beta_2 (\boldsymbol{n}_2 \otimes \boldsymbol{n}_2 - \boldsymbol{n}_3 \otimes \boldsymbol{n}_3), \end{aligned}$$

where β_1 and β_2 are the principal values and $\boldsymbol{n}_1$, $\boldsymbol{n}_2$ and $\boldsymbol{n}_3$ are the principal directions of $\boldsymbol{\beta}$. For the given back stress deviator $\boldsymbol{\beta}$ the equivalent stress (2.3.7) takes the form

$$\begin{aligned} \bar{\sigma}_{vM}^2 &= 3\tilde{J}_1^2 \left(1 - \frac{\beta_1}{\tilde{J}_1}\right)^2 + 3\tilde{J}_2^2 \left(1 - \frac{\beta_2}{\tilde{J}_2}\right)^2 + \frac{3}{2}\tilde{J}_1 \tilde{J}_2 \left(1 - \frac{\beta_1}{\tilde{J}_1}\right)\left(1 - \frac{\beta_2}{\tilde{J}_2}\right) \\ &+ 3I_{\boldsymbol{n}_1\boldsymbol{n}_2}^2 + 3I_{\boldsymbol{n}_1\boldsymbol{n}_3}^2 + 3I_{\boldsymbol{n}_2\boldsymbol{n}_3}^2, \end{aligned} \tag{2.3.23}$$

where the invariants $\tilde{J}_i$ are defined by Eqs (2.2.53) and the invariants $I_{\boldsymbol{n}_i\boldsymbol{n}_j}$ are defined by Eqs (2.2.48). Steady state creep with initial orthotropic symmetry is discussed in Sect. 2.2.2. In this case the von Mises type equivalent stress includes 6 invariants and 6 independent material constants. The equivalent stress (2.3.23) contains all 6 orthotropic invariants. However, the last three terms (three shear stresses with respect to the three planes of the orthotropic symmetry) are not affected by the hardening. Furthermore, in the steady state range these terms vanish since the back stress deviator $\boldsymbol{\beta}_*$ is coaxial with the stress deviator according to (2.3.20).

The possibilities to improve the predictions of the kinematic hardening model are:

- Introduction of additional state variables like isotropic hardening variable, e.g. [87], ageing variable, e.g. [238], or damage variables, e.g. [101]. Models with damage variables will be discussed in Sect. 2.4.
- Formulation of the creep potential as a general isotropic function of two tensors $\boldsymbol{\sigma}$ and $\boldsymbol{\alpha}$. Such an approach is proposed in [72] for the case of plasticity and includes different special cases of kinematic hardening,
- Consideration of the initial anisotropy of the material behavior, e.g. [148].

Creep models with kinematic hardening of the type (2.3.8) and different specific forms of the hardening evolution equation are discussed in [158, 159, 202, 238, 245, 272] among others. For the description of creep and creep-plasticity interaction at complex loading conditions a variety of unified models is available including the hardening variables as second rank tensors. For details we refer to [174, 176, 185, 208]. Several unified models are reviewed and evaluated in [148, 149]. The historical background of the development of non-linear kinematic hardening rules is presented in [87].

2.4 Tertiary Creep and Creep Damage

Tertiary creep stage is the final part of the creep process. In a uni-axial creep curve tertiary creep is observed as the increase of the creep rate. The shape of the final part of the creep curve and the duration of the tertiary creep depends on the material composition, the stress level and the temperature. For some structural steels, the tertiary creep is the major part of the whole creep process, e.g. [105, 242].

The origins of tertiary creep are progressive damage processes including the formation, growth and coalescence of voids on grain boundaries, coarsening of precipitates and environmental effects. The voids may nucleate earlier during the creep process, possibly at primary creep stage or even after spontaneous deformation. The initially existing micro-defects have negligible influence on the creep rate. As their number and size increase with time, they weaken the material providing the decrease in the load-bearing capacity. The coalescence of cavities or propagation of micro-cracks lead to the final fracture. Creep fracture is usually inter-granular [33]. Dyson [99] distinguishes three main categories of creep damage: the strain induced damage, the thermally induced damage and the environmentally induced damage. The strain induced damage may be classified as follows [101]

- excessive straining at constant load,
- grain boundary cavitation and
- progressive multiplication of the dislocation substructure

The first two damage mechanisms occur in all poly-crystalline materials, whereas the third one is essential for nickel-based super-alloys.

The thermally induced damage mechanisms include material ageing processes which lead to the loss of strength and contribute to the nucleation and growth of cavities. The example of the thermally induced ageing includes the coarsening of carbide precipitates for ferritic steels (increase of volume fraction of carbide precipitates or new precipitation), e.g. [251]. The rate of ageing does not depend on the applied stress, but is influenced by the temperature and can be identified by exposing test-pieces to thermal environment.

The environmentally induced damage (corrosion, oxidation, etc.) appears due to the attack of chemical species contained within the surrounding medium. The environmental damage rate can be inversely related to the test-piece (component) dimensions [99].

The dominance of a creep damage mechanism depends on the alloy composition, on the fabrication route and on the service conditions. For several metals and alloys, fracture mechanism maps are available [33]. By analogy with the deformation mechanism maps, regions with different fracture modes are indicated depending on the stress and the temperature ranges.

Physical modeling of creep damage is complicated by the fact that many different mechanisms may operate and interact in a specific material under given loading conditions. This interaction should be taken into account in the damage rate equations. Models related to the grain boundary cavitation are discussed and reviewed in [155, 271].

The characterization of tertiary creep under multi-axial stress states is the important step in a creep analysis of engineering structures. A lifetime prediction of a specific load bearing component designed for creep, or a residual lifetime estimation of a structure operating at elevated temperature requires a model which takes into account tertiary creep and damage evolution under multi-axial stress states.

The damage rate and consequently the creep rate are determined by the stress level, the accumulated damage and the temperature. These dependencies can be established based on experimental data from the uni-axial creep testing. If the material is subjected to multi-axial loading, the kind of stress state has a significant influence on the damage growth. Tension and compression lead to different creep rates. Different stress states corresponding to the same von Mises equivalent stress lead, in general, to different equivalent tertiary creep rates while the equivalent strain rate in the secondary stage is approximately the same. These facts are established from the data of creep tests under combined tension and torsion, e.g. [169, 170], as well as from biaxial and triaxial creep tests [282, 283]. Stress state effects must be considered in the damage evolution equation. In Sect. 2.4.1 we discuss various possibilities to characterize the tertiary creep behavior by means of scalar valued damage parameters. Under non-proportional loading conditions, the additional factor is the influence of the damage induced anisotropy. Examples are creep tests under combined tension and alternating torsion, e.g. [218], and creep tests under biaxial loading with alternating direction of the first principal stress [283]. In both cases the assumption of isotropic creep behavior and the scalar measure of damage lead to disagreement with experimental observations. In Sect. 2.4.2 we review some experimental results illustrating the damage induced anisotropy and discuss creep-damage models with tensor-valued damage variables.

2.4.1 Scalar-Valued Damage Variables

Many microstructural observations show the directional effect of creep damage. For example, during a cyclic torsion test on copper voids nucleate and grow predominantly on those grain boundaries, which are perpendicular to the first principal direction of the stress tensor, e.g. [134]. Creep damage has therefore an anisotropic nature and should be characterized by a tensor. However, if the initially isotropic material is subjected to constant or monotonic loading the influence of the damage anisotropy on the observed creep behavior, i.e. the strain vs. time curves, is not significant. If the state of damage is characterized by a tensor (see Sect. 2.4.2) then such a tensor can be assumed to be coaxial with the stress tensor under monotonic loading conditions. In such a case only the scalar damage measures will enter the creep constitutive equation. Below we introduce different models of tertiary creep including the phenomenological, the so-called micromechanically consistent and mechanism based models. The effect of damage is described by means of scalar valued damage parameters and corresponding evolution equations. The stress state influences are expressed in the equivalent stress responsible for the damage evolution.

2.4.1.1 Kachanov-Rabotnov Model. The phenomenological creep-damage equations were firstly proposed by L. Kachanov [150] and Rabotnov [263]. A new

internal variable has been introduced to characterize the "continuity" or the "damage" of the material. The geometrical interpretation of the continuity variable starts from changes in the cross-section area of a uni-axial specimen. Specifying the initial cross-section area of a specimen by A_0 and the area of voids, cavities, micro-cracks, etc. by A_D, the Kachanov's continuity is defined as follows (see [152])

$$\psi = \frac{A_0 - A_D}{A_0}$$

The value $\psi = 1$ means the virgin, fully undamaged state, the condition $\psi = 0$ corresponds to the fracture (completely damaged cross-section).

Rabotnov [263, 264, 265] introduced the dual damage variable ω. In [264] he pointed out that the damage state variable ω "may be associated with the area fraction of cracks, but such an interpretation is connected with a rough scheme and is therefore not necessary". Rabotnov assumed that the creep rate is additionally dependent on the current damage state. The constitutive equation should have the form

$$\dot{\varepsilon}^{cr} = \dot{\varepsilon}^{cr}(\sigma, \omega)$$

Furthermore, the damage processes can be reflected in the evolution equation

$$\dot{\omega} = \dot{\omega}(\sigma, \omega), \quad \omega|_{t=0} = 0, \quad \omega < \omega_*,$$

where ω_* is the critical value of the damage parameter for which the material fails. With the power functions of stress and damage the constitutive equation may be formulated as follows

$$\dot{\varepsilon}^{cr} = \frac{a\sigma^n}{(1-\omega)^m} \tag{2.4.1}$$

Similarly, the damage rate can be expressed by

$$\dot{\omega} = \frac{b\sigma^k}{(1-\omega)^l} \tag{2.4.2}$$

These equations contain the material dependent constants: a, b, n, m, l, k. It is easy to prove that for the damage free state ($\omega = 0$), the first equation results in the power law creep constitutive equation.

Setting $m = n$ the first equation can be written as

$$\dot{\varepsilon}^{cr} = a\tilde{\sigma}^n, \tag{2.4.3}$$

where $\tilde{\sigma} = \sigma/(1-\omega)$ is the so-called net-stress or effective stress. In this case (2.4.3) is a generalization of the Norton-Bailey secondary creep law for the description of tertiary creep process. Lemaitre and Chaboche [185] proposed the effective stress concept to formulate constitutive equations for damaged materials based on available constitutive equation for "virgin" materials. An interpretation can be given for a tension bar, Fig. 2.12. Here A_0 denotes the initial cross-section area of the bar, Fig. 2.12a. From the given tensile force F the stress can be computed as $\sigma = F/A_0$.

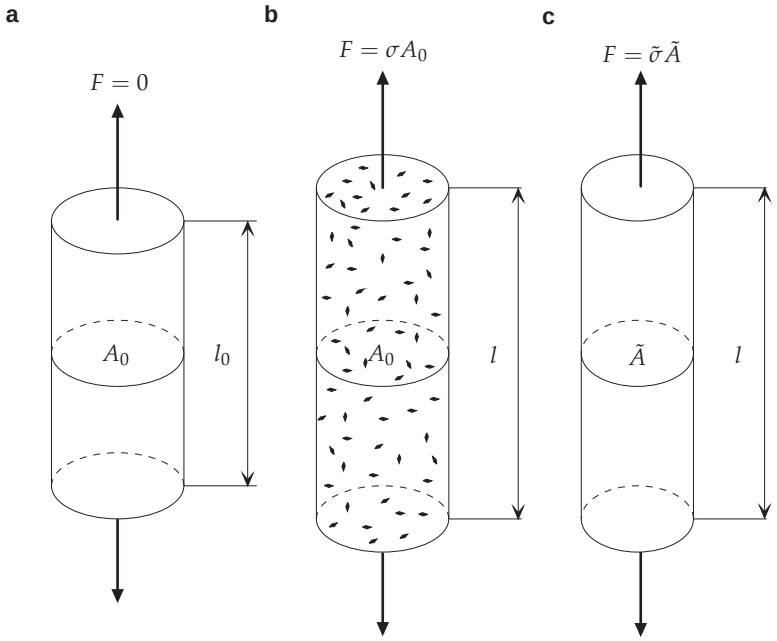

Figure 2.12 Strain and damage of a bar. **a** Initial state, **b** damaged state, **c** fictitious undamaged state

The axial strain for the loaded bar $\varepsilon = (l - l_0)/l_0$ can be expressed as a function of the stress and the actual damage $\varepsilon = f(\sigma, \omega)$, Fig. 2.12b. For the effective cross-section $\tilde{A} = A_0 - A_D$ the effective stress is

$$\tilde{\sigma} = \frac{F}{\tilde{A}} = \frac{\sigma}{1 - \omega} \tag{2.4.4}$$

Now a fictitious undamaged bar with a cross-section area $\tilde{A}$, Fig. 2.12c, having the same axial strain response as the actual damaged bar $\varepsilon = f(\tilde{\sigma}) = f(\sigma, \omega)$ is introduced. The strain equivalence principle [183] states that any strain constitutive equation for a damaged material may be derived in the same way as for a virgin material except that the usual stress is replaced by the effective stress. Thus the constitutive equation for the creep rate (2.4.3) is the power law generalized for a damaged material.

Let us estimate the material constants in the model

$$\dot{\varepsilon}^{cr} = a\tilde{\sigma}^n, \quad \dot{\omega} = \frac{b\sigma^k}{(1 - \omega)^l} \tag{2.4.5}$$

based on uni-axial creep curves, Fig. 2.13. Setting $\omega = 0$ the first equation yields the minimum creep rate. The material constants a and n can be determined from steady state creep. Let $\dot{\varepsilon}^{cr}_{min1}$ and $\dot{\varepsilon}^{cr}_{min2}$ be minimum creep rates at the constant stresses σ_1 and σ_2, respectively. Then the material constants can be estimated from

$$n = \frac{\log(\dot{\varepsilon}^{cr}_{min1}/\dot{\varepsilon}^{cr}_{min2})}{\log(\sigma_1/\sigma_2)}, \quad a = \frac{\dot{\varepsilon}^{cr}_{min1}}{\sigma_1^n} = \frac{\dot{\varepsilon}^{cr}_{min2}}{\sigma_2^n} \tag{2.4.6}$$

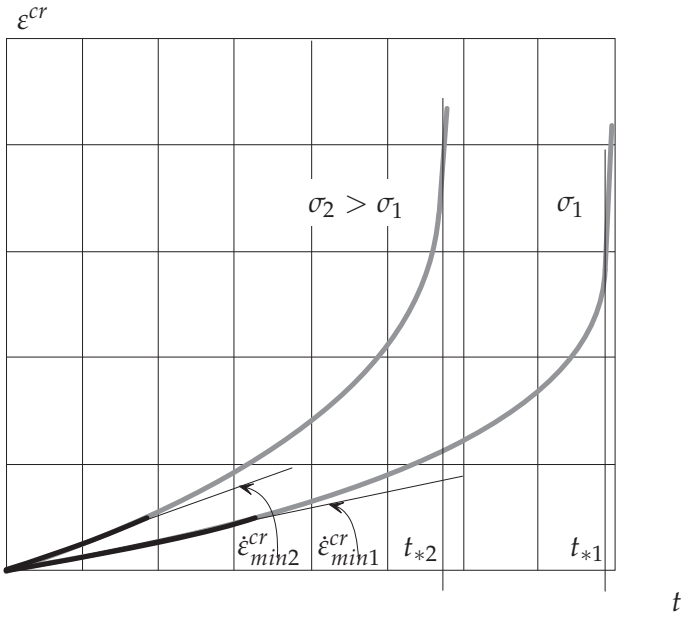

Figure 2.13 Phenomenological description of uni-axial creep curves

For a constant stress σ the second equation (2.4.5) can be integrated as follows

$$\int_0^{\omega_*} (1-\omega)^l d\omega = \int_0^{t_*} b\sigma^k dt$$

with t_* as time to fracture of the specimen. Setting the critical damage value $\omega_* = 1$ we obtain

$$t_* = \frac{1}{(l+1)b\sigma^k} \tag{2.4.7}$$

This equation describes the failure time - applied stress relation. For a number of metals and alloys the experimental data of the long-term strength can be approximated by a straight line in a double logarithmic scale. Note, that such an approximation is valid only for a specific stress range, Fig. 2.14. In the special case $k = l$ the material constants k and b may be estimated from the long-term strength curve as follows

$$k = \frac{\log(t_{*2}/t_{*1})}{\log(\sigma_1/\sigma_2)}, \quad b = \frac{1}{t_{*1}(k+1)\sigma_1^k} = \frac{1}{t_{*2}(k+1)\sigma_2^k}$$

with t_{*1}, t_{*2} as failure times corresponding to the applied stresses σ_1 and σ_2. Integration of the second Eq. (2.4.5) with respect to time by use of Eq. (2.4.7) provides

$$\omega(t) = 1 - \left(1 - \frac{t}{t_*}\right)^{\frac{1}{l+1}}$$

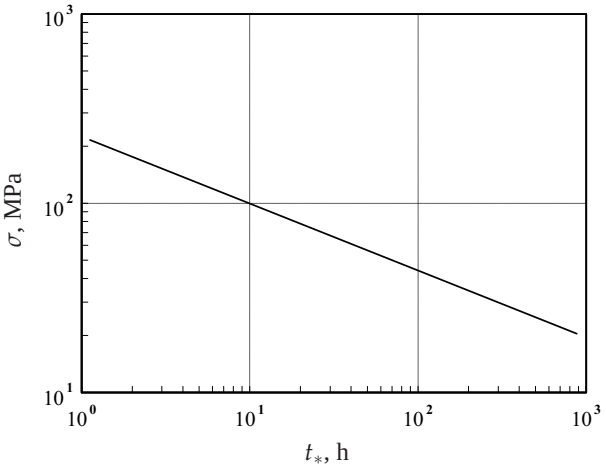

Figure 2.14 Long-term strength curve

After integration of the creep rate equation (2.4.5) with $\sigma = const$ we obtain

$$\varepsilon^{cr}(t) = \frac{a\sigma^{n-k}}{b(l+1-n)}\left[1-\left(1-\frac{t}{t_*}\right)^{\frac{l+1-n}{l+1}}\right]$$

The creep strain ε^{cr}_* at time t_* (fracture strain) can be calculated as

$$\varepsilon^{cr}_*(t_*) = \frac{a\sigma^{n-k}}{b(l+1-n)}$$

If $k > n$ then the fracture strain is a decreasing function of stress. This is usually observed in the case of moderate stresses.

The phenomenological model (2.4.5) characterizes the effect of damage evolution and describes the tertiary creep in a uni-axial test. For a number of metals and alloys material constants are available, see e.g. [18, 69, 77, 132, 141, 142, 143, 144, 163, 169, 184, 185, 216]. Instead of the power law functions of stress or damage it is possible to use another kind of functions, e.g. the hyperbolic sine functions in both the creep and damage evolution equations. In addition, by the introduction of suitable hardening functions or internal hardening variables, the model can be extended to consider primary creep.

In applying (2.4.5) to the analysis of structures one should bear in mind that the material constants are estimated from experimental creep curves, usually available for a narrow range of stresses. The linear dependencies between $\log \dot{\varepsilon}^{cr}_{min}$ and $\log \sigma$ or between $\log t_*$ and $\log \sigma$ do not hold for wide stress ranges. For example, it is known from materials science that for higher stresses the damage mode may change from inter-granular to transgranular, e.g. [33]. Alternatively, tertiary creep can be described by the introduction of several internal variables which are responsible for different interacting damage mechanisms. Examples for such models will be discussed later.

The model (2.4.5) is a system of two ordinary differential equations, which must be integrated over time in order to obtain the current creep strain and damage. For the analysis of statically indeterminate structures the integration must be performed numerically, even in the case of a uni-axial stress state. In some cases the effect of tertiary creep rate does not lead to significant stress redistribution and one can neglect the damage variable in the constitutive equation (2.4.1), e.g. [276]. The damage evolution equation can be integrated separately providing the time to fracture estimation for the given constant stress in the steady-state creep range.

To discuss multi-axial versions of (2.4.1) and (2.4.2) let us neglect primary creep effects and assume the von Mises type secondary creep material model introduced in Sect. 2.2.1

$$\dot{\boldsymbol{\varepsilon}}^{cr} = \frac{3}{2} a \sigma_{vM}^{n} \frac{\boldsymbol{s}}{\sigma_{vM}} \tag{2.4.8}$$

Rabotnov [264] assumed that the the creep potential for the damaged material has the same form as for the secondary creep. His proposition was the introduction of an effective stress tensor $\tilde{\boldsymbol{\sigma}} = \boldsymbol{f}(\boldsymbol{\sigma}, \omega)$. For the case of distinct principal values of the stress tensor $\sigma_I > \sigma_{II} > \sigma_{III}$ and $\sigma_I > 0$ the following expression is suggested [264]

$$\tilde{\boldsymbol{\sigma}} = \frac{\sigma_I}{1-\omega} \boldsymbol{n}_I \otimes \boldsymbol{n}_I + \sigma_{II} \boldsymbol{n}_{II} \otimes \boldsymbol{n}_{II} + \sigma_{III} \boldsymbol{n}_{III} \otimes \boldsymbol{n}_{III}$$

If we apply the strain equivalence principle [185] than the constitutive equation (2.4.8) can be modified by replacing the stress tensor $\boldsymbol{\sigma}$ with the effective one. Assuming the effective stress tensor in the form $\tilde{\boldsymbol{\sigma}} = \boldsymbol{\sigma}/(1-\omega)$, the constitutive equation (2.4.8) can be generalized as follows [182]

$$\dot{\boldsymbol{\varepsilon}}^{cr} = \frac{3}{2} a \left(\frac{\sigma_{vM}}{1-\omega} \right)^{n} \frac{\boldsymbol{s}}{\sigma_{vM}} \tag{2.4.9}$$

The next step is the formulation of the damage evolution equation. By analogy with the uni-axial case, the damage rate should have a form

$$\dot{\omega} = \dot{\omega}(\boldsymbol{\sigma}, \omega)$$

The dependence on the stress tensor can be expressed by means of the "damage equivalent stress" $\sigma_{eq}^{\omega}(\boldsymbol{\sigma})$ which allows to compare tertiary creep and long term strength under different stress states. With the damage equivalent stress, the uni-axial equation (2.4.2) can be generalized as follows

$$\dot{\omega} = \frac{b(\sigma_{eq}^{\omega})^{k}}{(1-\omega)^{l}} \tag{2.4.10}$$

The material constants a, b, n, k and l can be identified from uni-axial creep curves. In order to find a suitable expression for the damage equivalent stress, the data from multi-axial creep tests up to rupture are required. In general, σ_{eq}^{ω} can be formulated in terms of three invariants of the stress tensor, for example the basic invariants (see Sect. 2.2.1)

$$\sigma_{eq}^{\omega} = \sigma_{eq}^{\omega}[I_1(\boldsymbol{\sigma}), I_2(\boldsymbol{\sigma}), I_3(\boldsymbol{\sigma})]$$

Similarly to the uni-axial case, see Eq. (2.4.7), the damage evolution equation (2.4.10) can be integrated assuming that the stress tensor is a constant function of time. As a result, the relationship between the time to creep fracture and the equivalent stress can be obtained

$$t_* = \frac{1}{(l+1)b}(\sigma_{eq}^{\omega})^{-k} \tag{2.4.11}$$

Sdobyrev [288] carried out long-term tests on tubular specimens made from alloys EI-237B (Ni-based alloy) and EI-405 (Fe-based alloy) under tension, torsion and combined tension-torsion. The results of the tests are summarized for different temperatures with the help of equivalent stress vs. fracture time plots. The following dependence was established

$$\frac{1}{2}(\sigma_I + \sigma_{vM}) = f(\log t_*) \tag{2.4.12}$$

He found that the linear function f provides a satisfactory description of the experimental results. The equivalent stress responsible to the long term strength at elevated temperatures is then $\sigma_{eq}^{*} = \frac{1}{2}(\sigma_I + \sigma_{vM})$. Based on different mechanisms which control creep failure, the influence of three stress state parameters (the mean stress $\sigma_m = I_1/3$, the first positive principal stress or the maximum tensile stress $\sigma_{maxt} = (\sigma_I + |\sigma_I|)/2$ and the von Mises stress) is discussed by Trunin in [314]. The Sdobyrev criterion was extended as follows

$$\sigma_{eq}^{*} = \frac{1}{2}\left(\sigma_{vM} + \sigma_{maxt}\right) a^{1-2\eta}, \quad \eta = \frac{3\sigma_m}{\sigma_{vM} + \sigma_{maxt}}, \tag{2.4.13}$$

where a is a material constant. For special loading cases this equivalent stress yields

– uni-axial tension

$$\sigma_{eq}^{*} = \sigma, \quad \eta = \frac{1}{2}$$

– uni-axial compression

$$\sigma_{eq}^{*} = \frac{\sigma a^3}{2}, \quad \eta = -1$$

– pure torsion

$$\sigma_{eq}^{*} = \frac{\sqrt{3}+1}{2}\tau a, \quad \eta = 0$$

The constant a can be calculated from the ultimate stress values leading to the same fracture time for a given temperature. For example, if the ultimate tension and shear stresses are σ_u and τ_u, respectively, then

$$a = \frac{2}{\sqrt{3}+1}\frac{\sigma_u}{\tau_u}$$

Hayhurst [132] proposed the following relationship

$$t_* = A(\alpha\sigma_{maxt} + \beta I_1 + \gamma\sigma_{vM})^{-\chi}, \tag{2.4.14}$$

where A and χ are material constants, $I_1 = 3\sigma_m$ and $\alpha + \beta + \gamma = 1$. Comparing this equation with Eq. (2.4.11) one can obtain

$$A = \frac{1}{(l+1)b}, \quad \chi = k, \quad \sigma_{eq}^{\omega} = \alpha\sigma_{maxt} + \beta I_1 + \gamma\sigma_{vM} \tag{2.4.15}$$

Hayhurst introduced the normalized stress tensor $\bar{\boldsymbol{\sigma}} = \boldsymbol{\sigma}/\sigma_0$ and the normalized time to fracture $\bar{t}_* = t_*/t_{*0}$, where t_{*0} is the time to fracture in a uni-axial test conducted at the stress σ_0. From Eqs (2.4.7) and (2.4.11) it follows

$$\bar{t}_* = \left(\frac{\sigma_{eq}^{\omega}}{\sigma_0}\right)^{-k} = (\bar{\sigma}_{eq}^{\omega})^{-k}$$

By setting the normalized rupture time equal to unity, the equation $\bar{\sigma}_{eq}^{\omega} = 1$ follows, which is connecting the stress states leading to the equal rupture time. In [132] the data of biaxial tests (biaxial tension test, combined tension and torsion of tubular specimens) for different materials are summarized. It was found convenient to present the results in terms of the isochronous rupture surface, which is the plot of the equation $\bar{\sigma}_{eq}^{\omega} = 1$ for the specified values of α and β in the normalized stress space. For plane stress states the isochronous rupture loci can be presented in the normalized principal stress axes. Examples for different materials are presented in [132]. The coefficients α and β are specific for each material and, in addition, they may depend on the temperature. Figure 2.15 shows the isochronous rupture loci for three special cases: $\bar{\sigma}_{eq}^{\omega} = \bar{\sigma}_{maxt}$, $\bar{\sigma}_{eq}^{\omega} = \bar{\sigma}_{vM}$ and $\bar{\sigma}_{eq}^{\omega} = 3\bar{\sigma}_m$. The first two represent the extremes of the material behavior [182].

A more general expression for the damage equivalent stress can be formulated by the use of three invariants of the stress tensor. With the first invariant I_1, the von Mises equivalent stress σ_{vM} and

$$\sin 3\xi = -\frac{27}{2}\frac{(\boldsymbol{s}\cdot\boldsymbol{s})\cdot\cdot\boldsymbol{s}}{\sigma_{vM}^3}, \quad -\frac{\pi}{6} \le \xi \le \frac{\pi}{6},$$

as a cubic invariant, the following equivalent stress has been proposed in [27]

$$\sigma_{eq}^{\omega} = \lambda_1\sigma_{vM}\sin\xi + \lambda_2\sigma_{vM}\cos\xi + \lambda_3\sigma_{vM} + \lambda_4 I_1 + \lambda_5 I_1\sin\xi + \lambda_6 I_1\cos\xi \tag{2.4.16}$$

The identification of coefficients $\lambda_i, i = 1,\ldots,6$ requires six independent tests. Equation (2.4.16) contains a number of known failure criteria as special cases, see [27]. For example, setting $\lambda_1 = \lambda_2 = \lambda_4 = \lambda_5 = \lambda_6 = 0$ the equation provides the von Mises equivalent stress. Taking into account

$$\sigma_I = \frac{1}{3}\left[2\sigma_{vM}\sin\left(\xi + \frac{2\pi}{3}\right) + I_1\right] = -\frac{1}{3}\sigma_{vM}\sin\xi + \frac{\sqrt{3}}{3}\sigma_{vM}\cos\xi + \frac{1}{3}I_1$$

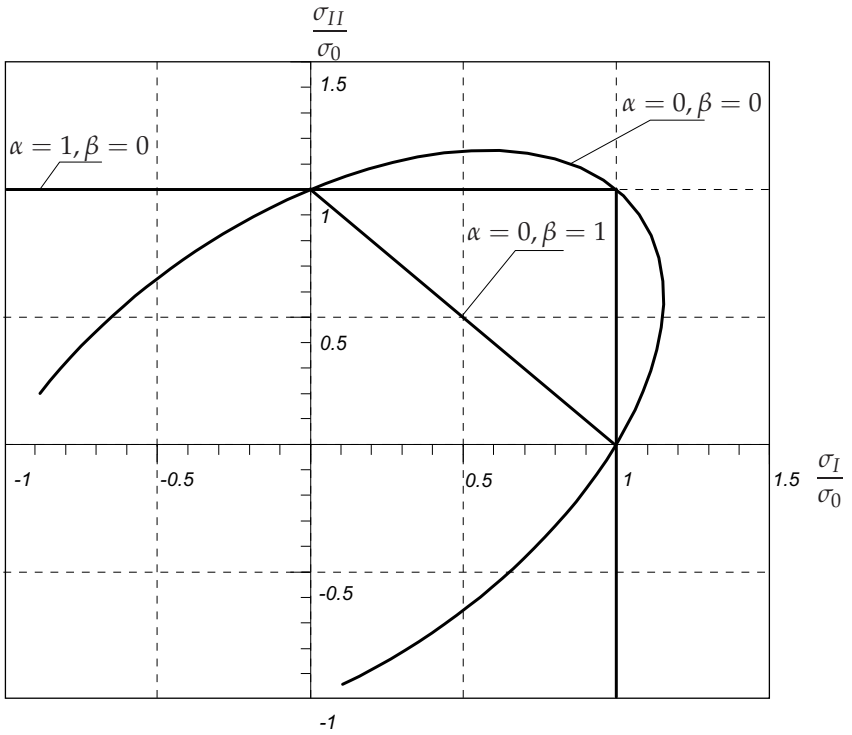

Figure 2.15 Plane stress isochronous rupture loci, for details see [132]

and with

$$\lambda_1 = -\frac{1}{6}, \quad \lambda_2 = \frac{\sqrt{3}}{6}, \quad \lambda_3 = \frac{1}{2}, \quad \lambda_4 = \frac{1}{6}, \quad \lambda_5 = \lambda_6 = 0$$

one can obtain $\sigma_{eq}^{\omega} = \frac{1}{2}(\sigma_I + \sigma_{vM})$. With

$$\lambda_1 = -\frac{1}{3}\alpha, \quad \lambda_2 = \frac{\sqrt{3}}{3}\alpha, \quad \lambda_3 = \beta, \quad \lambda_4 = 1 - \frac{2}{3}\alpha - \beta, \quad \lambda_5 = \lambda_6 = 0$$

Eq. (2.4.16) yields $\sigma_{eq}^{\omega} = \alpha\sigma_I + \beta\sigma_{vM} + (1 - \alpha - \beta)I_1$. Other examples are discussed in [3].

In order to identify the material constants, e.g., a in (2.4.13) or α and β in (2.4.14), the values of the ultimate stresses leading to the same failure time for different stress states are necessary. Therefore series of independent creep tests up to rupture are required. For each kind of the test the long term strength curve (stress vs. time to fracture curve), see Fig. 2.14, must be obtained. For example, a series of torsion tests (at least two) under different stress values should be performed. Usually, experimental data from creep tests under complex stress states are limited and the scatter of the experimental results is unavoidable. Therefore, the constitutive and the evolution equation (2.4.9) and (2.4.10) with the two-parametric damage equivalent stress (2.4.15) are widely used in modeling tertiary creep. Examples

of material constants as well as structural mechanics applications can be found in [18, 69, 77, 132, 142, 143, 144, 163, 169] among others.

2.4.1.2 Micromechanically-Consistent Models. The creep constitutive equation (2.4.9) includes the effect of damage by means of the equivalent stress concept. An alternative approach to formulate the creep constitutive equation can be based on micromechanics. Rodin and Parks [277] considered an infinite block from incompressible isotropic material containing a given distribution of cracks and subjected to a far field homogeneous stress. As a measure of damage they used $\rho = a^3 N/V$, where N is the number of cracks (voids) in a volume V and a is the averaged radius of a crack. Assuming power law creep, they found that the creep potential for such a material has the following form

$$W(\boldsymbol{\sigma}, \rho, n) = \frac{\dot{\varepsilon}_0 \sigma_0}{n+1} f\Big(\zeta(\boldsymbol{\sigma}), \rho, n\Big) \left(\frac{\sigma_{vM}}{\sigma_0}\right)^{n+1}, \tag{2.4.17}$$

where $\dot{\varepsilon}_0$ is the reference creep rate, σ_0 is the reference stress and n is a material constant. $\zeta(\boldsymbol{\sigma})$ is a function representing the influence of the kind of stress state. In [277] the following particular expression is proposed

$$\zeta(\boldsymbol{\sigma}) = \frac{\sigma_I}{\sigma_{vM}},$$

where σ_I is the maximum principal stress. The creep potential (2.4.17) and the flow rule (2.1.6) give

$$\begin{aligned} \dot{\boldsymbol{\varepsilon}}^{cr} &= \frac{\partial W}{\partial \boldsymbol{\sigma}} = \frac{\partial W}{\partial \sigma_{vM}} \frac{\partial \sigma_{vM}}{\partial \boldsymbol{\sigma}} + \frac{\partial W}{\partial \zeta} \frac{\partial \zeta}{\partial \boldsymbol{\sigma}} \\ &= \dot{\varepsilon}_0 \left(\frac{\sigma_{vM}}{\sigma_0}\right)^n \left[\frac{3}{2}\left(f - \frac{\zeta f_{,\zeta}}{n+1}\right) \frac{\boldsymbol{s}}{\sigma_{vM}} + \frac{f_{,\zeta}}{n+1} \boldsymbol{n}_I \otimes \boldsymbol{n}_I\right], \end{aligned} \tag{2.4.18}$$

where $\boldsymbol{n}_I$ is the first principal direction of the stress tensor. The function f must satisfy the following convexity condition [277]

$$f f_{,\zeta\zeta} - \frac{n}{n+1} f_{,\zeta}^2 > 0,$$

The form of the function f is established for the assumed particular distribution of cracks and by use of a self-consistent approach. In [278] the following expression is proposed

$$\begin{aligned} f(\zeta, \rho, n) &= \Big[1 + \alpha(\rho, n)\zeta^2\Big]^{\frac{n+1}{2}}, \\ \alpha(\rho, n) &= \frac{2\rho}{n+1} + \frac{(2n+3)\rho^2}{n(n+1)^2} + \frac{(n+3)\rho^3}{9n(n+1)^3} + \frac{(n+3)\rho^4}{108n(n+1)^4} \end{aligned}$$

Models of the type (2.4.18) are popular in materials science related literature, e.g. [121, 211]. They are based on micromechanical considerations and therefore

seem to be more preferable for creep-damage analysis. However, only idealized damage states, e.g. dilute non-interacting cracks or voids with a given density and specific distribution can be considered. Furthermore, at present there is no micromechanically-consistent way to establish the form of the evolution equation for the assumed damage variable. Different empirical equations are proposed in the literature. For example, Mohrmann and Sester [211] assume that the cavity nucleation is strain controlled and recommend the following equation

$$\frac{\rho}{\rho_f} = \left(\frac{\varepsilon_{vM}}{\varepsilon_f}\right)^{\gamma},$$

where ρ_f, ε_f and γ are material constants which should be identified from "macroscopic" creep responses.

Bassani and Hawk [36] proposed to use a phenomenological damage parameter ω (see Sect. 2.4.1.1) instead of ρ. The function f is then postulated as follows

$$f(\zeta,\omega,n) = \frac{1}{(1-\omega)^k}\left(1-\alpha_0\omega+\alpha_0\omega\zeta^2\right)^{\frac{n+1}{2}} \tag{2.4.19}$$

Here

$$\zeta = (1-\alpha_1)\frac{\sigma_I}{\sigma_{vM}} + \alpha_1\frac{\sigma_H}{\sigma_{vM}}$$

and k, n, α_0 and α_1 are material constants. From Eqs (2.4.18) and (2.4.19) follows

$$\begin{aligned}\dot{\boldsymbol{\varepsilon}}^{cr} &= \dot{\varepsilon}_0\left(\frac{\sigma_{vM}}{\sigma_0}\right)^n \frac{1}{(1-\omega)^k}(1-\alpha_0\omega+\alpha_0\omega\zeta^2)^{\frac{n-1}{2}}\times \\ &\times \left\{\frac{3}{2}(1-\alpha_0\omega)\frac{\boldsymbol{s}}{\sigma_{vM}} + \alpha_0\omega\zeta[(1-\alpha_1)\boldsymbol{n}_I\otimes\boldsymbol{n}_I + \alpha_1\boldsymbol{I}]\right\}\end{aligned} \tag{2.4.20}$$

With $\alpha_0 = 1$ and $k = n$ (2.4.20) yields the Kachanov-Rabotnov type constitutive equation (2.4.9). By setting $\alpha_0 = 1$, $k = (n+1)/2$ and $\omega \ll 1$ Eq. (2.4.20) approximates the Rodin and Parks micro-mechanical based model [277]. For the case $k = n$, $\alpha_0 = 1$ and $\alpha_1 = 1$ the constitutive equation for the creep rate can be presented as follows

$$\dot{\boldsymbol{\varepsilon}}^{cr} = \dot{\varepsilon}_0\left[\frac{\sigma_{vM}}{\sigma_0(1-\omega)}\right]^n (1-\omega+\omega\zeta^2)^{\frac{n-1}{2}}\left[\frac{3}{2}(1-\omega)\frac{\boldsymbol{s}}{\sigma_{vM}} + \omega\zeta\boldsymbol{I}\right]$$

From Eq. (2.4.20) one can calculate the volumetric creep rate

$$\dot{\varepsilon}_V = \operatorname{tr}\dot{\boldsymbol{\varepsilon}}^{cr} = \dot{\varepsilon}_0\left(\frac{\sigma_{vM}}{\sigma_0}\right)^n \frac{1}{(1-\omega)^k}(1-\alpha_0\omega+\alpha_0\omega\zeta^2)^{\frac{n-1}{2}}\left[\alpha_0\omega\zeta(1+2\alpha_1)\right]$$

We observe that the damage growth induces dilatation. Creep constitutive equations (2.4.18) or (2.4.20) include the first principal dyad of the stress tensor. It should be noted that the dyad $\boldsymbol{n}_I\otimes\boldsymbol{n}_I$ can be found only if $\sigma_I \neq 0$, $\sigma_I \neq \sigma_{II}$ and $\sigma_I \neq \sigma_{III}$. In this case, e.g. [199]

$$\boldsymbol{n}_I \otimes \boldsymbol{n}_I = \frac{1}{(\sigma_I - \sigma_{II})(\sigma_I - \sigma_{III})} \left[\boldsymbol{\sigma}^2 - (\mathrm{tr}\,\boldsymbol{\sigma} - \sigma_I)\boldsymbol{\sigma} + \frac{\det \boldsymbol{\sigma}}{\sigma_I} \boldsymbol{I} \right] \qquad (2.4.21)$$

Inserting (2.4.21) into (2.4.18) or into (2.4.20) we observe that not only the volumetric strain but also second order effects (see Sect. 2.2.1 for discussion) are "induced" by damage.

2.4.1.3 Mechanism-Based Models. The constitutive and evolution equations (2.4.9) and (2.4.10) are formulated in terms of power law functions of stress. It is known from materials science that the power law creep model guarantees the correct description only for a specific stress range (see Sect 2.2.3). In addition, the power law stress and damage functions used in Eqs. (2.4.9) and (2.4.10) may lead to numerical problems in finite element simulations of creep in structures with stress concentrations or in attempts to predict the creep crack growth [192, 281].

The uni-axial creep tests are usually performed under increased stress and temperature levels in order to accelerate the creep process. For the long term analysis of structures the material model should be able to predict creep rates for wide stress ranges including moderate and small stresses. Within the materials science many different damage mechanisms which may operate depending on the stress level and the temperature are discussed, e.g., [99]. Each of the damage mechanisms can be considered by a state variable with an appropriate kinetic equation.

Another way for the formulation of a creep-damage constitutive model is the so-called mechanism-based approach. The internal state variables are introduced according to those creep and damage mechanisms which dominate for a specific material and specific loading conditions. Furthermore, different functions of stress and temperature proposed in materials science can be utilized. The form and the validity frame of such a function depend on many factors including the stress and temperature levels, type of alloying, grain size, etc. The materials science formulations do not provide the values of material constants (only the bounds are given). They must be identified from the data of standard tests, e.g. uni-axial creep test. Examples of mechanism-based models can be found in [133, 134, 171, 243, 251]. Here we discuss the model proposed by Perrin and Hayhurst in [251] for a 0.5Cr-0.5Mo-0.25V ferritic steel in the temperature range 600 – 675°C.

The starting point is the assumption that the rate of the local grain boundary deformation is approximately a constant fraction of the overall deformation rate. From this follows that the constitutive equations for the overall creep rate can be formulated in terms of empirical relationships between the local grain boundary deformation rate and the stress, the temperature, the cavitation rate, etc.

For ferritic steels the nucleation of cavities has been observed at carbide particles on grain boundaries due to the local accumulation of dislocations. The nucleation kinetics can be therefore related to the local deformation. Furthermore, the cavity nucleation depends on the stress state characterized by σ_I / σ_{vM}. Cane [83] observed that the area fraction of intergranular cavities in the plane normal to the applied stress increases uniformly with the accumulated creep strain. He proposed that the nucleation and growth can be combined into an overall measure of cavitation. The cavitated area fraction A_f can be related to the von Mises equivalent creep strain,

the von Mises equivalent stress and the maximum principal stress by the equation

$$A_f = D\varepsilon_{vM}\left(\frac{\sigma_I}{\sigma_{vM}}\right)^{\mu}, \tag{2.4.22}$$

where D and μ are constants depending on the material microstructure. Perrin and Hayhurst define the damage state variable ω as the cavitated area fraction. The failure condition in a uni-axial creep test is the complete cavitation of all grain boundaries normal to the applied stress. The cavitated area fraction of such cavities at failure is approximately $1/3$. Therefore, the critical state at which the material fails, can be characterized by $\omega_* = 1/3$.

The important mechanism of creep damage for the ferritic steel under consideration is the temperature dependent coarsening of carbide precipitates. First, the carbide precipitates restrict the deformation of the grain interior and second, they provide sites for nucleation of cavities. Following Dyson [99], the particle coarsening can be characterized by the state variable $\phi = 1 - l_i/l$ related to the initial (l_i) and current (l) spacing of precipitates. The kinetic equation is derived from the coarsening theory [99, 101]

$$\dot{\phi} = \left(\frac{K_c}{3}\right)(1-\phi)^4 \tag{2.4.23}$$

with K_c as the material dependent constant for a given temperature. The rate of the coarsening variable is independent from the applied stress and can be integrated with respect to time. The primary creep is characterized by the work hardening due to the formation of the dislocation substructure. For this purpose a scalar hardening state variable H is introduced. This variable varies from zero to a saturation value H_*, at which no further hardening takes place. The proposed evolution equation is

$$\dot{H} = \frac{h_c\dot{\varepsilon}^{cr}_{vM}}{\sigma_{vM}}\left(1 - \frac{H}{H_*}\right) \tag{2.4.24}$$

with h_c as the material constant.

The creep rate is controlled by the climb plus glide deformation mechanism. For the stress dependence of the creep rate, the hyperbolic sine stress function is used. The materials science arguments for the use of hyperbolic sine function instead of power law function are discussed, for example, by Dyson and McLean [102]. With the assumed mechanisms of hardening, cavitation and ageing and the corresponding state variables the following equation for the von Mises creep rate is proposed

$$\dot{\varepsilon}^{cr}_{vM} = A\sinh\frac{B\sigma_{vM}(1-H)}{(1-\phi)(1-\omega)} \tag{2.4.25}$$

The previous equations are formulated with respect to a fixed temperature. The influence of the temperature on the processes of creep deformation, creep cavitation and coarsening can be expressed by Arrhenius functions with appropriate activation energies. Further details of the physical motivation are discussed in [251]. The following set of constitutive and evolution equations has been proposed

$$
\begin{aligned}
\dot{\boldsymbol{\varepsilon}}^{cr} &= \frac{3}{2}\frac{\boldsymbol{s}}{\sigma_{vM}} A \sinh \frac{B\sigma_{vM}(1-H)}{(1-\phi)(1-\omega)},\\
\dot{H} &= \frac{h_c \dot{\varepsilon}^{cr}_{vM}}{\sigma_{vM}} \left(1 - \frac{H}{H_*}\right),\\
\dot{\phi} &= \left(\frac{K_c}{3}\right)(1-\phi)^4,\\
\dot{\omega} &= DN\dot{\varepsilon}^{cr}_{vM} \left(\frac{\sigma_I}{\sigma_{vM}}\right)^{\mu},\\
A &= A_0 B \exp\left(-\frac{Q_A}{RT}\right), \quad B = B_0 \exp\left(-\frac{Q_B}{RT}\right),\\
K_c &= \frac{K_{c_0}}{B^3} \exp\left(-\frac{Q_{K_c}}{RT}\right), \quad D = D_0 \exp\left(-\frac{Q_D}{RT}\right),
\end{aligned}
\tag{2.4.26}
$$

where $N = 1$ for $\sigma_I > 0$ and $N = 0$ for $\sigma_I \leq 0$. A_0, B_0, D_0, K_{c_0}, h_c, H_*, Q_A, Q_B, Q_D and Q_{K_c} are material constants which must be identified from uni-axial creep tests. The material constant μ, the so-called stress state index, can be determined from multi-axial creep rupture data. These constants are identified in [251] based on the experimental data of uni-axial creep over the stress range of $28 - 110$ MPa and over the temperature range of $615 - 690^\circ$ C. In [252] Eqs (2.4.26) are applied to model creep in different zones of a weldment at 640° C including the weld metal, the heat affected zone and the parent material.

It should be noted that Eqs (2.4.26) are specific for the considered material and can only be applied with respect to the dominant mechanisms of the creep deformation and damage evolution. Further examples of mechanism based material models are presented in [244] for a nickel-based super-alloy and in [171] for an aluminium alloy.

2.4.1.4 Models Based on Dissipation. Sosnin [296, 297] proposed to characterize the material damage by the specific dissipation work. The following damage variable has been introduced

$$
q = \int_0^t \sigma \dot{\varepsilon}^{cr} d\tau \tag{2.4.27}
$$

For the variable q the evolution equation was postulated

$$
\dot{q} = f_\sigma(\sigma) f_T(T) f_q(q)
$$

For the multi-axial stress and strain states this variable is defined as follows

$$
q = \int_0^t \boldsymbol{\sigma} \cdot\cdot\, \dot{\boldsymbol{\varepsilon}}^{cr} d\tau
$$

In [297] Sosnin presented experimental data for various titanium and aluminium alloys in a form of q vs. time curves. He found that a critical value q_* exists at

which the material fails under creep conditions. The value q_* does not depend on the kind of applied stress and can be considered as a material constant.

For isotropic materials the creep rate equation can be formulated as follows (see Sect. 2.2.1)

$$\dot{\boldsymbol{\varepsilon}}^{cr} = \frac{3}{2}\frac{\dot{P}}{\sigma_{vM}}\boldsymbol{s}, \quad P = \boldsymbol{\sigma} \cdot\cdot\, \dot{\boldsymbol{\varepsilon}}^{cr} = \sigma_{vM}\dot{\varepsilon}^{cr}_{vM} \tag{2.4.28}$$

Sosnin assumed the dissipation power $\dot{P}$ to be a function of the von Mises equivalent stress, the temperature and the internal state variable q as follows

$$\dot{q} \equiv \dot{P} = f_\sigma(\sigma_{vM}) f_T(T) f_q(q)$$

In many cases the following empirical equation provides a satisfactory agreement with experimental results

$$\dot{q} = \frac{b\sigma^n_{vM}}{q^k(q^{k+1}_* - q^{k+1})^m}, \tag{2.4.29}$$

where b, n, k, m and q_* are material constants. In [297] experimental data obtained from uni-axial tests and tests on tubular specimens under combined tension and torsion are presented. Particularly the results of combined tension and torsion tests show that the q versus t curves do not depend on the kind of the stress state. The material constants are identified for titanium alloys OT-4, BT-5 and BT-9, for the aluminium alloy D16T and for the steel 45. In [28] the Sosnin's dissipation damage measure is applied to the description of creep-damage of the titanium alloy OT-4 and the aluminium alloy D16T considering stress state effects. In [341] Życzkowski calculated the dissipation power P starting from the Kachanov-Rabotnov constitutive equation (2.4.9). He found that for a class of materials it is possible to express the damage evolution equation (2.4.10) in terms of the dissipation power. He concluded that this approach allows to reduce the number of material constants to be determined from creep tests.

2.4.2 Damage-Induced Anisotropy

The dominant damage mechanism for many materials is the nucleation and growth of cavities and formation of micro-cracks. Cavities nucleate on grain boundaries having different orientations. At the last stage before creep rupture the coalescence of cavities and the formation of oriented micro-cracks is observed. The direction of the orientation depends on the material microstructure and on the kind of the applied stress. For example, micrographs of copper specimens tested under torsion show that the micro-cracks dominantly occur on the grain boundaries whose normals coincide with the direction of the maximum positive principal stress [134, 136, 212]. The strongly oriented micro-cracks may induce anisotropic creep responses particularly at the last stage of the creep process. Creep responses of the austenitic steel X8 CrNiMoNb 1616 and the ferritic steel 13 CrMo 4 4 are experimentally studied in [63, 105] with respect to different loading orientations. Figure 2.16 schematically

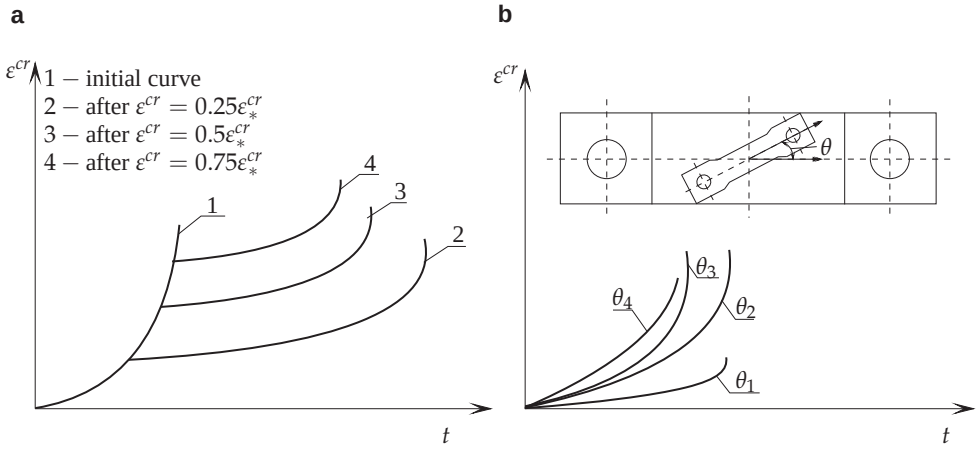

Figure 2.16 Uni-axial creep tests with different orientations of the loading direction. **a** Creep curve for a flat specimen and creep curves for small specimens after different prestraining, **b** creep curves for different loading directions after pre-straining of $0.75\varepsilon_*^{cr}$ (after [63, 105])

presents the results of testing. Uni-axial creep tests were carried out on flat specimens at different stress and temperature levels. In order to establish the influence of the creep history (pre-loading and pre-damage), series of flat specimens were tested up to different values of the creep strain. The values of the creep pre-straining were $\varepsilon^{cr} = 0.25\varepsilon_*^{cr}; 0.5\varepsilon_*^{cr}; 0.75\varepsilon_*^{cr}$, where ε_*^{cr} is the creep strain at fracture. After unloading, small specimens were manufactured from the pre-strained flat specimens with different orientation to the loading axis, Fig. 2.16b. The uni-axial tests performed on the small specimens show that the creep responses depend on the angle of the orientation θ. In [105] it is demonstrated that for small specimens pre-strained up to $0.25\varepsilon_*^{cr}$ the creep response is not sensitive to the angle θ. The significant dependence of the creep curves and the fracture times on the angle θ has been observed for specimens pre-strained up to $0.75\varepsilon_*^{cr}$.

In [218] creep tests were carried out on thin-walled copper tubes under combined tension and torsion. The loading history and the creep responses are schematically presented in Fig. 2.17. During the first cycle the specimens were preloaded by constant normal and shear stresses within the time interval $[0, t_1]$. In the second cycle from t_1 up to creep rupture the specimens were loaded under the same constant normal stress but the reversed constant shear stress. The stress state after the reversal is characterized by the change of the principal directions. The angle between the first principal direction in the reference state and after the reversal can be controlled by the values of the normal and the shear stresses. Creep responses for different angles are discussed in [218]. It is demonstrated that the creep-damage model with a scalar damage parameter, see Sect. 2.4.1, is not able to predict the creep behavior after the shear stress reversal. Particularly, it significantly underestimates the fracture time in all loading cases. Similar results are discussed in [219] based on tests on Nimonic 80A.

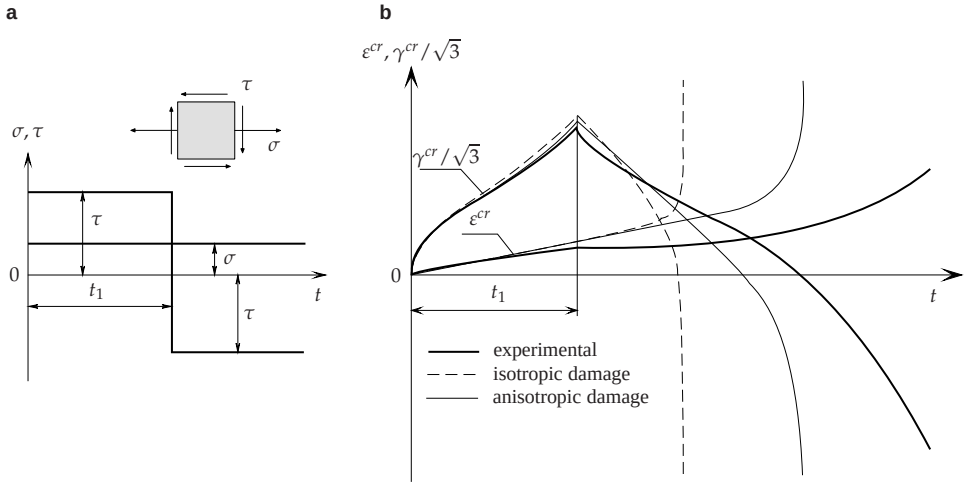

Figure 2.17 Creep tests at combined tension and torsion. **a** Loading history, **b** creep responses (after [218])

The introduced examples of experimental observations indicate that the creep rate and the lifetime of a specimen additionally depend on the orientation of microdefects with respect to the principal axes of the stress tensor. One way to consider such a dependence is the use of a tensor-valued damage parameter. A second rank damage tensor was firstly introduced by Vakulenko and M. Kachanov [316] for the description of elastic-brittle damage. The first attempt to use a tensor-valued damage parameter in creep mechanics is due to Murakami and Ohno [215, 217]. They considered a characteristic volume V in the material having N wedge cracks and specified the area of the grain boundary occupied by the kth crack by dA_g^k. They assumed that the state of damage can be characterized by the following second rank symmetric tensor

$$\boldsymbol{\Omega} = \frac{3}{A_g(V)} \sum_{k=1}^{N} \int_V [\boldsymbol{m}^k \otimes \boldsymbol{m}^k + w^k(\boldsymbol{I} - \boldsymbol{m}^k \otimes \boldsymbol{m}^k)] dA_g^k, \tag{2.4.30}$$

where $\boldsymbol{m}^k$ is the unit normal vector to the kth crack and $A_g(V)$ is the total area of all grain boundaries in V. w^k characterizes the effect of the kth crack on the area reduction in the planes whose normals are perpendicular to $\boldsymbol{m}^k$. Specifying the three principal values of $\boldsymbol{\Omega}$ by Ω_j, $j = 1, 2, 3$, and the corresponding principal directions by the unit vectors $\boldsymbol{n}_j$ the damage tensor can be formulated in the spectral form

$$\boldsymbol{\Omega} = \sum_{j=1}^{3} \Omega_j \boldsymbol{n}_j \otimes \boldsymbol{n}_j \tag{2.4.31}$$

The principal values of the damage tensor Ω_j are related to the cavity area fractions in three orthogonal planes with the unit normals $\pm\boldsymbol{n}_j$. The cases $\Omega_j = 0$ and $\Omega_j = 1$ correspond to the undamaged state and the creep-rupture in the jth plane,

respectively. By analogy with the uni-axial bar (see Fig. 2.12) Murakami and Ohno introduced a fictitious undamaged configuration in a solid by means of effective infinitesimal area elements. From three orthogonal planes having the unit normals $-\boldsymbol{n}_j$ an infinitesimal tetrahedron is constructed with area elements $-\tilde{\boldsymbol{n}}_i d\tilde{A}_i$ and $\tilde{\boldsymbol{n}} d\tilde{A}$ so that

$$\tilde{\boldsymbol{n}} d\tilde{A} = \sum_{j=1}^{3} \boldsymbol{n}_j d\tilde{A}_j = \sum_{j=1}^{3} (1 - \Omega_j) \boldsymbol{n}_j dA_j \tag{2.4.32}$$

With $\Omega_j \boldsymbol{n}_j = \boldsymbol{n}_j \cdot \boldsymbol{\Omega} = \boldsymbol{\Omega} \cdot \boldsymbol{n}_j$

$$\tilde{\boldsymbol{n}} d\tilde{A} = (\boldsymbol{I} - \boldsymbol{\Omega}) \cdot \boldsymbol{n} dA \tag{2.4.33}$$

The stress vector acting in the plane with the unit normal $\boldsymbol{n}$ can be specified by $\boldsymbol{\sigma}_{(\boldsymbol{n})}$. The resultant force vector acting in the plane dA is

$$dA\boldsymbol{\sigma}_{(\boldsymbol{n})} = dA\boldsymbol{n} \cdot \boldsymbol{\sigma} = d\tilde{A}\tilde{\boldsymbol{n}} \cdot (\boldsymbol{I} - \boldsymbol{\Omega})^{-1} \cdot \boldsymbol{\sigma} = d\tilde{A}\tilde{\boldsymbol{n}} \cdot \tilde{\boldsymbol{\sigma}}, \quad \tilde{\boldsymbol{\sigma}} \equiv (\boldsymbol{I} - \boldsymbol{\Omega})^{-1} \cdot \boldsymbol{\sigma}, \tag{2.4.34}$$

where $\tilde{\boldsymbol{\sigma}}$ is the effective stress tensor. Introducing the so-called damage effect tensor $\boldsymbol{\Phi} \equiv (\boldsymbol{I} - \boldsymbol{\Omega})^{-1}$ one can write

$$\tilde{\boldsymbol{\sigma}} = \boldsymbol{\Phi} \cdot \boldsymbol{\sigma} \tag{2.4.35}$$

According to the strain equivalence principle [185], the constitutive equation for the virgin material, for example the constitutive equation for the secondary creep, can be generalized to the damaged material replacing the Cauchy stress tensor $\boldsymbol{\sigma}$ by the net stress tensor $\tilde{\boldsymbol{\sigma}}$. The net stress tensor (2.4.35) is non-symmetric. Introducing the symmetric part

$$\tilde{\boldsymbol{\sigma}}^s = \frac{1}{2}(\boldsymbol{\sigma} \cdot \boldsymbol{\Phi} + \boldsymbol{\Phi} \cdot \boldsymbol{\sigma}) \tag{2.4.36}$$

the secondary creep equation (2.4.8) is generalized as follows [219]

$$\dot{\boldsymbol{\varepsilon}}^{cr} = \frac{3}{2} a \tilde{\sigma}_{vM}^{n-1} \tilde{\boldsymbol{s}}^s, \quad \tilde{\boldsymbol{s}}^s = \tilde{\boldsymbol{\sigma}}^s - \frac{1}{3}\mathrm{tr}\tilde{\boldsymbol{\sigma}}^s \boldsymbol{I}, \quad \tilde{\sigma}_{vM} = \sqrt{\frac{3}{2}\tilde{\boldsymbol{s}}^s \cdot\cdot \tilde{\boldsymbol{s}}^s} \tag{2.4.37}$$

The rate of the damage tensor is postulated as a function of the stress tensor and the current damage state. The following evolution equation is proposed in [218] for the description of creep damage of copper

$$\dot{\boldsymbol{\Omega}} = b[\alpha \tilde{\sigma}_I^s + (1 - \alpha)\tilde{\sigma}_{vM}^s]^k (\boldsymbol{n}_I^{\tilde{\boldsymbol{\sigma}}} \cdot \boldsymbol{\Phi} \cdot \boldsymbol{n}_I^{\tilde{\boldsymbol{\sigma}}})^l \boldsymbol{n}_I^{\tilde{\boldsymbol{\sigma}}} \otimes \boldsymbol{n}_I^{\tilde{\boldsymbol{\sigma}}}, \tag{2.4.38}$$

where b, α, k and l are material constants and the unit vector $\boldsymbol{n}_I^{\tilde{\boldsymbol{\sigma}}}$ denotes the direction corresponding to the first positive principal stress $\tilde{\sigma}_I$. The constitutive and evolution equations (2.4.37) and (2.4.38) have been applied in [219] for the description of creep-damage behavior of Nimonic 80A. The second rank damage tensor (2.4.31) and the net stress (2.4.36) have been used in [218] with McVetty-type creep equations for the prediction of creep-damage of copper. The results show that the model with the damage tensor provides better agreement with experimental data if

compared to the model with a scalar damage parameter, see Fig. 2.17. In [217] the following damage evolution equation is utilized

$$\dot{\boldsymbol{\Omega}} = b[\alpha\tilde{\sigma}_I^s + \beta\tilde{\sigma}_m + (1-\alpha-\beta)\tilde{\sigma}_{vM}^s]^k (\mathrm{tr}\,\boldsymbol{\Phi}^2)^{l/2} \left[\eta\boldsymbol{I} + (1-\eta)\boldsymbol{n}_I^{\tilde{\sigma}} \otimes \boldsymbol{n}_I^{\tilde{\sigma}}\right], \tag{2.4.39}$$

where β and η are material constants. This equation takes into account the influence of the mean stress on the damage rate. Furthermore, the isotropic part of the damage tensor associated with the growth of voids is included.

To discuss the damage tensor (2.4.31) let us consider a uni-axial homogeneous stress state $\boldsymbol{\sigma} = \sigma_0 \boldsymbol{m} \otimes \boldsymbol{m}$ with $\sigma_0 > 0$ and $\boldsymbol{m} = const$. Let us specify $\boldsymbol{\Omega} = \boldsymbol{0}$ as the initial condition. The evolution equation (2.4.38) takes the form

$$\dot{\boldsymbol{\Omega}}(t) = \dot{\omega}(t)\boldsymbol{m} \otimes \boldsymbol{m}, \quad \dot{\omega} = \frac{b\sigma_0^k}{(1-\omega)^{k+l}}, \quad \omega(0) = 0 \tag{2.4.40}$$

The equation for the scalar ω can be integrated as shown in Sect. 2.4.1. As a result one can find the relation between the time to fracture and the stress σ_0. Based on this relation and experimental data one can estimate the values of material constants b, k and l (Sect. 2.4.1). According to the introduced damage measure (2.4.31) the damage state $\boldsymbol{\Omega} = \omega \boldsymbol{m} \otimes \boldsymbol{m}$ corresponds to the case of uniformly distributed penny-shaped cracks (circular planes) with the unit normals $\boldsymbol{m}$.

Now let us assume that the damage state $\boldsymbol{\Omega} = \omega_0 \boldsymbol{m} \otimes \boldsymbol{m}$, $0 < \omega_0 < 1$ is induced as a result of the constant stress $\boldsymbol{\sigma} = \sigma_0 \boldsymbol{m} \otimes \boldsymbol{m}$ exerted over a period of time and in the next loading cycle $\boldsymbol{\sigma} = \sigma_0 \boldsymbol{p} \otimes \boldsymbol{p}$, $\boldsymbol{p} \cdot \boldsymbol{m} = 0$. In this case the solution of (2.4.38) can be written down as follows

$$\boldsymbol{\Omega}(t) = \omega_0 \boldsymbol{m} \otimes \boldsymbol{m} + \omega_1(t)\boldsymbol{p} \otimes \boldsymbol{p}, \quad \dot{\omega}_1 = \frac{b\sigma_0^k}{(1-\omega_1)^{k+l}}, \quad \omega_1(0) = 0 \tag{2.4.41}$$

The model predicts that in the second cycle the material behaves like a virgin undamaged material. The corresponding time to fracture does not depend on the initial damage ω_0. The rate of nucleation and growth of new voids (cracks) on the planes orthogonal to $\boldsymbol{p}$ will not be affected by cracks formed in the first loading cycle. Furthermore, if a compressive stress i.e. $\boldsymbol{\sigma} = -\sigma_0 \boldsymbol{p} \otimes \boldsymbol{p}$ is applied in the second cycle the model predicts no damage accumulation.

Let us note that the evolution equations (2.4.38) and (2.4.39) can only be applied if $\tilde{\sigma}_I \neq 0$, $\tilde{\sigma}_I \neq \tilde{\sigma}_{II}$ and $\tilde{\sigma}_I \neq \tilde{\sigma}_{III}$. In this case the dyad $\boldsymbol{n}_I^{\tilde{\sigma}} \otimes \boldsymbol{n}_I^{\tilde{\sigma}}$ can be found from the identity (2.4.21). For the stress states $\boldsymbol{\sigma} = a_0 \boldsymbol{I}$ or $\boldsymbol{\sigma} = a\boldsymbol{p} \otimes \boldsymbol{p} + b(\boldsymbol{I} - \boldsymbol{p} \otimes \boldsymbol{p})$, $a < b$, there is an infinite number of first principal directions. Such stress states are typical for several structural components. For example, the stress state of the type $\boldsymbol{\sigma} = a\boldsymbol{p} \otimes \boldsymbol{p} + b(\boldsymbol{I} - \boldsymbol{p} \otimes \boldsymbol{p})$ arises in the midpoint of a transversely loaded square plate with all for edges to be fixed (e.g. supported or clamped edges), [13]. In the loaded (top) surface of such a plate $b < a < 0$ while in the bottom surface $b > a$, $a < 0$, $b > 0$. Stress states of the same type arise in different rotationally symmetric problems of structural mechanics. For analysis of such problems a modified form of the evolution equation (2.4.39) is required [119].

Various forms of creep-damage constitutive equations with second rank damage tensors have been utilized. In [12] the effective stress tensor

$$\tilde{\boldsymbol{\sigma}} = \boldsymbol{\Phi}^{1/2} \cdot \boldsymbol{\sigma} \cdot \boldsymbol{\Phi}^{1/2} \tag{2.4.42}$$

proposed in [91] is applied to formulate the creep-damage constitutive equation. Mechanisms of damage activation and deactivation are taken into account. The model predictions are compared with experimental data of creep in copper. In [259, 260, 261, 262] a second rank damage tensor is applied for the modeling of creep of nickel-based single crystal super-alloys SRR 99 and CMSX-6 at 760° C. The proposed constitutive equations take into account both the initial anisotropy and the damage induced anisotropy.

The symmetry group of a symmetric second rank tensor includes at least nine elements (see Sect. 2.3.2). With the second rank damage tensor and the effective stress tensors (2.4.36) or (2.4.42) only restrictive forms of orthotropic tertiary creep can be considered (a similar situation is discussed in Sect. 2.3.2). Therefore in many works it is suggested to introduce higher order damage tensors. For different definitions of damage tensors one may consult [8, 10, 55, 172, 183, 291]. A critical review is given in [284]. At present, the available experimental data on creep responses do not allow to verify whether the orthotropic symmetry is an appropriate symmetry assumption for the modeling of anisotropic creep-damage processes. From the micro-structural point of view one may imagine rather complex three-dimensional patterns of voids and cracks which nucleate and propagate as the result of multi-axial non-proportional loadings. An attempt to predict these patterns would result in a complex mathematical model with a large (or even infinite) number of internal variables including tensors of different rank. A model to characterize different patterns of cracks may be based on the orientation distribution function, orientation averaging and the so-called orientation tensors. This approach is widely used in different branches of physics and materials science for the statistical modeling of oriented micro-structures. Examples include fiber suspensions [181], mixtures [112], polymers and polymer composites [21, 307]. The application of orientational averaging to characterize damage states under creep conditions is discussed in [212, 240, 300].

Finally let us note, that the material behavior at elevated temperature and non-proportional loading is a complex interaction of different deformation and damage mechanisms such as hardening, softening, creep-damage, fatigue-damage, etc. Several unified models utilize constitutive equations of creep with kinematic and/or isotropic hardening and include damage effects by means of the effective stress concept and the strain equivalence principle. In [158] the Malinin-Khadjinsky kinematic hardening rule, see Sect. 2.3.2 and isotropic Kachanov-Rabotnov type damage variable are discussed. The damage rate is additionally governed by the magnitude of the hardening variable, so that the coupling effect of damage and strain hardening/softening can be taken into account. It is shown that the kinematic hardening coupled with isotropic damage predicts well the effect of longer life-time after the stress reversal. In [98] the Chaboche-Rousselier visco-plasticity model is modified to predict the coupled creep-plasticity-damage behavior. The scalar damage variable is introduced as a sum of the accumulated time-dependent and cycle-dependent

components. Various approaches to formulate a unified material model within the framework of continuum damage mechanics and thermodynamics of dissipative processes are discussed in [85, 86, 88, 185].

The verification of a unified model with non-linear anisotropic hardening and damage coupling requires a large number of independent tests under non-proportional loading. As a rule, accurate experimental data are rarely available. Furthermore, non-uniform stress and strain fields may be generated in a standard uni-axial specimen under non-proportional cyclic loading conditions [189]. They may be the reason for the large scatter of experimental data and misleading interpretations.